

Final Report for CRADA No. 97-F001

October 2000

The U.S. Department of Energy
The National Energy Technology Laboratory
P.O. Box 10940, 626 Cochrans Mill Road
Pittsburgh, PA 15236-0940
and
P.O. Box 880, 3610 Collins Ferry Road
Morgantown, WV 26507-0880

and
The Foster Wheeler Development Corporation
12 Peachtree Hill Road
Livingston, NJ 07039

Disclaimer

This report was prepared as an account of work sponsored by an agency of the United States Government. Neither the United States Government nor any agency thereof, nor any of their employees, makes any warranty, express or implied, or assumes any legal liability or responsibility for the accuracy, completeness, or usefulness of any information, apparatus, product, or process disclosed, or represents that its use would not infringe privately owned rights. Reference therein to any specific commercial product, process, or service by trade name, trademark, manufacturer, or otherwise does not necessarily constitute or imply its endorsement, recommendation, or favoring by the United States Government or any agency thereof. The views and opinions of authors expressed therein do not necessarily state or reflect those of the United States Government or any agency thereof.

Table of Contents

I. Introduction

II Results and Discussion

- A. Task 1 - Continuing Validation of the MFIX Code
 - 1. Case 1: Simulation of NETL CFB cold flow unit
 - 2. Case 2: Simulation of FWDC CFB cold flow model
- B. Task 2 - Parametric MFIX Code Investigations
 - 1. Investigate Bubble Shape
 - 2. Spouted Bed Hydrodynamics
 - 3. Coal Chemistry Schemes
- C. Task 3 - MFIX Code Enhancements
 - 1. Improvements to the serial code
 - 2. Parallelization

III References

IV Appendices

- A. Appendix A CRADA Document
- B. Appendix B NETL Cold Flow Circulating Fluidized Bed Simulation
- C. Appendix C MFIX Code Modification to “usr0.f” and “b-force2.inc”
- D. Appendix D MFIX Predictions of Solids Distribution Within NETL Circulating Fluidized Bed
- E. Appendix E MFIX Input File for the Simulation of the FW Pilot Plant Cold Flow Unit
- F. Appendix F MFIX Input File for Bubble Shape Simulation
- G. Appendix G MFIX Input File Used to Predict Spouted Bed Behavior

I Introduction

This report documents the results of work conducted under the Cooperative Research And Development (CRADA) No. 97-F001 between the Foster Wheeler Development Corporation, FWDC, and the National Energy Technology Laboratory, NETL. Under this agreement, FWDC and NETL worked together to further investigate the applicability of the MFIX computer code to FWDC engineering problems. MFIX is a transient, finite difference, FORTRAN code that solves the equations of transport for interacting fluid and granular solid phases. It is designed to model fluidized bed reactors. Under the CRADA, work was divided into three tasks. The first task involved the continued validation of the hydrodynamic and chemistry capabilities of the MFIX code. The second task involved a parametric evaluation of the MFIX code's ability to predict bubble shape. Task 3 was to modify MFIX to make it execute faster and more easily on personal computers. Task 1 was accomplished by both FWDC and NETL while Tasks 2 and 3 were completed primarily by NETL. Non technical details of the CRADA can be found in Appendix A.

II Results and Discussion

Task 1 – Continuing Validation of the MFIX Code

Case 1: Simulation of NETL CFB cold flow unit

As part of its support to advanced coal conversion technologies, NETL has constructed a cold flow circulating fluidized bed unit. An MFIX simulation of this unit was conducted as part of the CRADA to help validate the code's predictions.

The NETL Experimental Facility

NETL's cold flow unit can be considered to consist of four major parts. The solids riser section, the cyclone to separate the gas flow from the solids flow, the solids standpipe, and the non-mechanical valve which connects the standpipe to the riser and controls the flow of solids from the standpipe to the riser. The overall nominal height of the entire unit is 60 feet. The riser inside diameter is 12 inches and the inside diameter of the standpipe as well as the non-mechanical valve is 10 inches. Gas flow up the riser can be larger than 100,000 SCFH and measured solids circulation rates have been larger than 100,000 pounds per hour. While NETL has tested three different non-mechanical valve configurations, "J" valve, "L" valve, and Loop Seal, only the "L" valve configuration was simulated. See Figure 1.

MFIX Simulation

MFIX was used to simulate the operation of the NETL cold flow circulating fluidized bed. Simulation results were compared against data collected on September 2, 1998 for operations using polyvinyl chloride bed material. A summary of important operating characteristics used in the MFIX simulation is listed in Table 1. The entire MFIX input file is listed in Appendix B.

Table 1. Important Experimental Quantities Used In MFIX Simulation

	Units	Value
Facility Height	cm	1828 (60 ft)
Facility Width	cm	178 (70 inches)
Riser Velocity	cm/sec	420.4 (13.79 ft/sec)
Standpipe Gas Velocity	cm/sec	1.94
Solids Density	gr/cc	1.42
Particle Diameter	cm	.02 (200 : m)
Minimum Solids Void Fraction		0.387

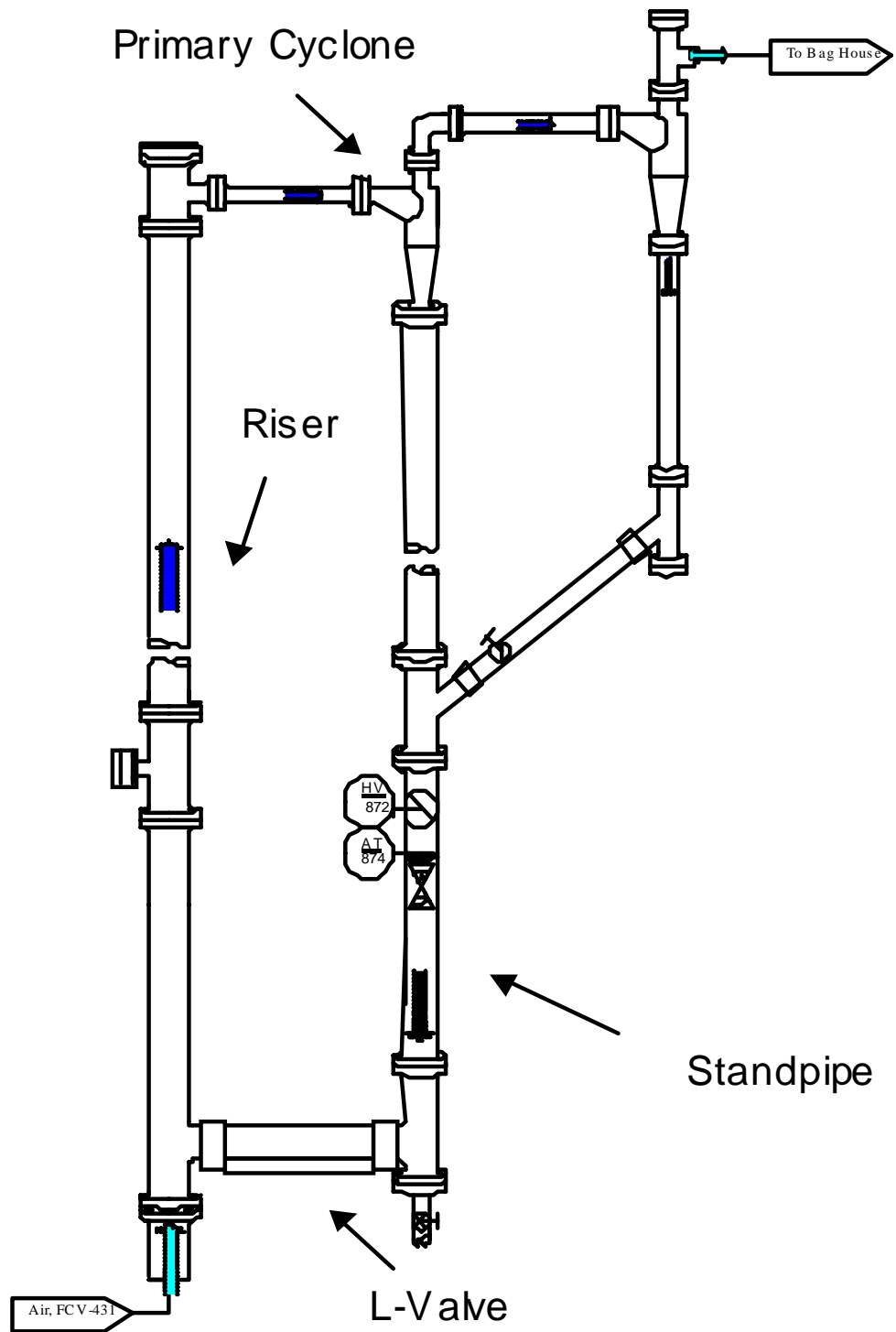


Figure 1. Diagram of NETL Cold Flow Circulating Fluidized Bed Facility

To simulate the NETL facility, the equipment was divided into computational cells 2 cm wide and 4 cm tall. With cells of these dimensions, the overall computational grid was 89 cells wide and 457 cells tall. A total of 40 seconds of operation were simulated. Figure 2 is a schematic of the overall simulation layout with dimensions rounded to the nearest inch.

Modeling of the primary cyclone separator at the top of the standpipe was achieved through the introduction of an “artificial” acceleration. Such an artificial construct was needed to incorporate the operation of the inherently 3D cyclone into the 2D simulation. This acceleration was located at the top of the standpipe and covered an area from 1716 cm to 1748 cm and extended 6 cm into the standpipe (56.3 ft to 57.3 feet extending 2.4 inches into the standpipe). This is the exact vertical location of the gas exit. The area over which this acceleration was imposed is shaded in Figure 2. An acceleration of 200,000 cm/sec² (about 200 times the acceleration due to gravity) to the right and away from the gas exit was imposed. The two modified MFIX routines used to impose this acceleration are listed in Appendix C. Portions of the code which have been added or modified are shaded.

Simulation Results

The solids distribution throughout the circulating system is shown in Figure 3. In this figure, areas of high solids loading (void fraction = 0.4) are shown in red while areas of low solids loading (void fraction = 1.0) are blue. Intermediate colors represent intermediate void fractions. The time, in seconds, from the beginning of the simulation is reported at the top of each figure. Figures showing the solids distribution at other times can be found in Appendix D.

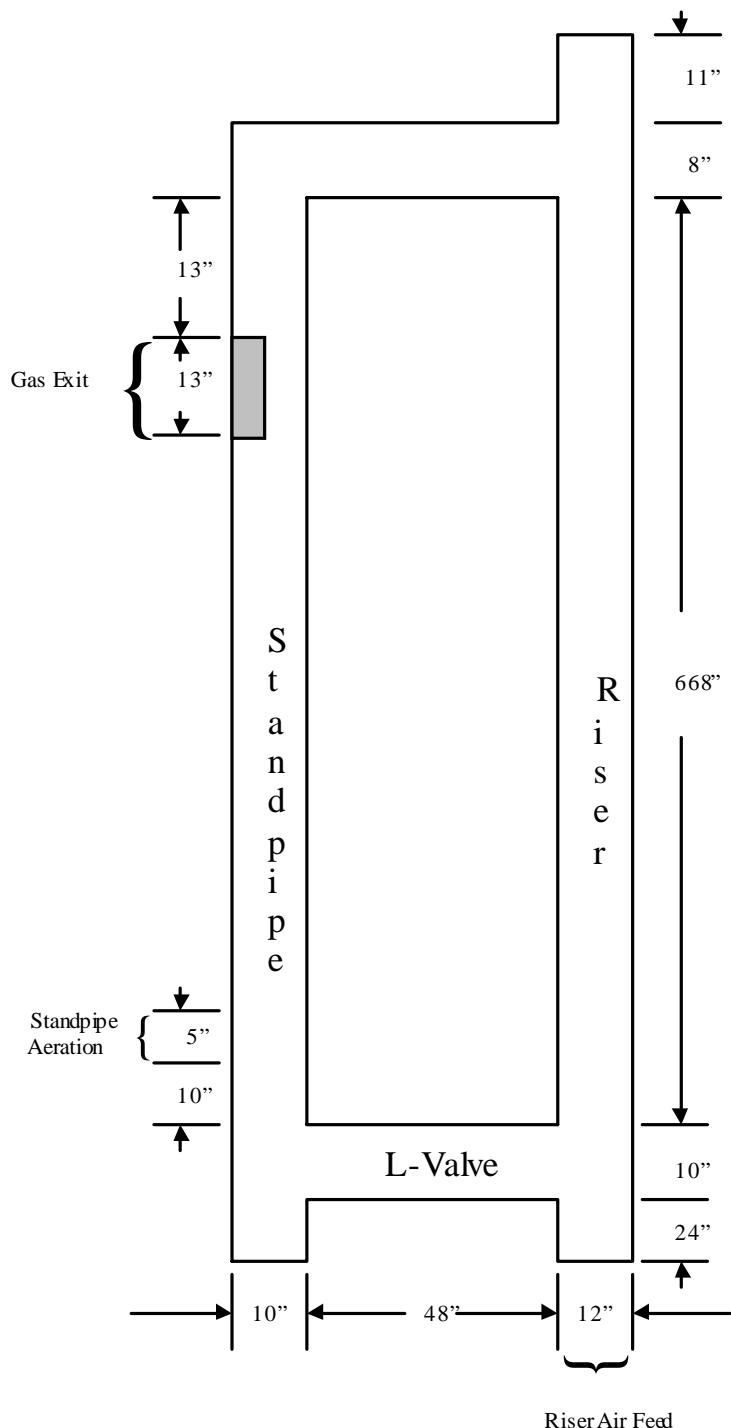


Figure 2. Schematic Diagram of NETL Cold Flow Unit Used For MFIX Simulation



Figure 3. MFIX Simulation of NETL Cold Flow Circulating Fluidized Bed

In addition to calculating the solids distribution within the cold flow unit, MFIX predicts virtually all of the other important flow field properties. One such property, gas pressure along the length of the riser, was compared against experimentally measured values. See Figure 4.

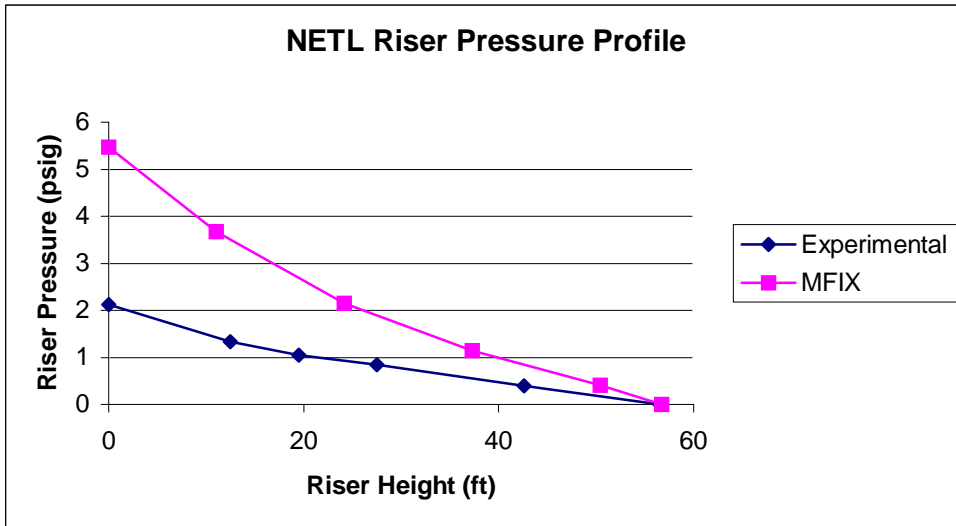


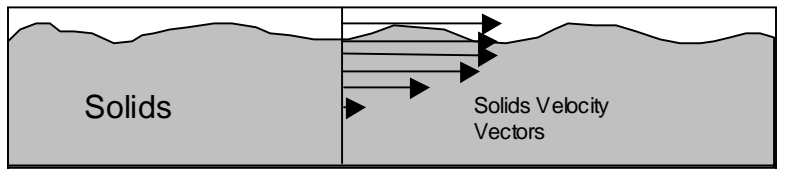
Figure 4. Comparison of Experimental and MFIX Predictions For Riser Pressure Profile

MFIX data used in Figure 4 was time averaged for the period of 30 and 35 seconds at each elevation. As seen in Figure 4, MFIX over predicts the pressure drop across the riser by a considerable factor. This over prediction is attributed to an over prediction of the solids circulation rate. The experimentally measured five minute average solids circulation rate for the 9/2/98 data was slightly less than 20,000 lbs/hr. This solids flow compares to a value of slightly more than 189,500 lbs/hr predicted by MFIX. The MFIX value was calculated by using POSTMFIX to report the mass flux in the Y direction (FLUX_{sy}) at 39 feet elevation for the riser and time averaged between 30 and 35 seconds. Values for the mass flux were averaged across the width of the riser. The mass flux average was then multiplied by the actual area of the riser to yield the total mass circulation rate. Certainly, a higher circulation rate predicted by MFIX leads to a higher solids inventory within the riser and as a result a higher pressure drop.

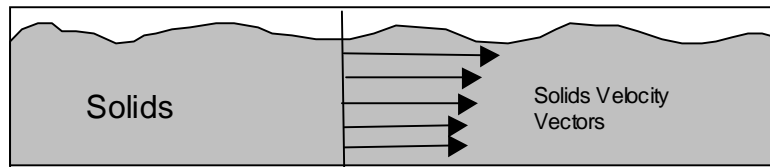
The high mass circulation rate predicted by MFIX is thought to be a result of the way MFIX treats the solids phase. Within MFIX, the solids phase is considered a continuous fluid in a manner very similar to the more conventional gas or liquid phase. As a result of this treatment, MFIX can not predict behavior which might be termed "hour-glass" flow. In this type of solids behavior, solids switch between a stationary pile of particles acting as a single solid mass and a flowing collection of particles behaving more like a fluid. In MFIX, the solids always act as a fluid. MFIX predicts that a conical pile of solids will flow into a uniformly thick layer (even without the influence of a fluidizing air flow).

Higher than expected circulation rates result when this characteristic is considered during L-valve operation. During actual L-valve operation, it is believed that there is a relatively thick

layer of solids at the bottom of the valve where the solids have velocities close to zero. It is only the top few inches of solids within the L-valve, which actually move and result in the overall solids circulation rate. MFIX, on the other hand, can not predict this stationary solids layer and instead predicts that the entire L-valve cross sectional area is available for solids flow. See Figure 5.



Experimental L-Valve Solids Flow



MFIX L-Valve Solids Flow

Figure 5. Comparison of Solids Velocities Within the L-Valve

Task 1 – Continuing Validation of the MFIX Code

Case 2: Simulation of FWDC CFB cold flow model

Foster Wheeler Development Corporation has conducted cold flow tests on its 1/3 scale CFB cold flow test facility in Livingston, New Jersey. A typical test run has been selected for MFIX simulations. A brief description and operating conditions of the cold flow experiment will be given in this section, followed by the model setup and results of the MFIX simulation.

The FWDC Experimental Facility

The cold flow test facility is a 1/3 scale model of a 60 MWe CFB boiler. A schematic of the test facility is shown in Figure 6. The dimensions of the furnace part are shown in Figure 7.

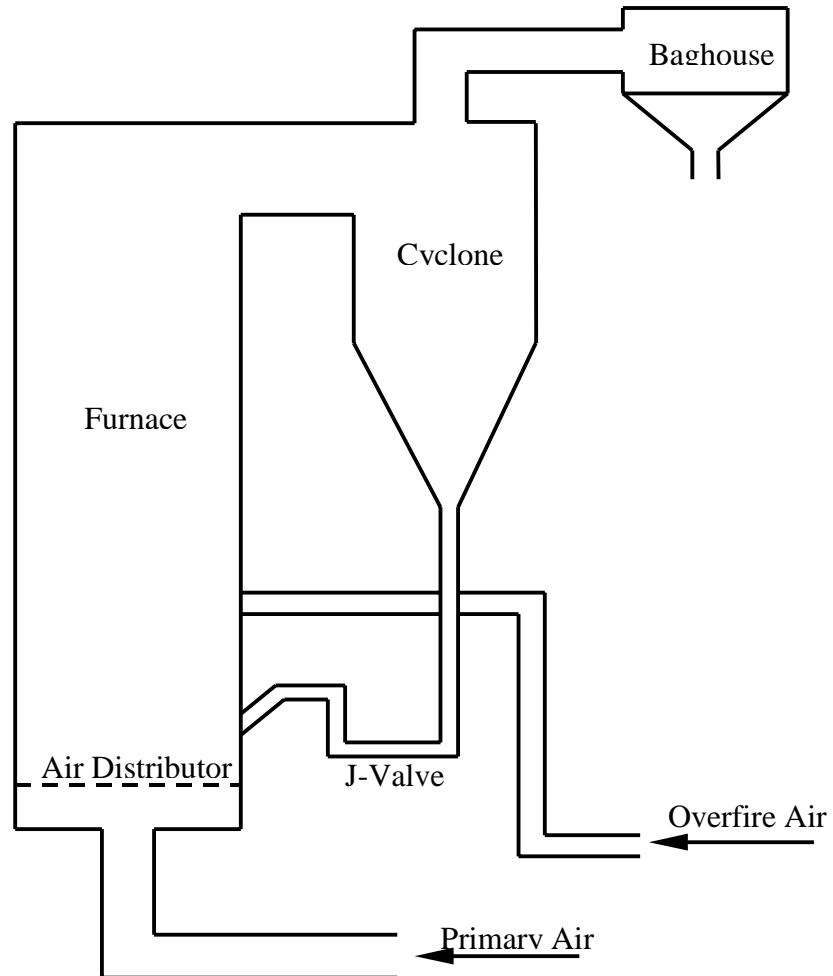


Figure 6. Schematic of cold flow test facility

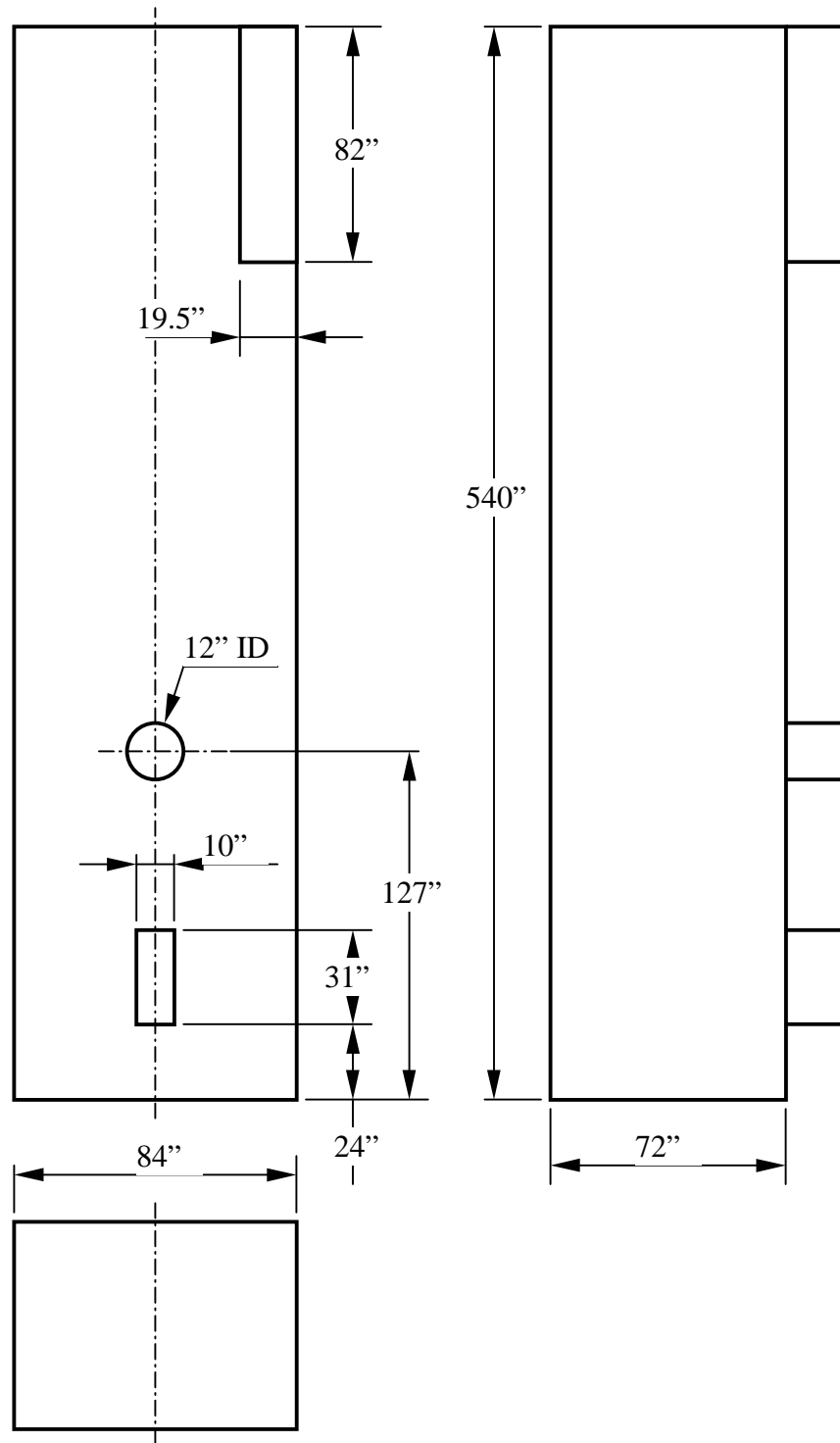


Figure 7. Dimensions of CFB furnace cold flow model

Air for the fluidization is introduced through an air distributor at the bottom of the furnace and, if needed, through the overfire air ports. The bed materials are entrained by the air and separated by the cyclone connected to the furnace exit. Most part of the solid materials return to the bed through a J-valve, while a small part of fine particles escape at the top of the cyclone and are collected by a baghouse. A typical test run without overfire air was selected for MFIX simulation. The operating conditions for the case are listed in Table 2.

Table 2. Operating conditions of the cold model test

	Unit	Operating Condition
Solid Material		Sand
Mean Size (Diameter)	micron	426
Density	kg/m ³	1510
Grid Velocity	ft/s	8.0
Free Board Velocity	ft/s	8.0
Air Temperature	°F	112
Solid Circulation Rate	lb/s	47.8
Operating Pressure	inch H ₂ O	41

MFIX Model Setup

3-D Cartesian coordinate system is used for the simulation. The furnace is meshed uniformly in each direction with 3 cells in z (depth) direction, 10 cells in x (width) direction and 137 cells in y (height) direction as shown in Figure 8. Inlet boundaries include the primary air entrance (air distributor) at the furnace bottom, recirculating particle/air injection surface at the J-valve and the furnace exit plane at the top of the furnace. The rest of the model boundary is furnace wall. Velocity and particle mass flow rate and void fraction are imposed at the inlets. Constant pressure is imposed at the furnace exit. For the cold-state test, the process is isothermal and thus the energy equation is not solved. Gaseous and particle phase reactions are turned off. Only one particle size is used for the simulation. The entire MFIX input file for this simulation can be found in Appendix E.

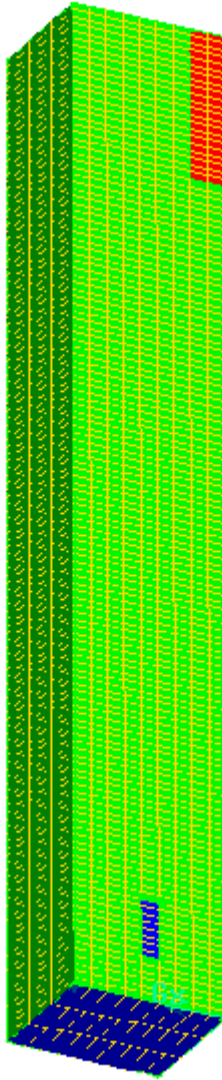


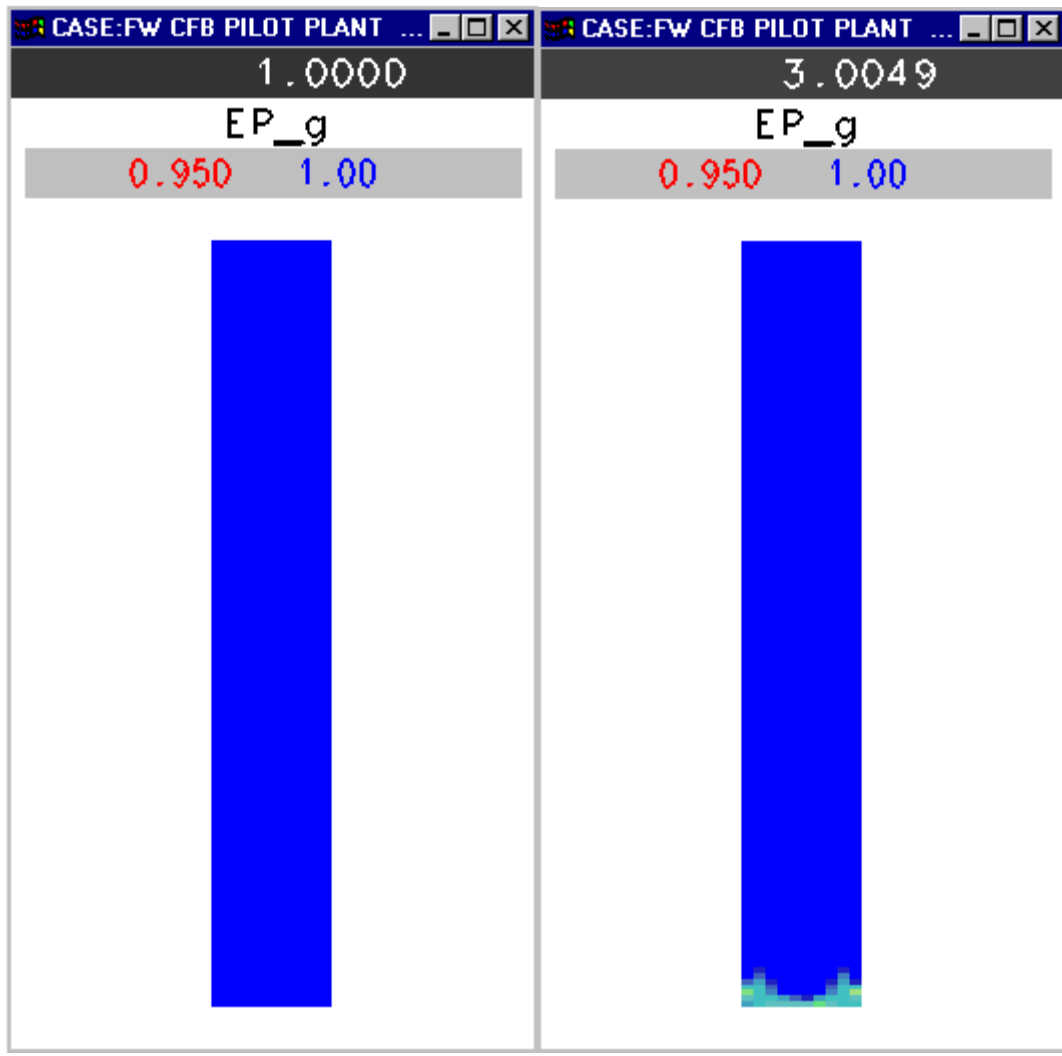
Figure 8. Computational mesh used by MFIX

Simulation Results

The simulation is started at time $t=1$ second. Initially, it is assumed that the bed is empty (void fraction equals to 1) and an upward air velocity is imposed everywhere in the furnace. After the run starts, a constant mass flow rate is imposed at the J-valve. A lower void fraction of 0.5 is set at the J-valve. The injection of solid particles causes the reduction of void fraction. Figure 9 shows the void fraction across a vertical plane half way between the front and rear walls at different moment during the transient simulation. Figure 10 is the corresponding plot of gas pressure and velocity vector. The contour and vector plots are drawn by MFIX animation code on the same color scale. The following trend can be seen from the two figures. At the very beginning ($t=1$ second), the void fraction is 1.0 everywhere in the furnace and the gas velocity and pressure are uniformly distributed in the furnace. At $t=3$ second, the solid particles start to

build up at the bottom of the furnace and so does the gas pressure. At $t=5$ second, more solid particles are accumulated above the distributor and gas flows at different directions near the air distributor due to the gas/solid interaction. At $t=10$ second, about one quarter of the furnace height is filled with solid particles. Around $t=20$ second, half of the furnace contains particles. At $t=50$ second, the particles buildup extends to the entire furnace. Later, the flow pattern reaches pseudo-steady state with a constant average void fraction in the furnace. The flow directions as shown in the velocity vector plots become more “random” in the entire reactor. The gas pressure at the bottom of the reactor is about 0.03 atm higher than that at the reactor exit, which is mainly caused by the particle weight inside the reactor.

A comparison between the MFIX simulation and actual test measurements is not possible since no comparable test was performed with a single particle size (426 micron). It is generally observed, however, that the MFIX pressure profile is far more linear with bed height than the test measurements, which exhibit a small decrease in pressure in a large freeboard and transport disengaging height (TDH) zone and a sharp decrease in a small dense bed region. Thus, in general, the MFIX predicts a far larger dense bed region than was shown in the cold model test. It is possible that a run simulating a longer span of time, especially with increased grid resolution at the walls to model particle reflex, may develop the trends toward those seen in the cold model tests.



(a)

(b)



Figure 9. Void fraction at different times

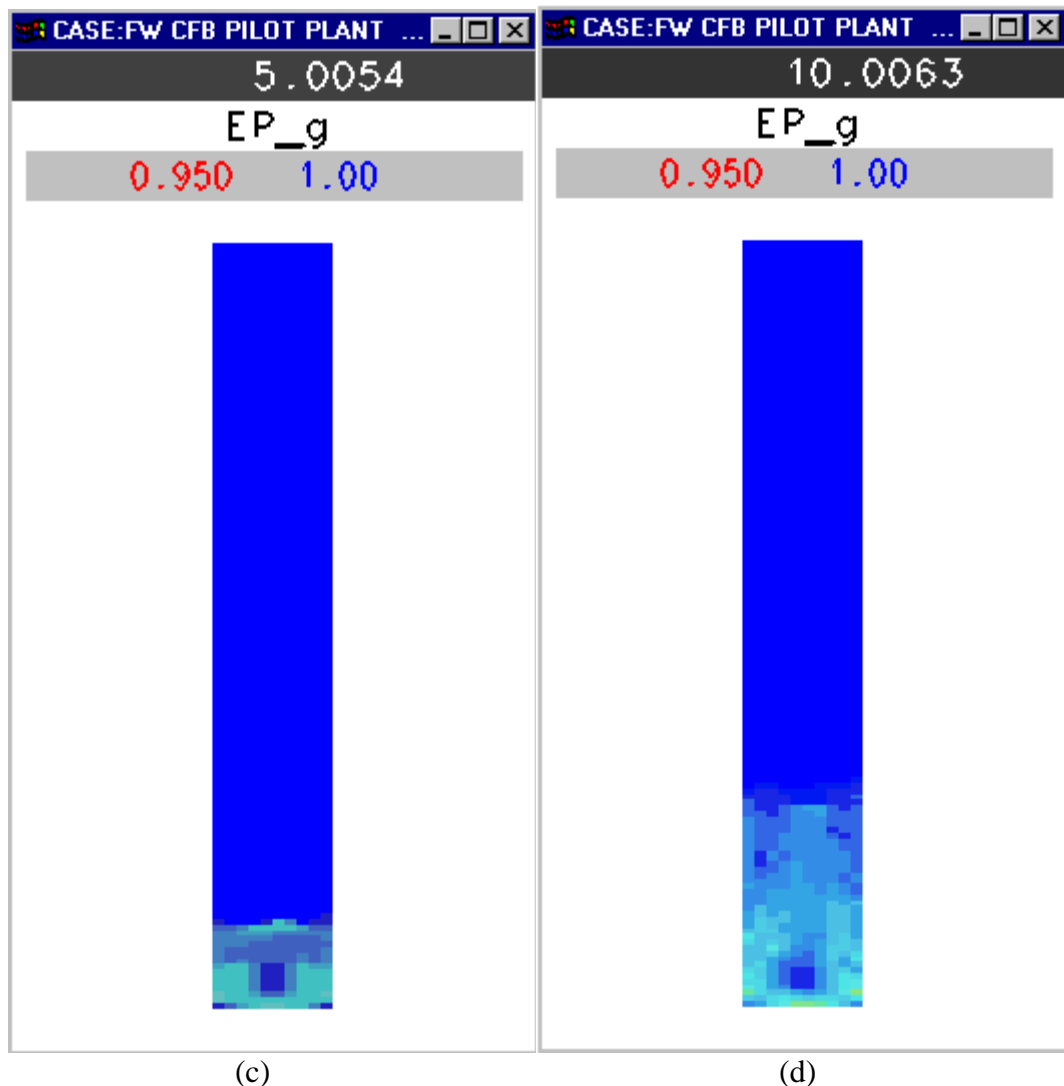


Figure 9. Void fraction at different times
(continued)

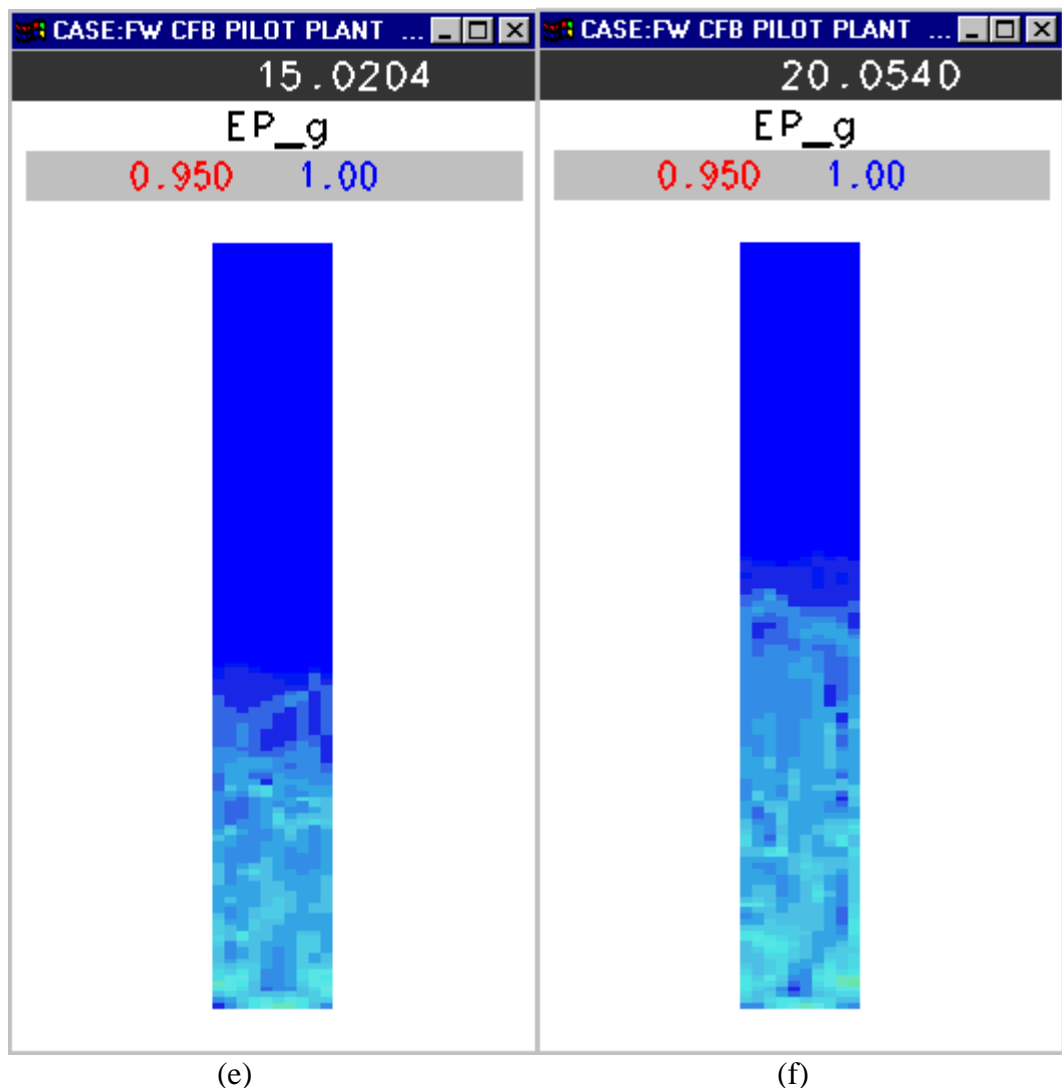


Figure 9. Void fraction at different times
(continued)

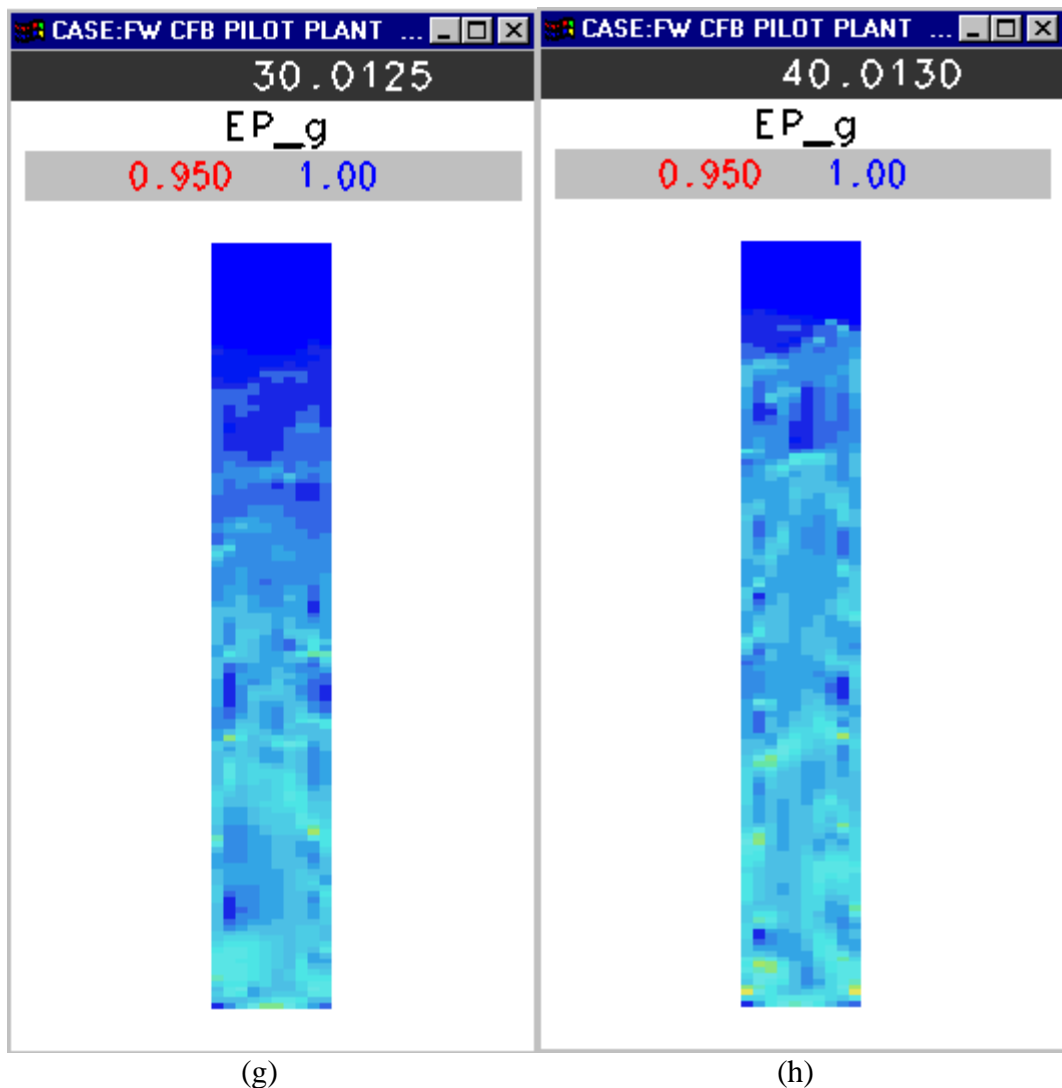


Figure 9. Void fraction at different times
(continued)

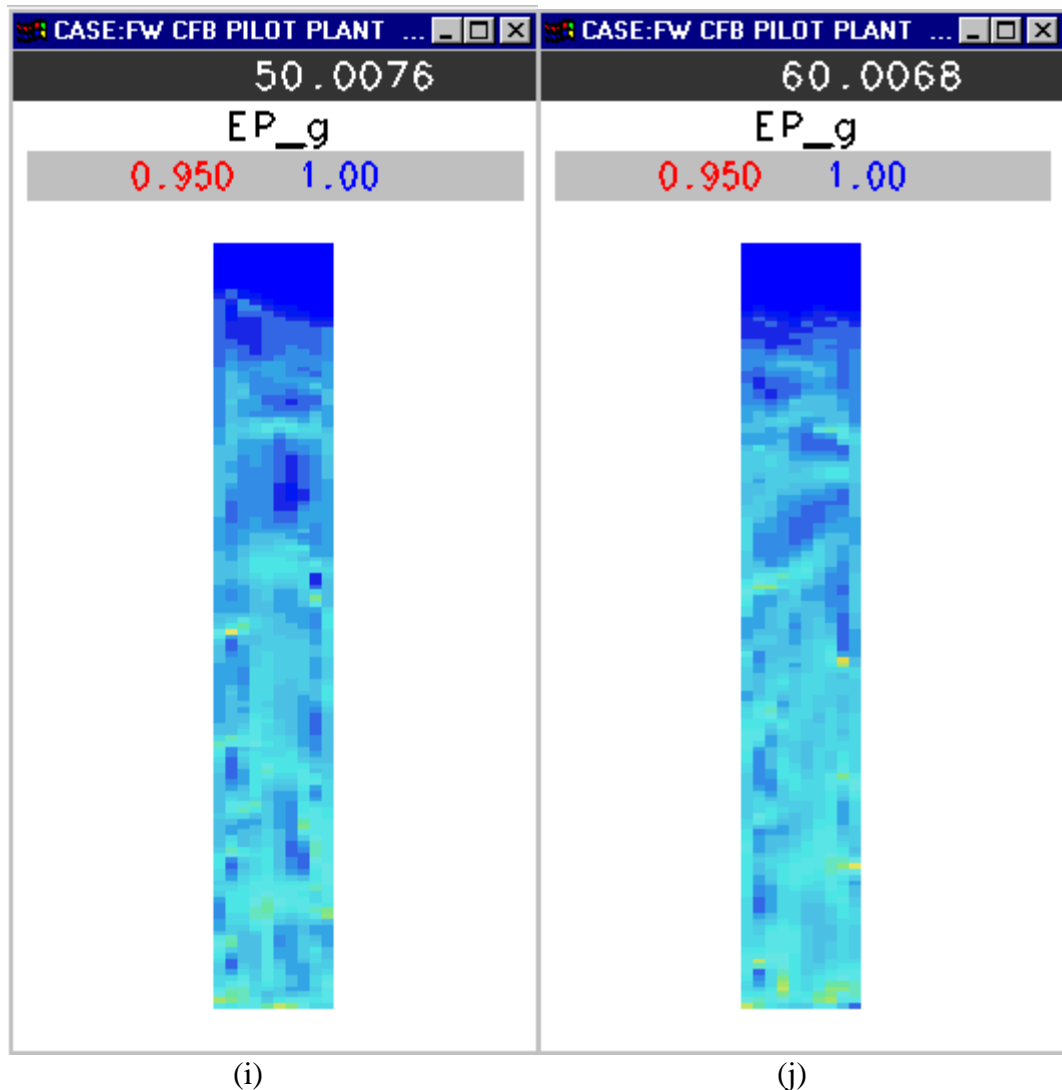


Figure 9. Void fraction at different times
(continued)

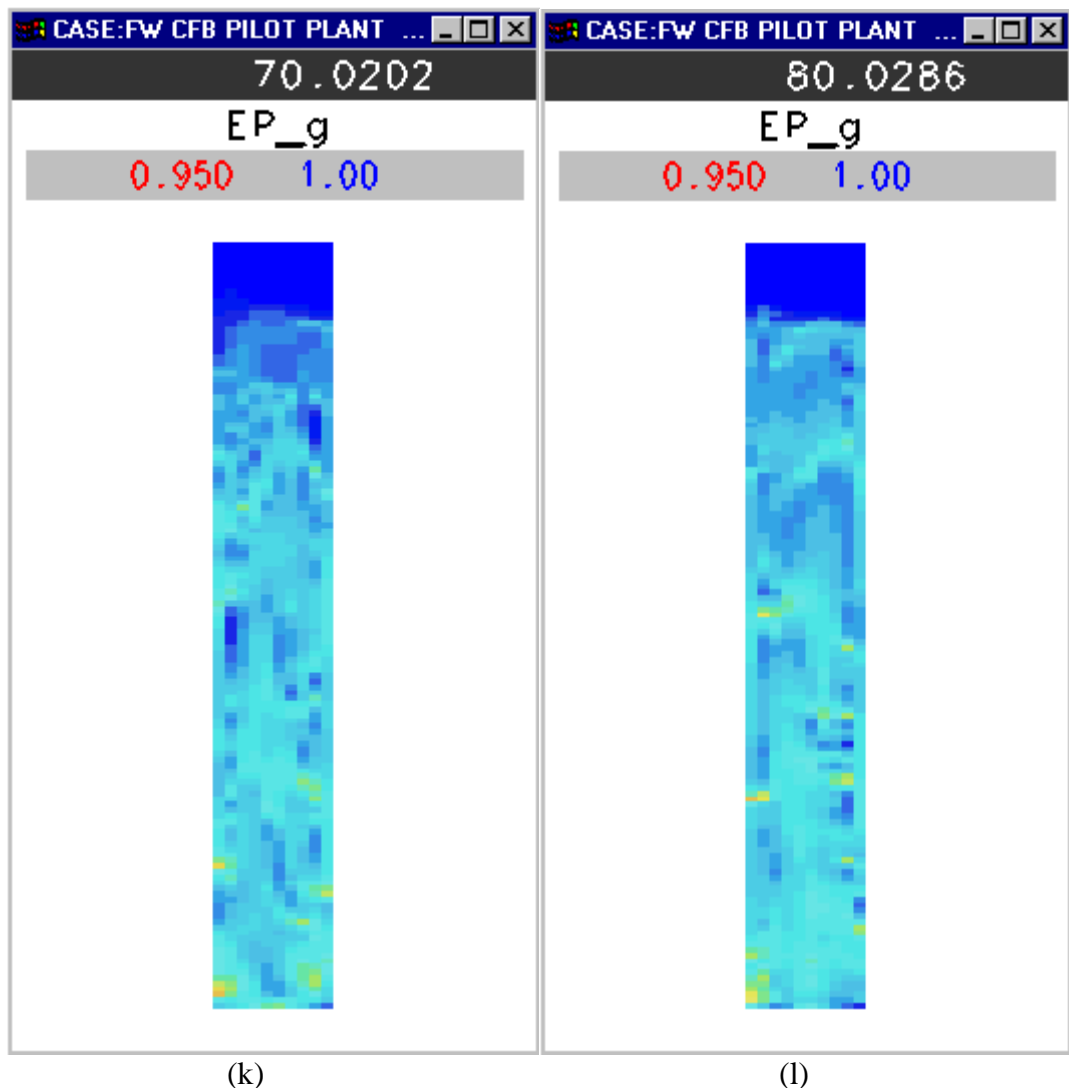


Figure 9. Void fraction at different times
(continued)

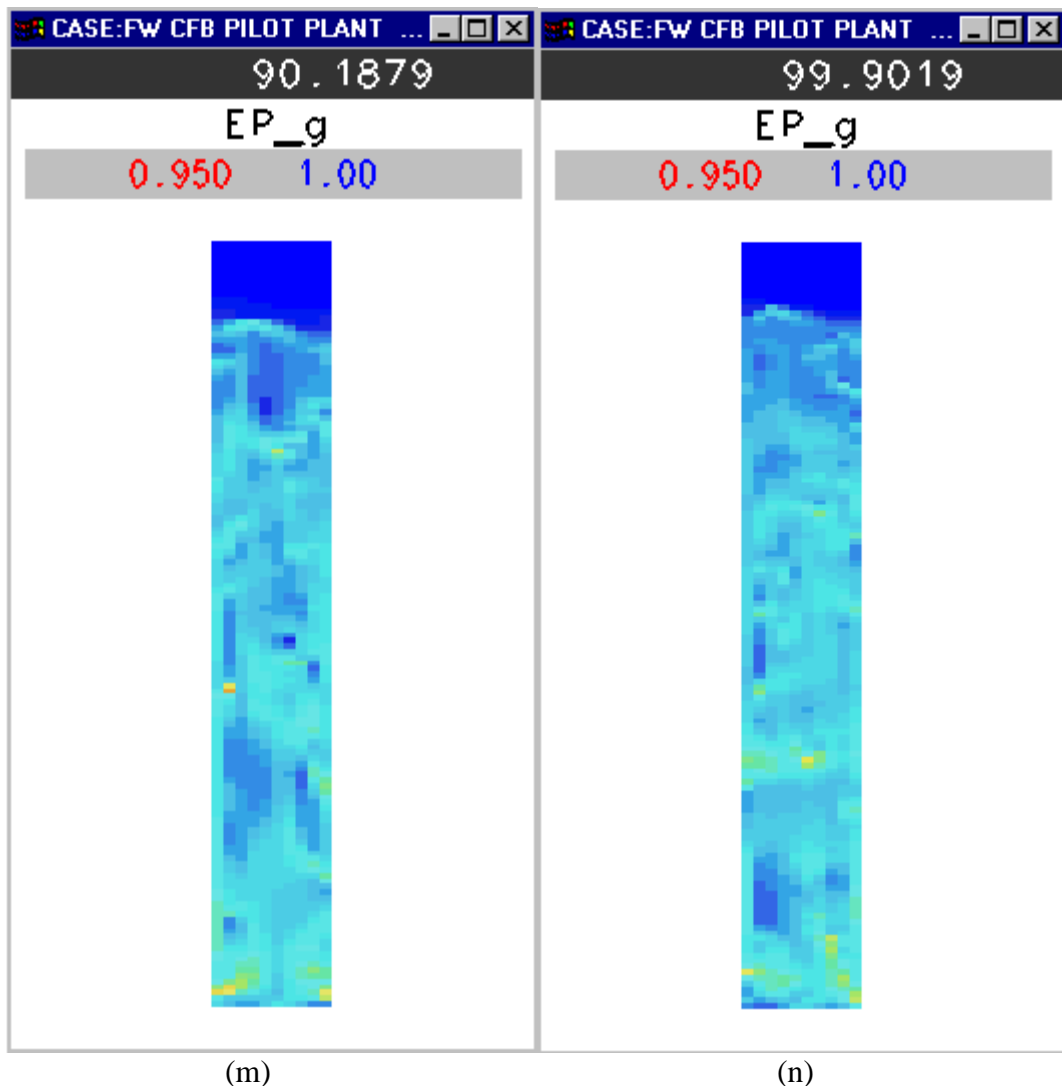
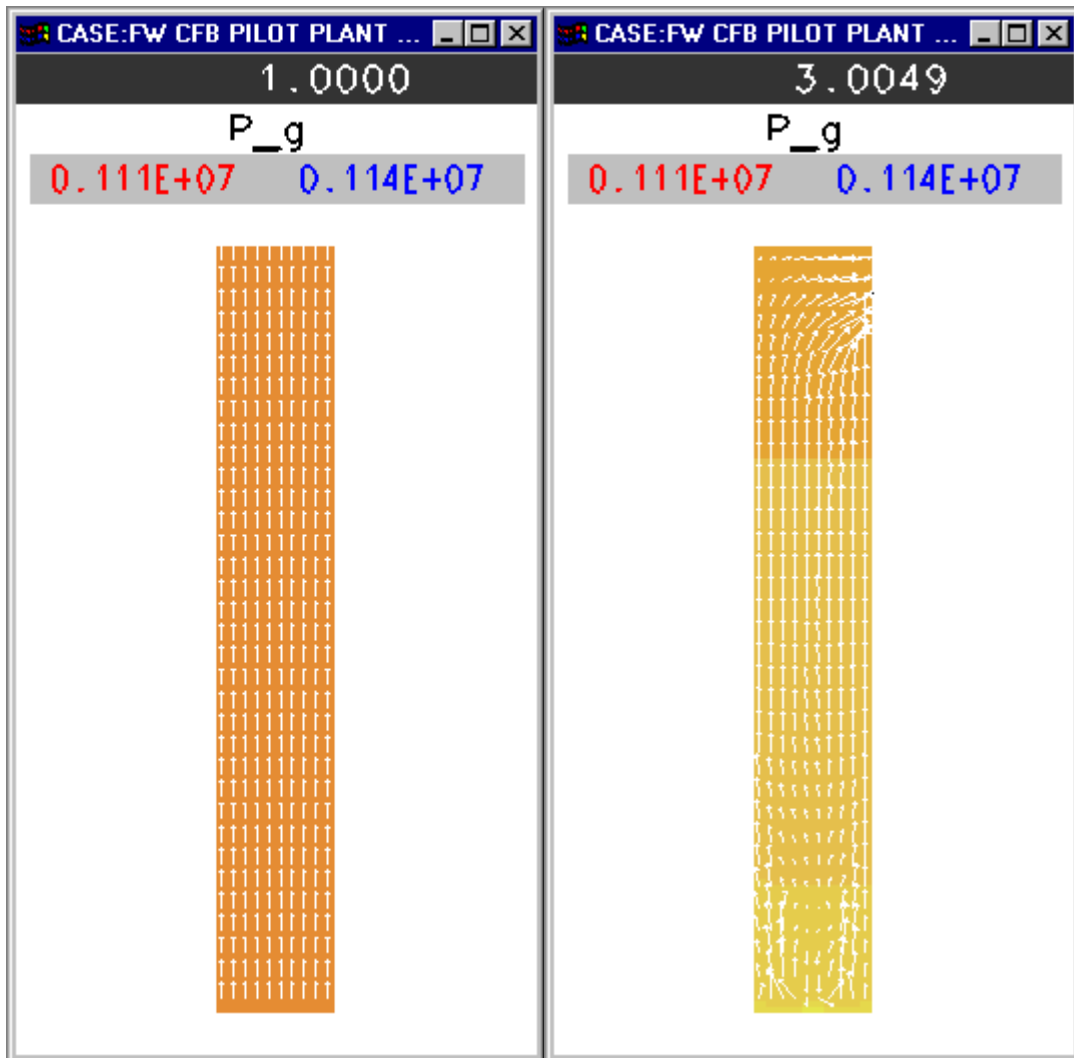


Figure 9. Void fraction at different times
(continued)



(a)

(b)

 0.111×10^7 0.114×10^7 Pressure Color Scale [gr/(cm-sec²)]**Figure 10. Gas pressure and velocity vector**

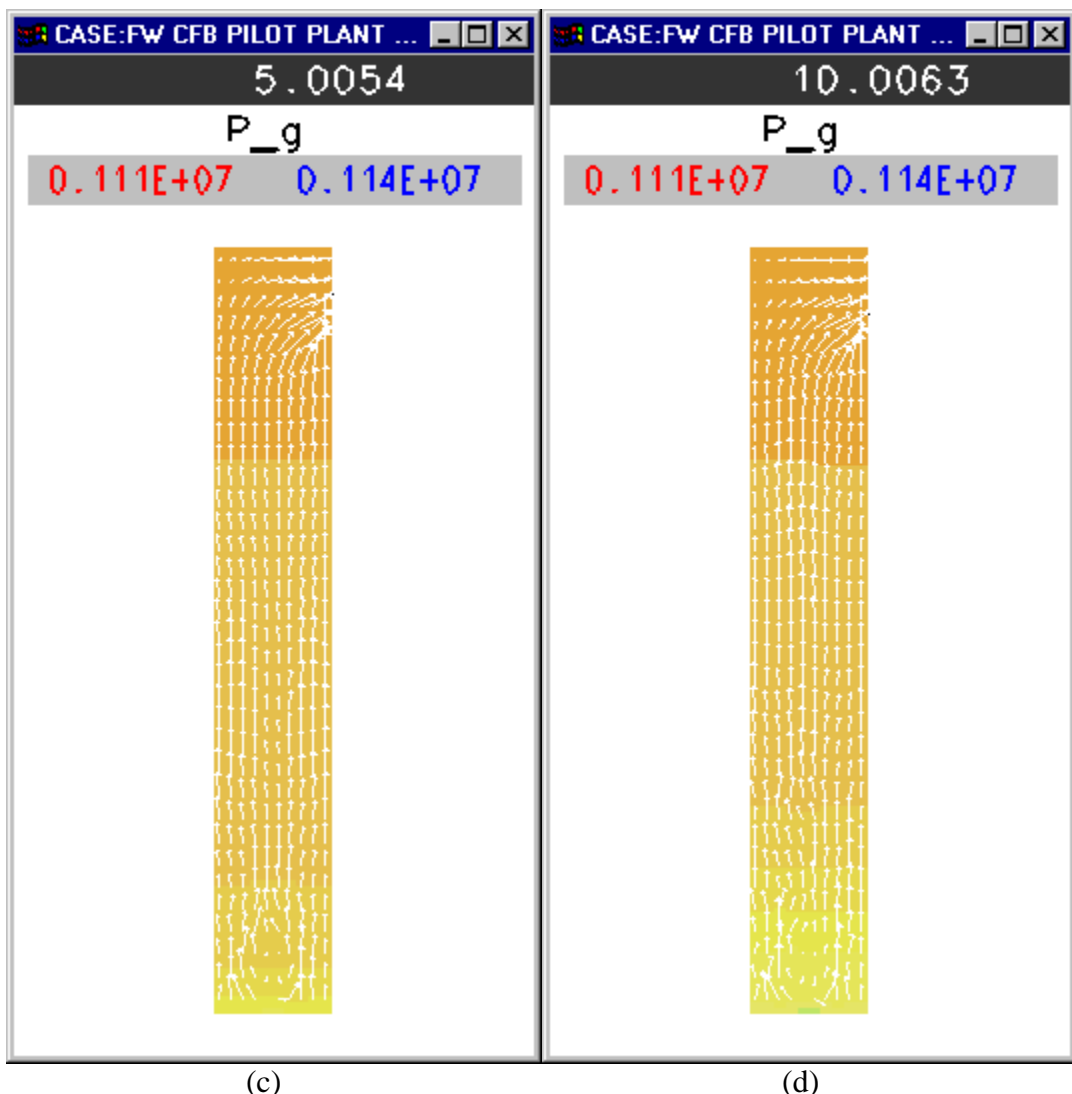


Figure 10. Gas pressure and velocity vector
(continued)

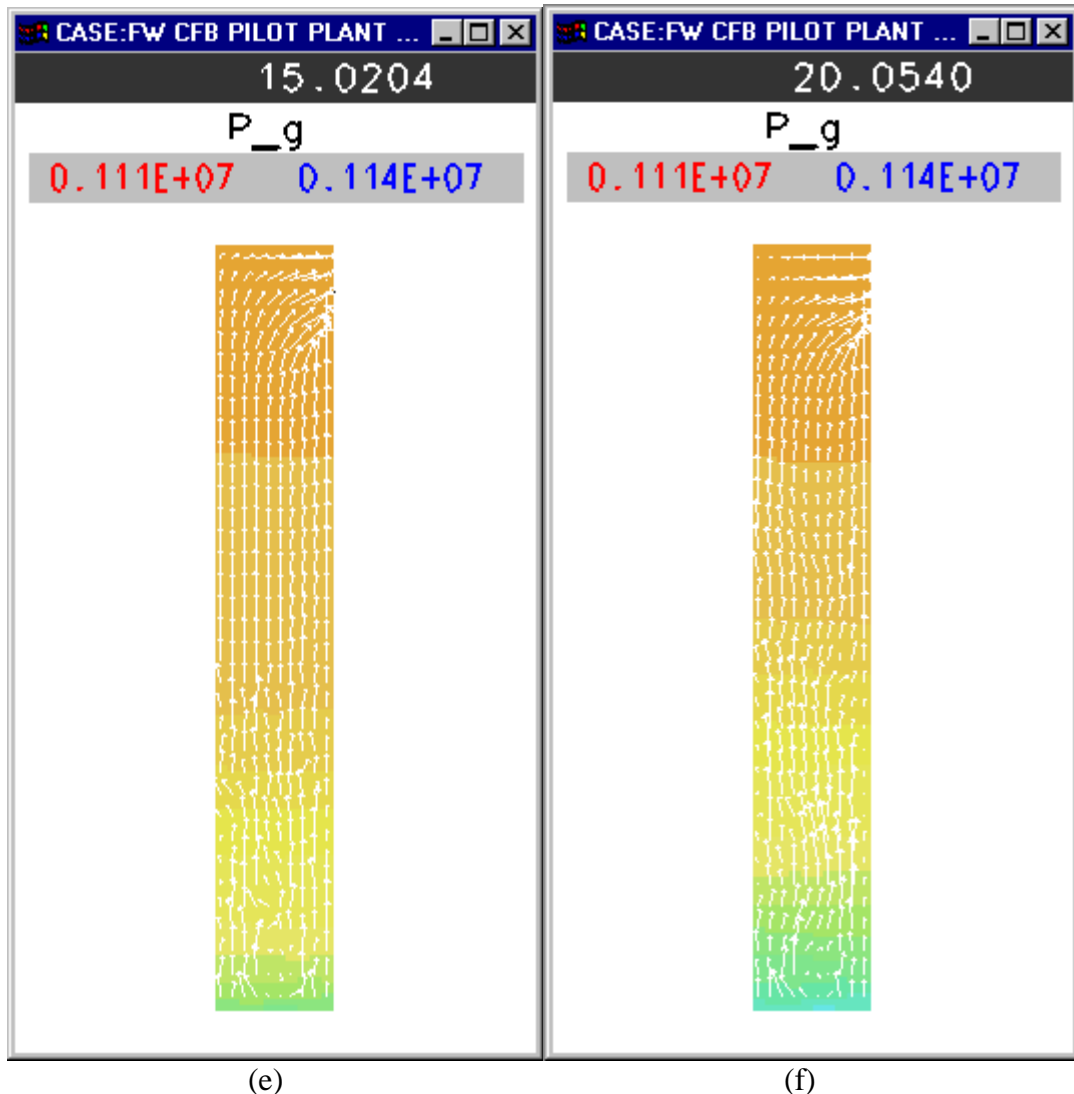


Figure 10. Gas pressure and velocity vector
(continued)

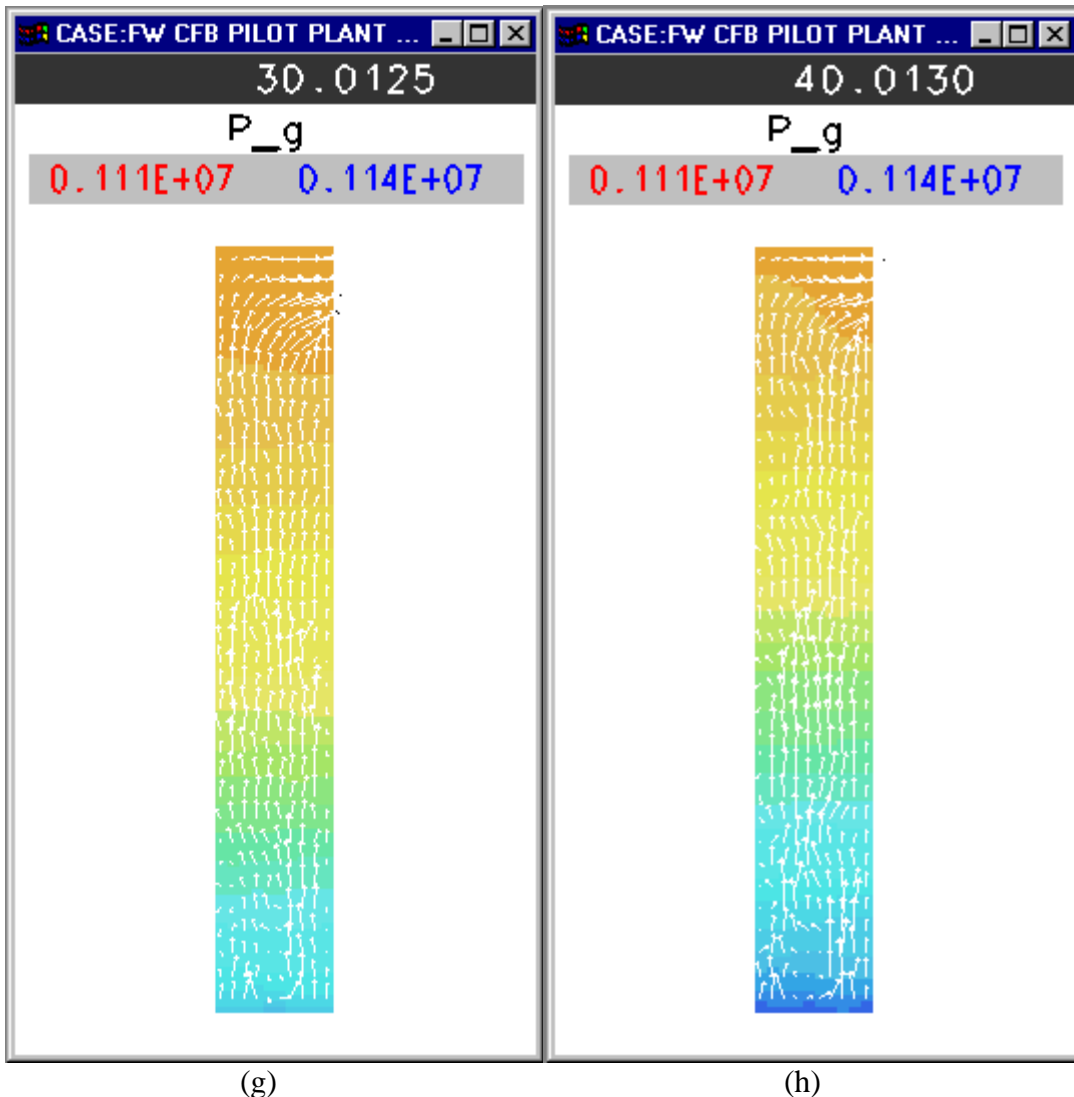


Figure 10. Gas pressure and velocity vector
(continued)

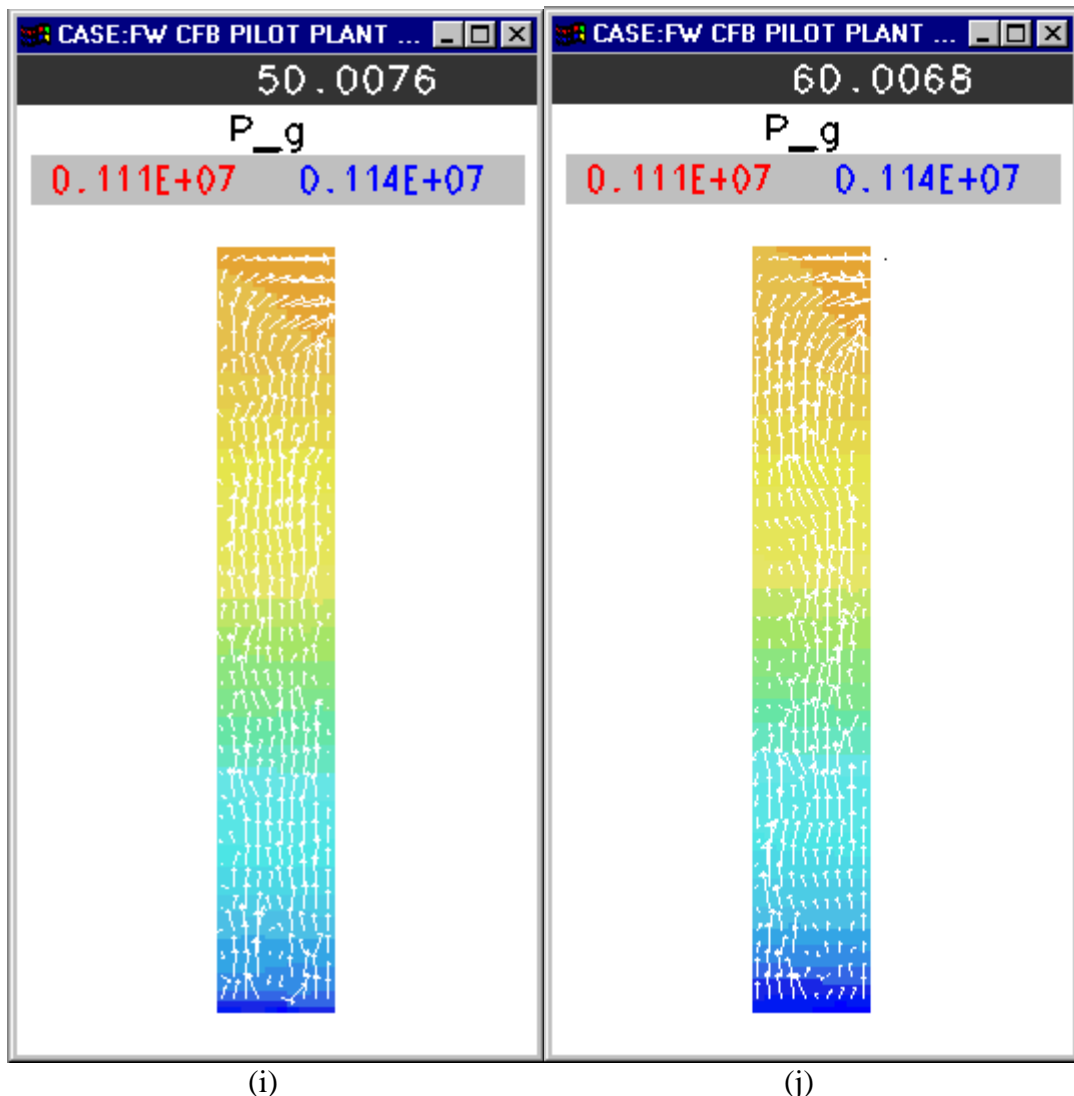
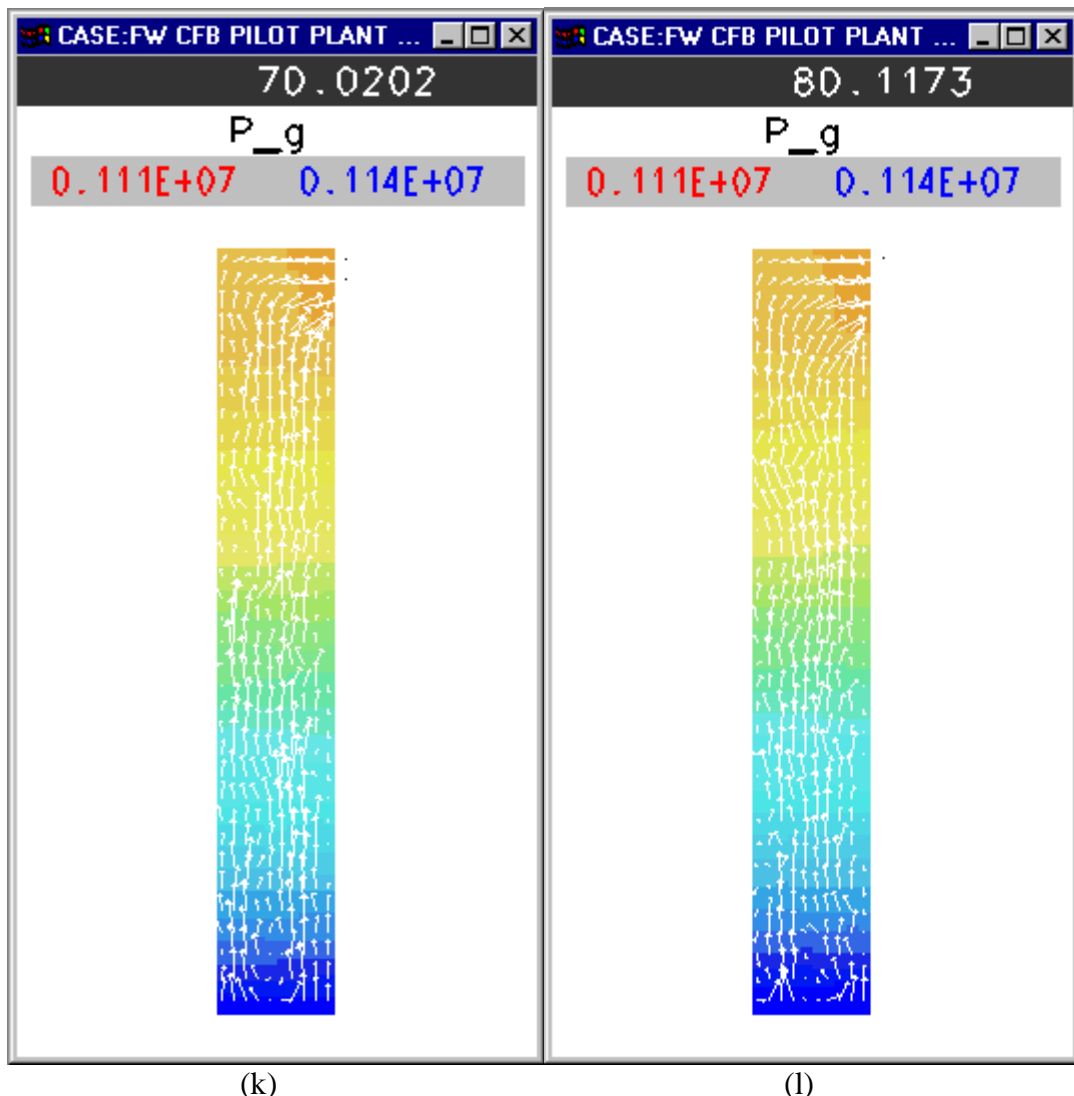


Figure 10. Gas pressure and velocity vector
(continued)



(k)

(l)

Figure 10. Gas pressure and velocity vector
(continued)

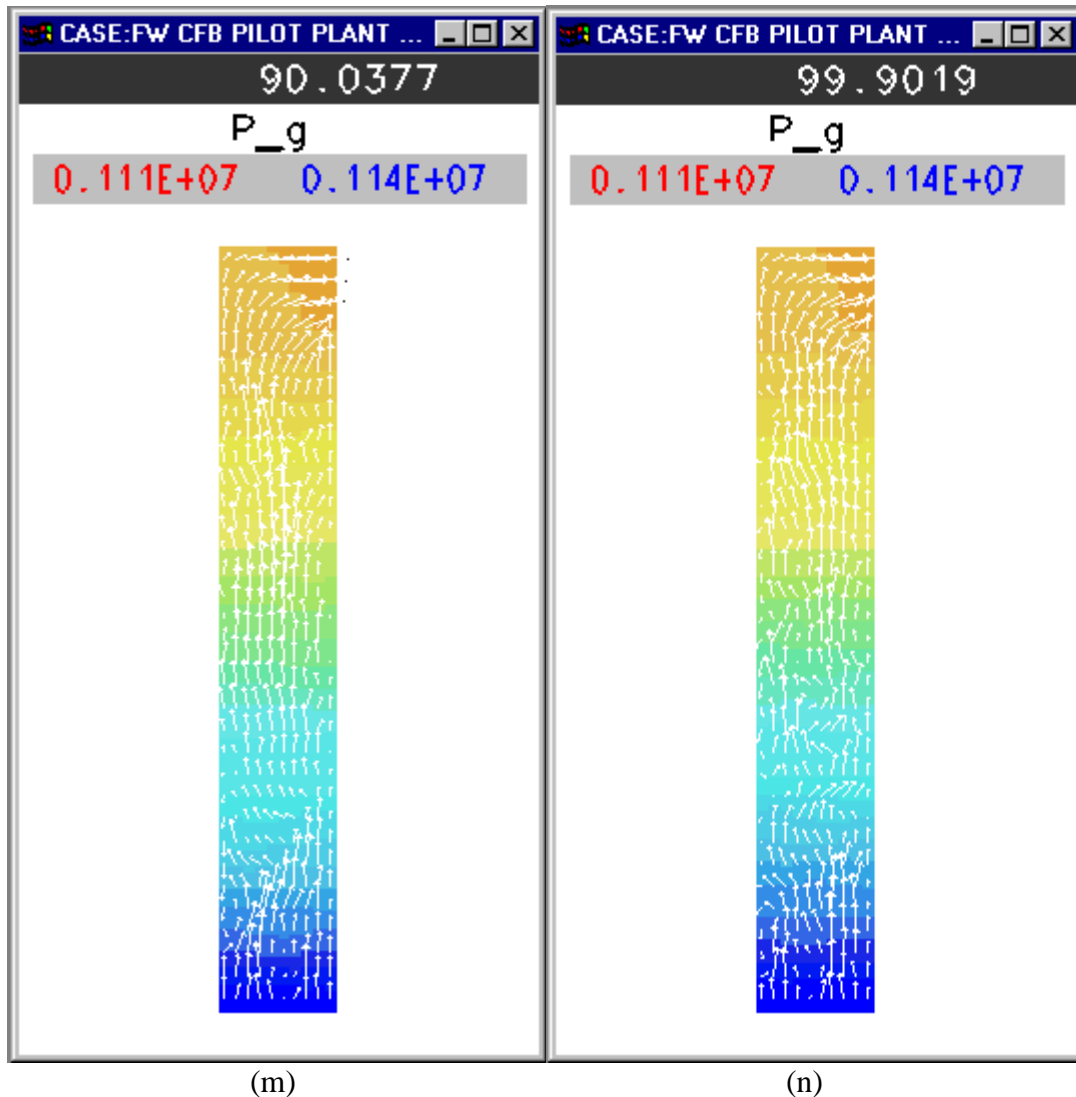


Figure 10. Gas pressure and velocity vector
(continued)

Task 2 – Parametric MFIX Code Investigations

Bubble Shape Investigation

MFIX simulations of bubbling-fluidized beds simulations show the formation and propagation of high void-fraction regions, called bubbles. Bubble characteristics such as the rise velocity, wake angle, void fraction distribution, and pressure distribution have been compared with experimental data (e.g. Gidaspow 1994, Syamlal and O'Brien 1989). It has been shown that the simulations qualitatively predict experimentally observed solids movement in the bubble wake and *slow* and *fast* bubbles (Syamlal and O'Brien 1989).

The predicted bubble shapes, observed from contour plots of void fraction, differ from experimental observations in one peculiar manner: the nose of the calculated bubble is pointed unlike the rounded shape of experimental bubbles. This problem appears in the simulation results published by various authors using different computational techniques (Gidaspow 1994, Syamlal and O'Brien 1989, Kuipers et. al. 1992, Boemer et.al. 1995, Sanyal et. al. 1994). To get physically realistic predictions, researchers have attempted to modify the theory. During the performance period of this CRADA, it was shown that the pointed bubble shape is a numerical artifact resulting from the usage of first order accurate discretization schemes and coarse grids. By using second-order accurate discretization schemes it is possible to predict a rounded bubble shape. This is clear from Figure 11, which compares the predictions of a second-order scheme (superbee) and first order upwind scheme (FOU). The bubble shape observed in an experiment, with operating conditions similar to that of the simulation, is shown in Figure 12. An MFIX input file predicting bubble formation can be found in Appendix F. Details about this second order discretization approach can be found in Syamlal (1997) and Guenther and Syamlal (2000).

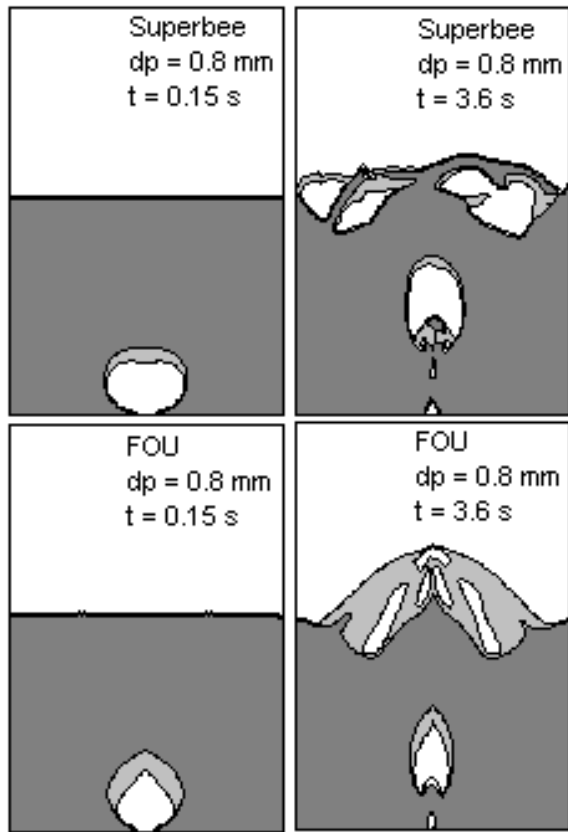


Figure 11. Void fraction contours for two discretization schemes at two instances (white - $\epsilon > 0.9$; light gray - $0.7 < \epsilon < 0.9$; dark gray - $\epsilon < 0.7$)

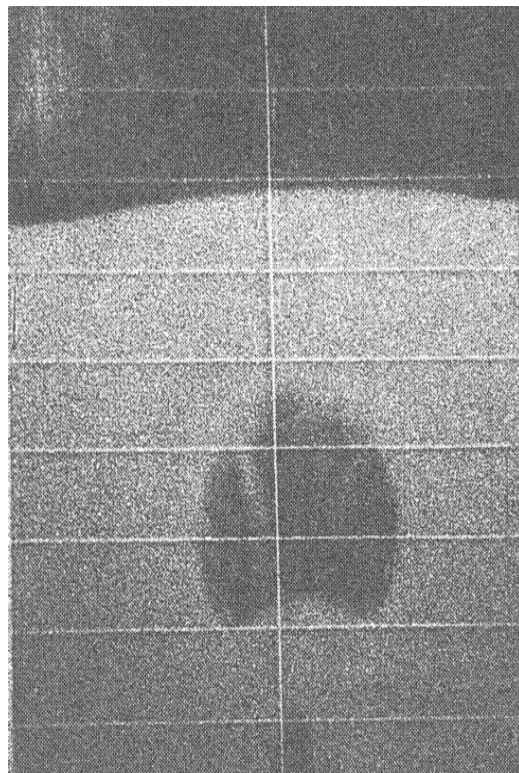


Figure 12. Photograph of a fluidized bed with a bubble (Gidaspow, 1994)

Task 2 – Parametric MFIX Code Investigations

Spouted Bed Hydrodynamics

During the performance of the previous CRADA with FWDC, Foster Wheeler had identified the simulation of spouted bed as a means for validating MFIX hydrodynamics and selected a set of experiments conducted by Professor John Grace's group at University of British Columbia (He et al. 1994 a, b). The version of MFIX available during the previous CRADA was unable to predict the spout formation. Last summer we revisited the problem and conducted simulations with the current version of MFIX. The MFIX input file used for this investigation is included in Appendix G. Table 3 includes the important bed characteristics used in the MFIX simulations.

Table 3. Spouted Bed Characteristics Used

Bed Material	Glass Beads
Bed density	2,503 kg/m ³
Particle Diameter	1.41 mm
Bed Dimensions	0.152m dia. X 1.4 m Height
Inlet Orifice Diameter	1.9 cm
Jet Velocity	38, 41, 45 m/s
Bed Height	0.325 m
Grid Resolution	49 x 362 cells
U _{mf} (. U _{ms})	0.54 m/s

As can be seen in Table 4, the qualitative features of the spouted bed were captured very well in the simulation demonstrating such features as a spout, an annulus, and a fountain. See Figure 13.

Table 4. Comparison of MFIX Predictions with Experimental Results

Fountain height (m) at U/U _{ms}	1.1	1.2	1.3
MFIX	0.13	0.18	0.23
Experiment	0.15	0.23	0.37

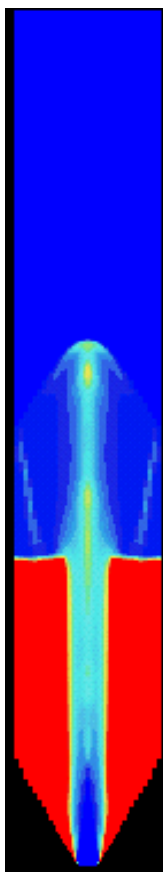


Figure 13. MFIX Simulation of Spouted Bed

The following figures show comparisons between experimental data and simulation results for the largest jet velocity (45 m/s or $U/U_s = 1.3$). The calculated particle velocity at the center of the spout is compared with experimental data in Figure 14.

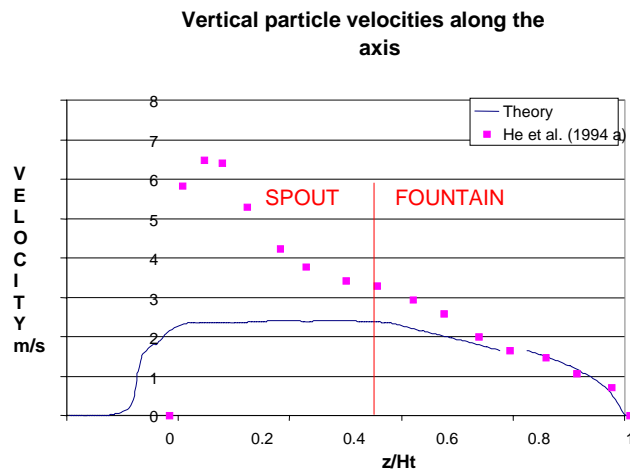


Figure 14. Comparison of Particulate Velocities Along Vertical Axis

The agreement is good in the fountain region (above the bed) and poor in the entrance region. The cause for this discrepancy is under investigation. From discussions with Prof. Grace it was realized that a lip near the jet entrance was not included in the simulations.

Calculated and experimental radial velocities in the spout are compared in Figure 15, which again shows considerable deviation from experiment in the entrance region.

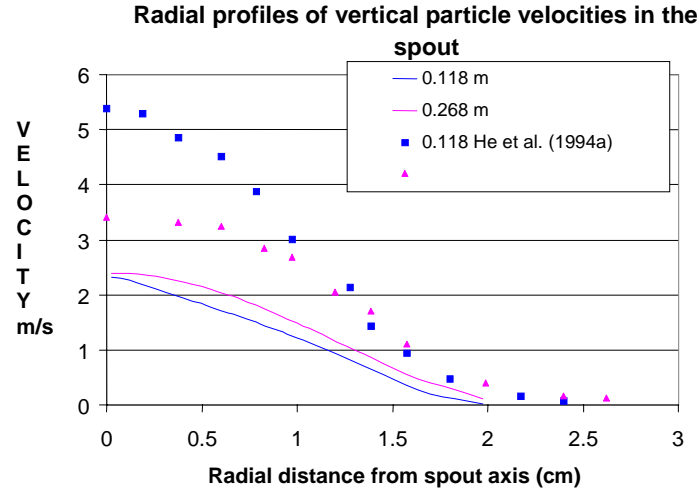


Figure 15. Calculated and Measured Radial Velocity Profiles

Figure 16 shows the radial profiles of void fraction in the spout. The agreement between data and simulation results is reasonable.

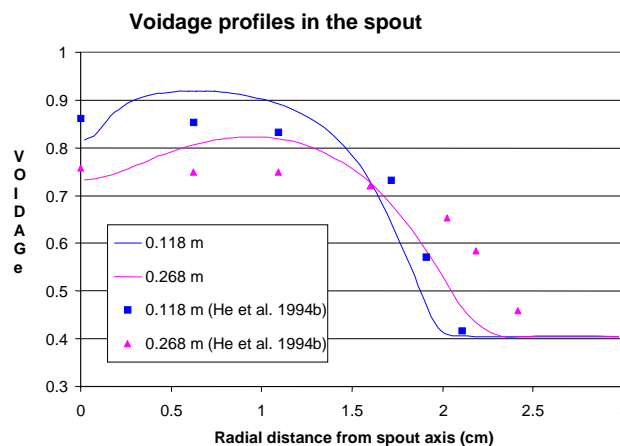


Figure 16. Comparison of Voidage Profiles

Figure 17 compares the calculated and experimental particle velocity in the (dense) annular region. The agreement is not good. It is possible that agreement may be improved, however, with a better frictional flow model.

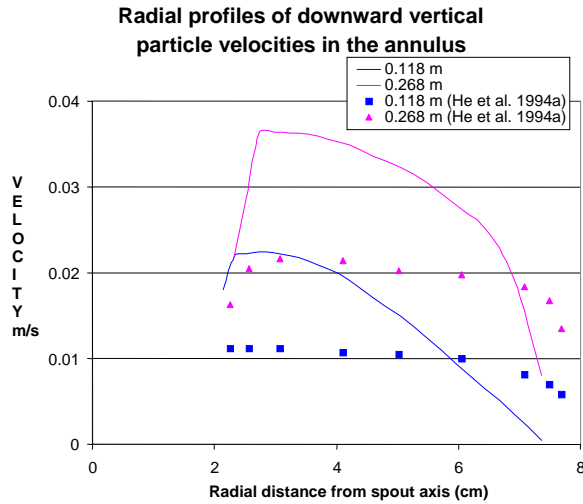


Figure 17. Comparison of Annular Velocity Profiles

Figure 18 compares the calculated and experimental radial particle velocities in the fountain region. The data and simulation results agree reasonably well in this case. This simulation study is ongoing, and final results will be published in the open literature.

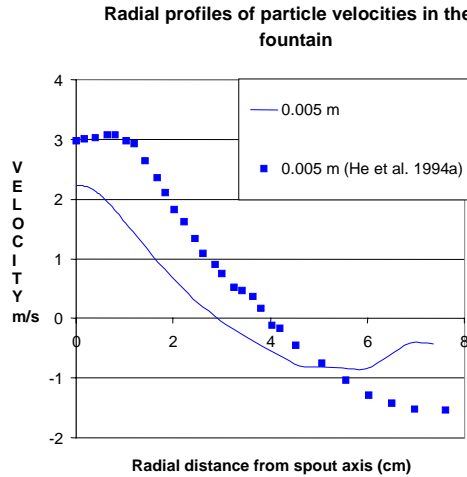


Figure 18. Comparison of Velocity Profiles Within the Fountain Region

Task 2 – Parametric MFIX Code Investigations

Coal Chemistry Schemes

Foster Wheeler and NETL personnel compared the coal chemistry schemes used in MFIX and Foster Wheeler's version of PCGC-3. A brief description of the two chemistry schemes is given below.

MFIX Model of Coal Chemistry

The MFIX model of coal chemistry is shown in Figure 19. This is a modified version of the reaction scheme in MGAS (Syamlal and Bissett 1992) and is based on gasification kinetic equations proposed by Wen et al. (1982). The solids phase consists of coal and sorbent. Coal contains the four pseudo-species: Ash, Moisture, Volatile Matter, and Fixed Carbon. Ash does not take part in any reactions. Moisture is released in an initial stage reaction, drying.

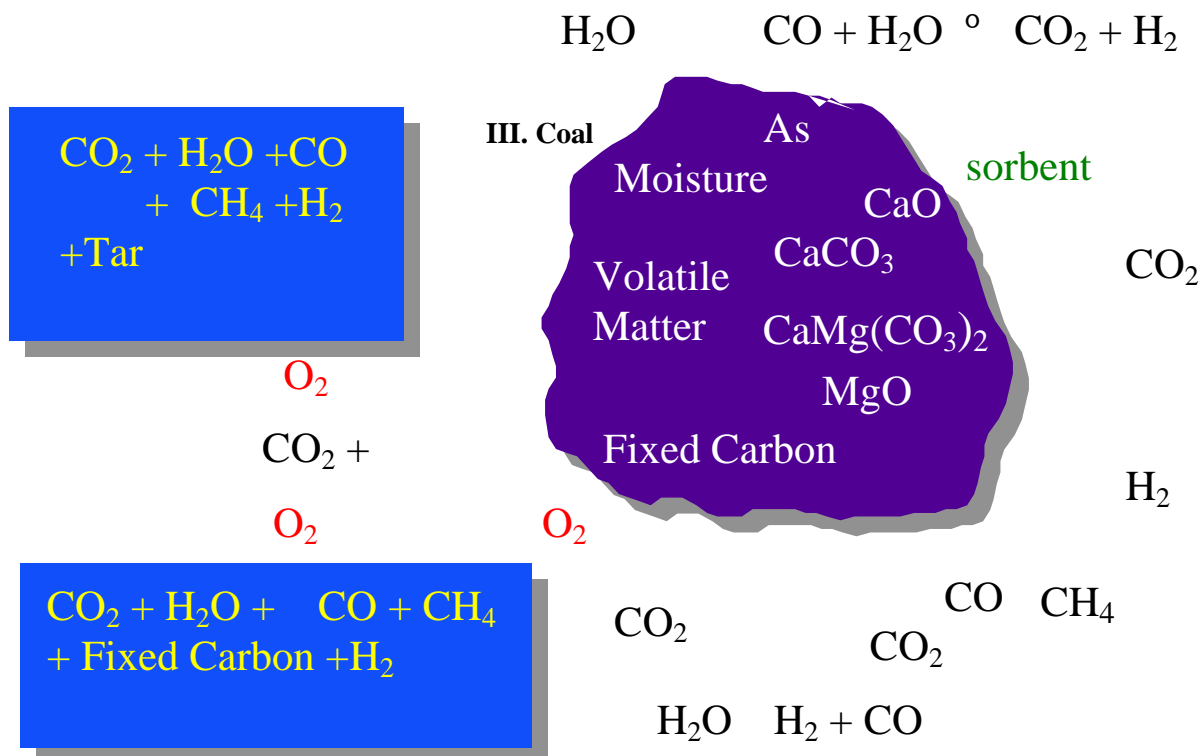


Figure 19. Chemical reactions in a gasifier

Volatile Matter produces several gas-phase species through devolatilization. Fixed Carbon takes part in combustion and in $(\text{H}_2\text{O}, \text{CO}_2, \text{CH}_4)$ gasification reactions. The sorbent undergoes thermal decomposition to produce CO_2 . The gas-phase reactions are tar decomposition, CO , CH_4 and H_2 combustion, and water-gas shift reaction.

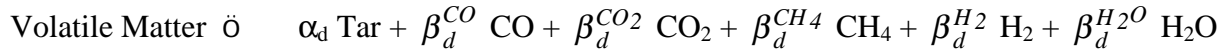
The rate expressions for the various reactions are given below.

1. Initial Stage Reactions

1.1 Drying: Moisture (coal) → H₂O (Syamlal and Bissett 1992)

$$Rate = 1.1 \cdot 10^5 \exp\left(\frac{-21200}{RT_s}\right) \varepsilon_s \rho_s X_{s3} \text{ (g/cm}^3 \cdot \text{s}),$$

1.2 Devolatilization: (Syamlal and Bissett 1992)



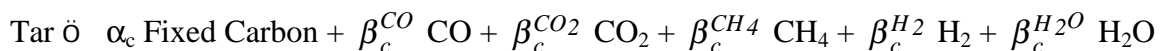
$$Rate = \begin{cases} 1.1 \cdot 10^5 \exp\left(\frac{-21200}{RT_s}\right) \varepsilon_s \rho_s (X_{s2} - X^*) & X_{s2} \geq X^* \\ 0 & X_{s2} < X^* \end{cases} \text{ (g/cm}^3 \cdot \text{s})$$

$$X^* = (X_{s1}^0 + X_{s2}^0) X_0^* ,$$

and

$$X_0^* = \begin{cases} \frac{\left(\frac{867.2}{(T_s - 273)}\right)^{3.914}}{100} & T_s < 1223 \\ 0 & T_s \geq 1223 \end{cases} .$$

1.3 Tar-cracking: (Syamlal and Bissett 1992)



$$Rate = 2.5 \cdot 10^7 \exp\left(\frac{-29000}{RT_g}\right) \varepsilon_g \rho_g X_{g8} \text{ (g/cm}^3 \cdot \text{s})$$

The stoichiometric coefficients (α 's and β 's) in the above reaction scheme are determined by assuming certain phenomenological rules as discussed in the MGAS manual (Syamlal and Bissett 1992).

2. Gasification Reactions

2.1 Steam gasification: $C + H_2O \rightarrow CO + H_2$. (Wen et al. 1982)

$$Rate = 930 \exp\left(\frac{-45000}{RT_g}\right) \left(\frac{\varepsilon_s \rho_s X_{s1}}{12}\right) p_{H2O} - p_{H2O}^* \quad (mol/cm^3 \cdot s),$$

where

$$p_{H2O}^* = \frac{p_{H2} p_{CO}}{\exp(17.29 - 16326/T_g)}.$$

2.2 CO₂ gasification: $C + CO_2 \rightarrow 2CO$. (Wen et al. 1982)

$$Rate = 930 \exp\left(\frac{-45000}{RT_g}\right) \left(\frac{\varepsilon_s \rho_s X_{s1}}{12}\right) p_{CO2} - p_{CO2}^* \quad (mol/cm^3 \cdot s),$$

where

$$p_{CO2}^* = \frac{p_{CO}^2}{\exp(20.92 - 20282/T_g)}.$$

2.3 Methanation: $\frac{1}{2}C + H_2 \rightarrow \frac{1}{2}CH_4$. (Wen et al. 1982)

$$Rate = \exp(-7.087 - 8078/T_g) \left(\frac{\varepsilon_s \rho_s X_{s1}}{12}\right) p_{H2} - p_{H2}^* \quad (mol/cm^3 \cdot s),$$

where

$$p_{H2}^* = \sqrt{\frac{p_{CH4}}{\exp(-13.43 + 10999/T_g)}}.$$

3 Combustion Reactions

3.1 Carbon combustion: $2C + O_2 \rightarrow 2CO$.

$$Rate = \frac{-6 \varepsilon_s p_{O_2}}{d_p \left(\frac{1}{k_f} + \frac{1}{k_a} + \frac{1}{k_r} \right)} \text{ (mol/cm}^3 \cdot \text{s)}$$

where the film resistance is given by

$$k_f = \frac{D_{O_2} Sh}{d_p R_{O_2} T_f}$$

The Sherwood number is given by (Gunn 1978)

$$Sh = (7 - 10 \varepsilon_g + 5 \varepsilon_g^2) (1 + 0.7 Re^{0.2} Sc^{1/3}) + (1.33 - 2.4 \varepsilon_g + 1.2 \varepsilon_g^2) Re^{0.7} Sc^{1/3} .$$

The ash layer resistance is given by

$$k_a = \frac{2 r_d D_e}{(1 - r_d) d_p R_{O_2} T_s}$$

and the ratio of core diameter to particle diameter is

$$r_d = \left(\frac{X_{s4}^0 - X_{s1}}{X_{s1}^0 - X_{s4}} \right)^{\frac{1}{3}}$$

$$k_r = 8710 \exp \left(- \frac{27000}{1.987 T_s} \right) r_d^2$$

The surface reaction rate is given by (Desai and Wen 1978)

3.2 CO combustion: $CO + \frac{1}{2} O_2 \rightarrow CO_2$ (Westbrook and Dryer 1981)

$$Rate = 3.98 \cdot 10^{14} \exp\left(\frac{-40000}{RT_g}\right) \varepsilon_g \left(\frac{\rho_g X_{g1}}{Mw_1}\right)^{0.25} \left(\frac{\rho_g X_{g2}}{Mw_2}\right) \\ \left(\frac{\rho_g X_{g6}}{Mw_6}\right)^{0.5} \text{ (mol/cm}^3\text{.s)}$$

3.3 CH₄ combustion: CH₄ + 2O₂ → CO₂ + 2H₂O (Westbrook and Dryer 1981)

$$Rate = 6.7 \cdot 10^{12} \exp\left(\frac{-48400}{RT_g}\right) \varepsilon_g \left(\frac{\rho_g X_{g1}}{Mw_1}\right)^{1.3} \left(\frac{\rho_g X_{g4}}{Mw_4}\right)^{0.2} \text{ (mol/cm}^3\text{.s)}$$

3.4 H₂ combustion: H₂ + ½O₂ → H₂O (Peters 1979)

$$Rate = 1.08 \cdot 10^6 \ exp\left(\frac{-30000}{RT_g}\right) \varepsilon_g \left(\frac{\rho_g X_{g1}}{Mw_1}\right) \left(\frac{\rho_g X_{g5}}{Mw_5}\right) \text{ (mol/cm}^3\text{.s)}$$

3.5 Tar combustion: Tar + f₁ O₂ → f₂ CO₂ + f₃ H₂O

The rate is assumed to be the same as the rate for C₁₀H₂₂ from Westbrook and Dryer (1981):

$$Rate = 3.8 \cdot 10^{11} \ exp\left(\frac{-30000}{RT_g}\right) \varepsilon_g \left(\frac{\rho_g X_{g1}}{Mw_1}\right)^{1.5} \left(\frac{\rho_g X_{g8}}{Mw_8}\right)^{0.25} \text{ (mol/cm}^3\text{.s)}$$

4 Other Reactions

4.1 Water gas - shift reaction: CO + H₂O → CO₂ + H₂. (Wen et al. 1982)

$$Rate = 2.877 \cdot 10^5 w_{g3} f_3 P^{(0.5-P/250)} \exp\left(\frac{-27760}{RT_g}\right) X_{g2} X_{g6} - \frac{X_{g3} X_{g5}}{K_3} \text{ (mol/cm}^3\text{.s)},$$

where

$$f_3 = \varepsilon_g (1 - \varepsilon_g) X_{s4}^0 \rho_{s1} \exp(-8.91 + 5553/T_g) ,$$

$$K_3 = \exp(-3.63061 + 3.955.71/T_g) .$$

$w_{g3} = 0.0068$, P is pressure (P_g) in atm.

4.2 Calcite Decomposition: $\text{CaCO}_3 \rightarrow \text{CaO} + \text{CO}_2$ (Campbell 1978)

$$Rate = 3.1 \cdot 10^{10} \exp\left(\frac{-55000}{R T_{gs}}\right) \left(\frac{\rho_s \varepsilon_{s1} X_{s5}}{Mw_{s5}}\right) \left(1 - \frac{P_{CO2}}{K_{CaO}}\right) (\text{mol/cm}^3 \cdot \text{s})$$

where

$$K_{CaO} = 1.03 \cdot 10^8 \exp(-21830/T_g)$$

4.3 Dolomite Decomposition: $\text{CaMg}(\text{CO}_3)_2 \rightarrow \text{CaCO}_3 + \text{MgO} + \text{CO}_2$ (Campbell 1978)

$$Rate = 2 \cdot 10^8 \exp\left(\frac{-51000}{R T_{gs}}\right) \left(\frac{\rho_s \varepsilon_{s1} X_{s6}}{Mw_{s6}}\right) (\text{mol/cm}^3 \cdot \text{s})$$

Nomenclature

d_p	mm	Diameter of the particles constituting the solids phase
D_{O_2}	cm^2/s	Oxygen diffusivity;
D_e	cm^2/s	Effective diffusivity through the ash layer;
m		Index of the solids phase: 1 - Char, 2 - Coal. (0 indicates gas phase)
Mw_n		Molecular weight of n^{th} gas species
Mw_{sn}		Molecular weight of n^{th} solids species
n		Index of the n^{th} chemical species: Gas species: 1 - O_2

2 - CO

3 - CO₂

4 - CH₄

5 - H₂

6 - H₂O

7 - N₂

8 - Tar.

Solids species: 1 - Fixed carbon

2 - Volatile matter

3 - Moisture

4 - Ash

5 - CaCO₃

6 - CaMg(CO₃)₂

7 - CaO

8 - MgO.

P_g Pa Pressure in the gas phase

p_n atm Partial pressure of nth species

R cal/mol.K Universal gas constant

R_{O₂} atm.cm³/g.K Gas constant for oxygen;

Re Solids phase particle Reynolds Number

Sc Schmidt number = $\frac{\mu_g}{\rho_g D_{O_2}}$

Sh_m Sherwood number

T_g K Temperature of the gas phase

T_f Film temperature: (T_g+T_s)/2

T_s K Temperature of solids phase

X* Minimum volatile fraction at the given temperature

X_{gn} Mass fraction of the nth chemical species in the gas phase

X_{sn} Mass fraction of the nth chemical species in the solids phase

X_{sn}⁰ Initial value of X_{sn}

GREEK LETTERS

ϵ_g		Volume fraction of the gas phase (void fraction)
ϵ_s		Volume fraction of the solids phase
μ_g	g/cm.s	Molecular viscosity of the gas phase
ρ_g	g/cm ³	Microscopic (material) density of the gas phase
ρ_s	g/cm ³	Microscopic (material) density of the solids phase

PCGC-FW Model of Coal Chemistry

In PCGC-FW, coal is assumed to contain inert ash, moisture and organic part (dry ash free coal). Upon being injected to a furnace, a coal particle will undergo moisture vaporization, devolatilization and char oxidation simultaneously.

Depending on the furnace condition, the rate of moisture vaporization can either be limited by the mass transfer or by heat transfer if the water in the particle is boiling. In pulverized coal combustion system, the moisture vaporization process happens in coal pulverizer; the particles entering the furnace are moisture-free.

The organic part of coal will undergo a coal devolatilization process to form char and volatile matters. It is assumed that the coal devolatilization happens everywhere inside the coal particle and hence the devolatilization rate per particle is related to the mass of organic coal remained in the particle. Based on the coal devolatilization research in the literature, the percentage of volatiles released in a furnace depends on the particle heating rate or the history of the particle temperature increase. The real yield of volatiles is usually higher than the yield in the ASTM standard test. There are three coal devolatilization models available in PCGC-FW code, namely, one-equation model, two-equation model and CPD model. The two-equation model is generally used for simplicity and reasonable accuracy. The one-equation model is not able to predict the dependency of volatiles yield on heating rate. The CPD model is a complicated network model and requires extensive NMR coal analysis data. In addition to reaction rate, size change or swelling of the coal particle is also modeled in PCGC-FW. The particle diameter increase is assumed to be proportional to the extent of devolatilization.

Char oxidation kinetics is modeled using a global mechanism. The char oxidation rate is correlated to the external surface area of the particle and the concentration of oxygen gas at the surface. The reaction order with respect to oxygen gas is not necessarily the first order; half order kinetics was observed for most bituminous coals. Char gasification by steam and CO_2 is not considered. Particle size change is modeled and related to coal type and extent of char oxidation. The products of char oxidation are assumed to be CO and CO_2 and the mole ratio of CO to CO_2 produced is related to the particle temperature. Because the char oxidation kinetics is not necessarily first order, the concentration of oxygen at the particle surface is solved iteratively by equating the oxygen consumption rate at the surface to the mass transfer rate. A blowing factor due to a potentially high mass transfer rate is also considered in calculating the mass transfer coefficient.

PCGC-FW does not consider the kinetics in the gas phase reactions. The species concentrations in the gas phase are obtained by assuming that all gaseous species of interest reach the chemical equilibrium.

The expressions regarding chemical reaction, mass transfer, and related variables are listed below.

Moisture Vaporization

A. Boiling

$$r_w = \frac{q}{\Delta H_v}$$

B. Non-Boiling

$$r_w = -\frac{k_w \rho_g (x_{w,s} - x_{w,b}) + x_{w,s} \sum_{i \neq w} r_i}{1 - x_{w,s}}$$

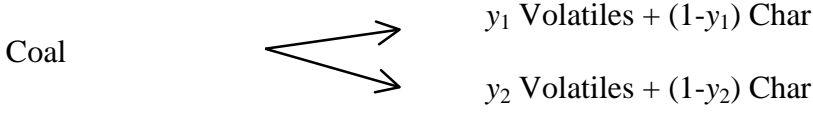
where

$$k_w = \frac{Sh D_{wm}}{d_p} \left(\frac{B}{e^B - 1} \right)$$

$$Sh = 2 + 0.6 Re^{1/2} Sc^{1/3}$$

$$B = \frac{d_p \sum r_i}{\rho_g Sh D_{wm}}$$

Coal Devolatilization (two-equation model)



$$r_c = -\frac{m_p \omega_c}{S_{ex}} \left[A_1^d \exp\left(-\frac{E_1^d}{RT_p}\right) + A_2^d \exp\left(-\frac{E_2^d}{RT_p}\right) \right]$$

$$r_v = \frac{m_p \omega_c}{S_{ex}} \left[y_1 A_1^d \exp\left(-\frac{E_1^d}{RT_p}\right) + y_2 A_2^d \exp\left(-\frac{E_2^d}{RT_p}\right) \right]$$

$$r_h^d = \frac{m_p \omega_c}{S_{ex}} \left[(1-y_1) A_1^d \exp\left(-\frac{E_1^d}{RT_p}\right) + (1-y_2) A_2^d \exp\left(-\frac{E_2^d}{RT_p}\right) \right]$$

$$d_p = d_{p,o} + \gamma d_{p,o} \left(1 - \frac{\omega_c}{\omega_{c,o}} \right)$$

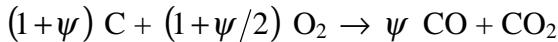
Char Oxidation

$$r_h^o = -A^o p_{O_2,s}^n \exp\left(-\frac{E^o}{RT_p}\right)$$

$$r_{O_2} = \frac{k_{O_2} \rho_g (x_{O_2,s} - x_{O_2,b}) + x_{O_2,s} \sum_{i \neq w} r_i}{1 - x_{O_2,s}}$$

$$\text{where } k_{O_2} = \frac{Sh D_{O_2,m}}{d_p} \left(\frac{B}{e^B - 1} \right)$$

On the particle external surface,



$p_{O_2,s}$ is solved based on,

$$\frac{r_h^o}{M_C (1 + \psi)} = \frac{r_{O_2}}{M_{O_2} (1 + \psi/2)}$$

where

$$\psi = A^r \exp \left(-\frac{E^r}{RT_p} \right)$$

$$\frac{d_p}{d_{p,ad}} = \left(\frac{m_p}{m_{p,ad}} \right)^{\frac{1-\alpha}{3}}$$

Nomenclature

A	Pre-Exponential factor
B	Blowing factor parameter due to high mass transfer rate
D_{im}	m^2/s
	Diffusivity of species i in gas mixture
d_p	m
	Particle diameter
E	J/mol
	Activation energy
ΔH_v	J/kg
	Heat of vaporization
m_p	kg
	Mass of a coal particle
k	m/s
	Mass transfer coefficient
M	g/mol
	Molecular/Atomic weight
n	
	Reaction order with respect to O_2 gas
q	W/m^2
	Heat flux added to particle
R	J/mol-K
	Universal gas constant
Re	
	Reynolds number
r_i	kg/s-m^2
	Reaction or vaporization rate per external particle surface area
S_{ex}	m^2
	External surface area of particle
Sc	
	Schmidt number
Sh	
	Sherwood number

T_p	K	Particle temperature
y_i		Fraction of volatiles product
x_i		Mass fraction of species i
α		Char oxidation mode parameter
γ		Coal particle swelling coefficient
ρ_g	kg/m ³	Gas density
ω_c		Mass fraction of coal organic in particle
ψ		CO to CO ₂ mole ratio

Subscript

ad	After devolatilization
b	Bulk
c	Coal
C	Carbon
h	Char
i	Species index
•	Initial
O_2	Oxygen gas
s	At particle external surface
w	Water (moisture)

Superscript

d	In coal devolatilization
•	In char oxidation
r	For CO to CO ₂ ratio

TASK 3 - MFIX Code Enhancements

Improvements to the Serial Code

During the course of this CRADA several improvements were made to MFIX. The improvements to the serial code are described in this section, and the development of a parallel version of the code is described in the next section.

To speed up the code, its numerical technique was replaced with a semi-implicit scheme that uses automatic time-step adjustment. The essence of the method used in the old version of MFIX was developed by Harlow and Amsden (1975) and was implemented in the K-FIX code (Rivard and Torrey 1977). The method was later adapted for describing gas solids flows at the Illinois Institute of Technology (Gidaspow and Ettehadieh 1983). In MFIX 2.0 that method was replaced by a method based on SIMPLE (Semi Implicit Method for Pressure Linked Equations), which was developed by Patankar and Spalding (Patankar 1980). Several research groups have used extensions of SIMPLE (e.g., Spalding 1980, Fogt and Peric 1994, Laux and Johansen 1997), and this appears to be the method of choice in commercial CFD codes (Fluent manual 1996, Witt and Perry 1996). Two modifications of standard extensions of SIMPLE have been introduced in MFIX to improve the stability and speed of calculations. One, MFIX uses a solids-volume-fraction correction equation (instead of a solids pressure correction equation), which appears to help convergence when the solids are loosely packed. That equation also incorporates the effect of solids pressure, which is a novel feature of the MFIX implementation that helps to stabilize the calculations in densely packed regions. Two, MFIX uses automatic time-step adjustment to ensure that the run progresses with the highest execution speed. In various test cases conducted MFIX 2.0 was found to run 3-30 times faster than the old version of the code.

To improve the accuracy of the code, second-order accurate schemes for discretizing convection terms were added to MFIX. Reducing the discretization errors is harder when first-order upwind (FOU) method is used for discretizing convection terms. For example, FOU method leads to the prediction of pointed bubble shapes in simulations of bubbling fluidized beds. This unphysical shape, caused by numerical diffusion, could not be corrected with certain affordable grid refinement. With the same grid, however, the use of a second-order accurate discretization scheme gave the physically realistic rounded bubble shape (Syamlal 1997).

The serial version of MFIX was migrated from FORTRAN 77 to Fortran 90. Fortran 90 allows the use of allocatable arrays, so that the problem size can be determined at run-time, and temporary storage can be dynamically allocated (for example, in the linear solvers). Also, programmer productivity will be increased as the code development is continued because of the advanced features of Fortran 90 (for example, notation for matrix/vector operations). In the future, this will also allow the use of Object Oriented programming.

The translator VAST/77to90TM (Pacific-Sierra Research 1995) was used at Oak Ridge National Laboratory (ORNL) to create a first draft of this version. Each include-type file and common block was converted into a module (except the include-type files containing statement functions); instead of the construct ‘include param.inc’, Fortran 90 construct ‘use param’ is used

and the contents of the file *param.inc* is inserted into the file *param_mod.f90*. Some of the automatically generated modules, however, had misplaced comment lines and several explicitly inserted parametric values. Hand editing was required to correct this. The translator also produced subroutine interface to place/encapsulate closely related subroutine files into modules. Very aggressive array constructs, like ‘where’, were not used since the resulting code was too different from the original code and not easy to read. Since there is inter-dependence on the modules, the modules have to be compiled in a certain order, in particular almost all routines depend on *param_mod.f90* and *param1_mod.f90* and so these routines should be compiled first. The makefile was modified so that all modules are compiled before being ‘used’ by other routines.

Several weeks of “clean-up” work were required to reinstall the internal documentation disrupted during the conversion. Additional routines were written to allocate memory and create temporary arrays. A “lock” and “unlock” feature was developed for the temporary arrays so that they can be safely reused without being accidentally overwritten.

This version of the code was brought into CVS (Concurrent Versions System, <http://www.cs.utah.edu/csinfo/texinfo/cvs/>), for version control of all further modifications. CVS has also facilitated the development of the code by multiple developers at different locations (Morgantown, WV; Oak Ridge, TN; and Phoenix, AZ).

The code was ported to run on a PC under Windows 95, Windows 98, Windows NT, and Linux. Substantial changes were made to *animate_mfix*, which was previously available only on Silicon Graphics machines. *Animate_mfix* was revised to use the industry standard OpenGL graphics routines and was given a user-interface based on Glut. Now *animate_mfix* is portable to many machines including PCs.

Parallelization

MFIX, at the start of the CRADA, could be run only on a serial computer, which has a single processor with its associated memory (Figure 20). To run large 3-D problems it was necessary to develop a version that can be run on shared memory and distributed memory parallel computers.

Shared Memory Parallel (SMP) Version

A shared memory parallel computer has multiple processors that access the same memory (Figure 21). Dr. Ed D Azevado at Oak Ridge National Laboratory (ORNL) developed a parallel version of MFIX for shared memory machines by inserting OpenMP directives into the code. This is now being used on dual- and quad-processor PCs and the SGI Power Challenge at NETL and the Pittsburgh Supercomputer Center.

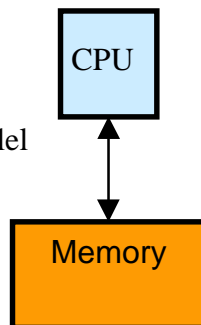


Figure 20. Serial Computer

An SMP version of MFIX, developed from the Fortran 90 version of MFIX, was parallelized using portable OpenMP directives (<http://www.openmp.org>). Profiling information suggested that over 70% of the overall runtime was consumed in the linear solvers. The remaining time was spread across many routines. The do-loops of the most time consuming routines were parallelized with OpenMP directives. Some care was required to appropriately declare local, shared and reduction variables.

The original version of MFIX supports several options for the linear solvers, including simple SOR (Successive Over Relaxation), and SLAP library routines for GMRES, Conjugate Gradients preconditioned by incomplete LU (ILU) factorization or simple diagonal (Jacobi) scaling. The SOR routine, with a fixed number of iterations, is most effective in solving the diagonally dominant linear system arising from the momentum equations, whereas ILU with GMRES is often used to solve the pressure equations.

The SOR, with the original sweep order, has data dependencies and cannot be easily parallelized on a shared memory machine. A variant of SOR, based on sweeping along hyper-planes ($I+J+K=constant$), was attempted. However, this was not found to be effective since there were insufficient opportunities for parallelism on typical grid configurations that are long and slender along the J-axis.

The SLAP library routines store a sparse matrix internally in a column-oriented “IA,JA” data structure. In order to use this GMRES routine, some overhead is incurred in sorting and copying from the “I,J,K” to the “IA,JA” SLAP format on each invocation. The SLAP library exposes very limited opportunities for parallelism. The factorization and forward and backward triangular solves are inherently serial. Moreover, the column-orient matrix vector multiply performs indirect summation through an index vector. Straightforward parallelization would require expensive locks and critical sections to ensure correctness.

Two new options for the linear solver, based on line or plane relaxation accelerated with BiCGSTAB or GMRES, were implemented. These routines take advantage of the logically rectangular “I,J,K” structure. Numerical experiments on typical problems suggest that relaxation sweeps along the J-direction, which is often the dominant flow direction, were most effective in reducing the residual. The tridiagonal line solves are performed by the LINPACK routine DGTSL.

BiCGSTAB is a variant of BiCG that uses a three-term recurrence in expanding the Krylov space. The implementation requires only extra storage for a few vectors. Each iteration performs 4 inner products, 6 DAXPY, 2 matrix-vector products, and 2 solves by the preconditioner. In our numerical experiments, our implementation of BiCGSTAB is often more efficient than our GMRES. However, BiCGSTAB does not guarantee monotone reduction in

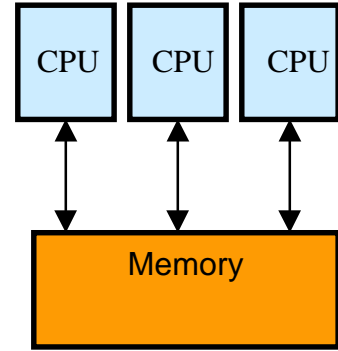


Figure 21. Shared Memory Parallel Computer

residual. In a few rare cases, BiCGSTAB did not converge in the fixed number of iterations specified. In those few cases, GMRES is called to solve the linear systems.

Unlike BiCGSTAB, an m-step GMRES method requires extra storage for m-vectors. On the i-th iteration, it requires (i+1) inner products, (i+1) DAXPY, 1 matrix vector product and 1 preconditioned solve. The QR updating of the Hessenberg matrix is not parallelized. GMRES does have the advantage of ensuring monotone progress in reducing the residual.

Since in most practical devices the flow is along narrow ducts, the coupling is strongest in the long dimension, which is usually the main direction of flow. In either Cartesian or cylindrical coordinates, this direction is the “J” direction. Since the code uses line relaxation, the node order was reassigned to be J-fastest, then I, K-slowest. This reordering was accomplished easily by modifying `funijk()`, which is a macro in the file `function.inc`. In order to maintain compatibility with post-processors, and to read archived restart files, a new routine `funijk_io()` was introduced, which maintains the original order: I-fastest, then J, K-slowest.

The SMP version of MFIX has been benchmarked, using several machines to determine its scaling performance. In Table 5, the CPU time required for execution for several fixed jobs is presented as a function of the number of processors, normalized to the performance of the SMP version running on one processor. The benchmark problem used 115,200 cells to describe the hydrodynamics of a uniformly fluidized bed in 3D. The tests were conducted on an 8-processor SGI Power Challenge.

Table 5. Performance of SMP version of MFIX on SGI Power Challenge

No of Processors	Elapsed time, s	Speed up	Parallel efficiency
1	13,953	1.00	100
2	7,492	1.86	93
4	4,264	3.27	82
8	2,363	5.90	74

Distributed Memory Parallel (DMP) Version

A disadvantage of the SMP machine is that it is not scalable, or the number of processors cannot be indefinitely increased to solve large problems. This lead to the development of DMP machines. Furthermore the availability of commodity PCs and networking equipment and software promoted the construction and usage of cheap PC clusters (known as Beowulf clusters) to solve large-scale problems. In DMP machines each processor has its associated memory and inter processor communication takes place through a switch (Figure 22). Because the memory is distributed the problem is broken into several pieces and solved on the different machines. If a processor needs information from a memory location that it does not own, it receives the information through the switch from the processor that owns the memory location. This communication is slow compared with direct memory access and should be minimized to improve the computational speed. Therefore, the conversion of the code for a DMP machine is much more difficult than that for the SMP machine. This more ambitious task was completed by

the following team: Dr. Ed D Azevado (ORNL), Dr. Sreekanth Pannala (ORNL), Dr. Aytekin Gel (Aeolus), Mr. Mike Prinkey (Aeolus, NETL), Dr. M. Syamlal (Fluent, NETL), Dr. Tom O'Brien (NETL), Mr. Phil Nicoletti (Parsons, NETL). This 1.7 person-year effort was completed in a year. For this development 58,302 lines of code were reviewed and 14,732 lines of code were added to MFIX.

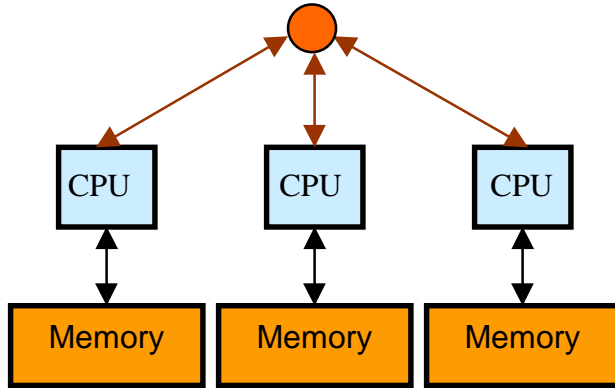


Figure 22. Distributed Memory Parallel Computer

The approach used is termed domain decomposition. For example, say we need to run a problem that has 12 cells in the J-direction on a DMP machine with three processors. We will solve for the values on the grid with J=1-4 on Processor 1, J=5-8 on Processor 2, and J=9-12 on Processor 3. Suppose Processor 1 needs a value at J=5, then that value is obtained from Processor 2 over the network. The communications are handled with the MPI message-passing library, which results in a portable code. ORNL developed several modules that hide the complexity of MPI function calls. These modules were called from the MFIX routines, which leaves the solver code simple and readable. The use of such modules also reduced the development and debugging time. Two ghost layers, for which no computations are performed, were added on each processor to considerably reduce inter processor communications. In the above example, Processor 1 will also have memory locations for J=5 and 6 as ghost layers.

The input data file is read by all the processors because it takes only a tiny fraction of the over all computational time. Each processor also writes out its own error messages. A designated processor writes all the output data files, however. So the output files are identical to those produced by serial and SMP versions of MFIX and no modifications were required in the post processing codes.

The project has produced a unified version of MFIX for Serial, SMP and DMP computing, which is easier to maintain than three separate versions. The users can easily select the version of the code at compile time by answering two yes/no questions.

The DMP parallel version of the code was subjected to extensive testing. The following options in MFIX were tested: 2-D, 3-D cylindrical and Cartesian grids; cyclic and non-cyclic

boundary conditions; all transport equations; and different discretization schemes. These tests were done with the suite of test problems given in Table 6.

Table 6. Test Problems Used For verification

Conduction
Conduction + Convection
Developed Pipe Flow
Developed Slit Flow
Scalar Transport
Scalar Transport in a Cyclic Domain
Lid-driven Cavity
Granular Shear Flow
Plug Flow Reactor
Rotary Drum
Liquid-Solids Settling Tank
Gas-Solids Riser
Bubble Fluidized Bed
Ozone Decomposition in 3D Domain

For benchmarking the code, we used the problem of the catalytic decomposition of O_3 in a bubbling fluidized bed. The 0.229-m diameter, 2-m tall reactor was represented in 3D-cylindrical coordinates with a grid resolution of 72 x 112 x 16 (129,024) cells. The memory requirement for the problem is 220 MB. The gas flow rate was five times the minimum fluidization velocity. The problem was run on the DMP machines shown Table 7.

The code performed best on the IBM SP machine as shown by the performance numbers given in Table 8. A factor of ten speedup is obtained with 16 processors.

The performance on the 24-node Beowulf cluster at NETL is shown in Table 9. A factor of seven speedup is obtained with 18 processors. Fine-tuning of the DMP version is ongoing to improve the performance of the code on the Beowulf cluster.

Table 7. Machines used for testing the DMP version of MFIX

Beowulf Cluster (NETL) 23 Nodes: Pentium II 400 MHz, 256 MB memory, Head Node: dual Pentium II, 512 MB memory, 24 port 3Com Fast Ethernet switch
Silicon Graphics (NETL) 8 processors: R10000, 194 MHz, 2.5 GB memory
IBM SP (ORNL) 62 "Winterhawk -II" nodes x four 375 MHz Power3+, 8 MB of L2 cache, 2 GB memory
Compaq (ORNL) 16 Nodes x four 500 MHz Alpha EV6, 2 GB memory, 365 GB of fiber Channel Disk
CRAY T3E (Pittsburgh Supercomputing Center) 512 processors: 450 MHz Alpha EV5, 128 MB memory
IBM SP (NERSC) 256 "Winterhawk-I" nodes x 2 200 MHz Power3, 4 MB of L2 cache, 1 GB memory

Table 8. Performance of DMP version of MFIX on IBM SP

No. of Processors	Elapsed Time, s	Speed-up	Parallel Efficiency
1	1,485	1.0	100%
2	702	2.1	106%
4	371	4.0	100%
8	230	6.4	81%
16	154	9.7	60%

Table 9. Performance of DMP version on MFIX on the Beowulf Cluster at NETL

No. of Processors	Elapsed Time, s	Speed-up	Parallel Efficiency
1	3,526	1.0	100%
2	1,799	2.0	98%
4	1,034	3.4	85%
8	708	5.0	62%
12	542	6.5	54%
18	506	7.0	39%

REFERENCES

Boemer, A., H. Qi, U. Renz, S. Vasquez, and F. Boysan, Eulerian Computation of Fluidized Bed Hydrodynamics—A Comparison of Physical Models, in Fluidized Bed Combustion - Volume 2, ASME, pp. 775-787 (1995).

Campbell, J.H. , 1978. The Kinetics of Decomposition of Colorado Oil Shale: II. Carbonate Minerals. Lawrence Livermore Laboratory Report, UCRL-52089 Part 2.

Desai, P.R., and Wen, C.Y., 1978, "Computer Modeling of the MERC Fixed Bed Gasifier," MERC/CR-78/3.

Epstein, N., J.R. Grace, Spouting of Particulate Solids, in *Handbook of Powder Science and Technology*, eds. M.E. Fayed and L. Otten, Van Nostrand Reinhold Co., New York, 1984.

Fluent User's Manual, 1996, Fluent, Inc., Lebanon, NH.

Fogt, H., and Peric, M., 1994, "Numerical calculation of gas-liquid flow using a two-fluid finite-volume method," FED-Vol. 185, *Numerical Methods in Multiphase Flows*, ASME, 73-80.

Gidaspow, D., Multiphase Flow and Fluidization, Academic Press, New York (1994).

Gidaspow, D., and B. Ettehadieh, 1983, "Fluidization in Two-Dimensional Beds with a Jet; 2. Hydrodynamic Modeling," *I&EC Fundamentals*, 22, 193-201.

Guenther, C. and M. Syamlal, "The effect of numerical diffusion on isolated bubbles in a gas-solid fluidized bed," accepted for publication, *Powder Tech* (2000).

Gunn, D.J., 1978, "Transfer of Heat or Mass to Particles in Fixed and Fluidized Beds," *Int. J. Heat Mass Transfer*, **21**, 467-476.

Harlow, F.H., and A.A. Amsden, 1975, "Numerical Calculation of Multiphase Fluid Flow," *J. of Comp. Physics*, 17, 19-52.

He, Y.L-, S.-Z. Qin, C.J. Lim, and J.R. Grace, *Can. J. Chem. Eng.*, 72, 561-568 (1994a).

He, Y.L-, C.J. Lim, J.R. Grace, J.-X. Zhu and S.-Z. Qin, *Can. J. Chem. Eng.*, 72, 229-234 (1994b).

Kuipers, J.A.M., K.J. Van Duin, F.P.H. Van Beckum, and W.P.M. Van Swaaij, A Numerical Model of Gas-Fluidized Beds, *Chem. Engng Sci*, **47** (8), pp. 1913-1924 (1992).

Laux, H., and Johansen, S.T., "Computer Simulation of Bubble Formation in a Gas-Fluidized Bed, 1997, Submitted to Fluidization IX conference.

Patankar, S.V., 1980, *Numerical Heat Transfer and Fluid Flow*, Hemisphere Publishing Corporation, New York.

Peters, N., 1979, "Premixed Burning in Diffusion Flames—The Flame Zone Model of Libby and Economos," *Int. J. Heat Mass Transfer*, **22**, 691-703.

Rivard, W.C., and M.D. Torrey, 1977, "K-FIX: A Computer Program for Transient, Two-Dimensional, Two-Fluid Flow," LA-NUREG-6623, Los Alamos National Laboratory, Los Alamos.

Sanyal, J., E. Cesmebasi, On the Effect of various Momentum Transfer Coefficient Models on Bubble Dynamics in a Rectangular Gas Fluidized Bed, *Chem. Engng Sci*, **49** (23), pp. 3955-3966 (1994).

Seager, M.K., and A. Greenbaum, 1988, "The Linear Algebra Package SLAP Ver 2.0," Lawrence Livermore National Lab.

Spalding, D.B., 1980, "Numerical Computation of Multi-phase fluid flow and heat transfer," in *Recent Advances in Numerical Methods in Fluids*, C. Taylor et al., eds, Pineridge Press.

Syamlal, M., Higher Order Discretization Methods for the Numerical Simulation of Fluidized Beds, Fluidization and Fluid-Particle Systems: Recent Research and Development, ed. H. Arastoopour, AIChE Symposium Series No. 138. (1998).

Syamlal, M., and Bissett, L.A., 1992, "METC Gasifier Advanced Simulation (MGAS) Model," Technical Note, NTIS report No. DOE/METC-92/4108 (DE92001111).

Syamlal, M., and T.J. O'Brien, Computer Simulation of Bubbles in a Fluidized Bed, in Fluidization and Fluid Particle Systems: Fundamentals and Applications, L.S. Fan (Ed), AIChE Symposium Series No. 270, **85**, pp. 22-31 (1989).

Wen, C.Y., Chen, H., and Onozaki, M., 1982, "User's Manual for Computer Simulation and Design of the Moving Bed Coal Gasifier," DOE/MC/16474-1390, NTIS/DE83009533.

Westbrook, C.K., and Dryer, F.L., 1981, "Simplified Mechanisms for the Oxidation of Hydrocarbon Fuels in Flames," *Combustion Sci. Tech.*, **27**, 31-43.

Witt, P.J., and Perry, J.H., 1996, "A Study in Multiphase Modelling of Fluidised Beds," in Computational Techniques and Applications CTAC95, eds. R.L. May and A.K. Easton, World Scientific Publishing Co.

APPENDIX A: CRADA Document

**COOPERATIVE RESEARCH AND DEVELOPMENT
AGREEMENT (hereinafter “CRADA”) No. 97-F001
BETWEEN
FEDERAL ENERGY TECHNOLOGY CENTER
U.S. DEPARTMENT OF ENERGY (hereinafter “FETC”)
AND
FOSTER WHEELER DEVELOPMENT CORPORATION
(hereinafter “Participant”)**

both being hereinafter jointly referred to as the “Parties.”

ARTICLE I: DEFINITIONS

- A. “Government” means the United States of America and agencies thereof.
- B. “DOE” means the Department of Energy, an agency of the United States of America.
- C. “METC” is a Government-owned and operated facility engaged in the conduct of fossil energy research and development.
- D. “Laboratory Director” means the Director of METC, acting in accordance with and under the general and enumerated authority of P.L. 99-502 and P.L. 101-189.
- E. “Generated Information” means information produced in the performance of this CRADA.
- F. “Proprietary Information” means information which is developed at private expense outside of this CRADA, is marked as Proprietary Information, and embodies (i) trade secrets or (ii) commercial or financial information which is privileged or confidential under the Freedom of Information Act (5 U.S.C. 552(b)(4)).

“Protected CRADA Information” means Generated Information which is marked as being Protected CRADA Information by a Party to this CRADA and which would have been Proprietary Information had it been obtained from a non-federal entity.

“Unlimited Rights” means the right to use, disclose, reproduce, prepare derivative works distributed to the public, and perform publicly or display publicly in any manner or for any purpose or to permit others to do so.

- I. “Subject Invention” means any invention of the Parties conceived or first actually reduced to practice in the performance of work under this CRADA.
- J. “Intellectual Property” means patent applications, patents, and other forms of comparable property rights protected by Federal law and its foreign counterparts.

ARTICLE II: STATEMENT OF WORK

Background

MFIX is a transient, finite difference, FORTRAN code that solves the equations of transport for interacting fluid and granular solid phases. It is designed to model fluidized bed reactors.

Recently the Foster Wheeler Development Corporation (FWDC) and the Morgantown Energy Technology Center completed a year long CRADA whose objectives were to validate MFIX and transfer it to FWDC for their use. MFIX has been transferred successfully and validated against four experimental studies. It was shown to capture general features of fluid bed behavior such as pressure drop fluctuations, temperature fluctuations, solids circulation cells, and bubble formation, consolidation, and growth. Those validation studies also have discovered aspects of fluid bed behavior such as bubble shape, bubble frequency and spouting that MFIX does not capture well with the existing physical models. This CRADA will: further clarify which aspects of fluid bed behavior MFIX is able to predict well; extend the studies to high pressure, high temperature and reactive cases; and amend the MFIX code if necessary. Work under this CRADA is divided into three tasks. The first task involves the continuing validation of the hydrodynamic and chemistry capabilities of the MFIX computer code. Foster Wheeler Development Corporation and FETC both will contribute to this task. The second task involves a parametric evaluation of the MFIX code's ability to predict bubble shape and the dependence of code results to particle size distribution and gasification chemistry. Task 3 is an enhancement of the MFIX code to make it execute faster and more easily used on personal computers. FETC will have primary responsibility for the second and third tasks.

TASK 1 - Continuing Validation of the MFIX Code

Together, FWDC and FETC will select results from previously conducted experimental studies to use for the continuing validation of the MFIX code. These experimental studies will involve the Foster Wheeler carbonizer, jetting fluidized beds, pressurized fluidized beds and/or spouting beds. Simulation responsibilities for these studies will be divided between FWDC and FETC, and the determination of the responsible Party will depend upon each organization's resource availability. The results of the validation studies will be documented in a technical report written by FETC.

TASK 2 - Parametric MFIX Code Investigations

As a result of the validation studies conducted in Task 1 and in the previous CRADA work, FETC will perform the following MFIX code investigations:

Investigate bubble shape

FETC will use the MFIX code to predict the shape of bubbles in a two dimensional fluid bed. Perceived bubble shape in a three-dimensional simulation of a three-dimensional bed will also be predicted.

- Study the effect of particle size distribution on bed behavior

FETC will simulate a fluid bed composed of three particle size fractions and simulate the same bed using an average particle size. The differences in bed behavior will be documented.

- Adjust gasification chemistry

FETC will adjust the gasification chemistry parameters within the MFIX code so that the predicted exit gases more closely match those observed by FWDC during experimental run 8.9.

Once a match has been achieved, at least two other Foster Wheeler carbonizer experiments will be simulated, and the predicted results compared to the experimental results.

TASK 3 - MFIX Code Enhancements

In order to make the MFIX code more readily usable, FETC will modify the MFIX code with the following goals:

- To increase MFIX execution speed

FETC will modify portions of the MFIX code in order to reduce the time needed to simulate circulating fluidized bed by at least half. The modified code will be transferred to FWDC.

- To make MFIX more portable

FETC will modify the MFIX code so that it runs on a Pentium-class personal computer. The modified code will be transferred to FWDC.

CRADA EVALUATION

To aid FETC in evaluating its CRADA program, the Participant will provide FETC with a short narrative at the end of the CRADA addressing the following:

- Were your CRADA expectations met, not met, or exceeded?
- Estimate the cost savings to future projects due to the CRADA?
- Did the CRADA result in any product or knowledge which can be applied to future company programs without FETC involvement?
- Would you enter into another CRADA with the FETC?
- What would you change about the CRADA development or CRADA implementation process?
- What is the largest potential impact this CRADA may have on your company (e.g., an increase in productivity, sales, new jobs created, new products, etc.)?

ARTICLE III. CONTRIBUTIONS OF THE PARTIES

The estimated value of the Participant's contribution is \$30,000. The estimated value of the Government's contribution is \$78,000, subject to available funding.

The Parties have no obligation to continue or complete performance of the work at an amount in excess of the estimated contribution in (A) above, including any subsequent amendment.

C. Each Party agrees to provide thirty (30) days advance notice to the other Party if the actual amount to complete performance will exceed the estimated contribution. If the Parties agree to continue the project, the Parties shall agree on the estimated increased contribution for each Party in a duly executed amendment to this CRADA.

ARTICLE IV: PERSONAL PROPERTY

Any tangible personal property produced in conducting the work under this CRADA shall be owned by the Party paying for it. There will be no jointly funded property. Personal property shall be disposed of as directed by the owner at the owner's expense.

ARTICLE V: DISCLAIMER

THE GOVERNMENT AND THE PARTICIPANT MAKE NO EXPRESS OR IMPLIED WARRANTY AS TO THE CONDITIONS OF THE RESEARCH OR ANY INTELLECTUAL

PROPERTY OR PRODUCT MADE, OR DEVELOPED UNDER THIS CRADA, OR THE OWNERSHIP, MERCHANTABILITY OR FITNESS FOR A PARTICULAR PURPOSE OF THE RESEARCH OR RESULTING PRODUCT.

IN NO EVENT SHALL EITHER PARTY OR ITS SUBCONTRACTORS OR VENDORS BE LIABLE, WHETHER IN CONTRACT, TORT (INCLUDING NEGLIGENCE), WARRANTY, STRICT LIABILITY OR ANY OTHER LEGAL THEORY, FOR ANY SPECIAL, INDIRECT, INCIDENTAL OR CONSEQUENTIAL DAMAGES. THE REMEDIES OF THE PARTIES SET FORTH IN THIS CRADA ARE EXCLUSIVE.

AS BETWEEN THE PARTIES TO THIS AGREEMENT, THEIR SUBCONTRACTORS AND VENDORS, WHETHER IN CONTRACT, TORT (INCLUDING NEGLIGENCE), WARRANTY, STRICT LIABILITY OR ANY OTHER LEGAL THEORY, THE LIABILITY OF EACH PARTY SHALL NOT EXCEED THE AMOUNT OF ITS CONTRIBUTION UNDER ARTICLE III. HOWEVER, LIABILITY TO THIRD PARTIES IS IN NO WAY LIMITED BY THIS ARTICLE.

ARTICLE VI: HOLD HARMLESS

Except for any liability resulting from any negligent acts or omissions of the Government, the Participant agrees to hold the Government harmless for all damages, costs and expenses, including attorney's fees, arising from personal injury or property damage occurring as a result of the making, using or selling of a product, process or service by or on behalf of the Participant, its assignees or licensees, which was derived from the work performed under this CRADA.

ARTICLE VII: PROPRIETARY INFORMATION

Each Party agrees to not disclose Proprietary Information provided by the other Party, without the written permission of said other Party, to anyone other than the providing Party, except to Government employees who are subject to 18 U.S.C. 1905.

ARTICLE VIII: OBLIGATIONS AS TO PROTECTED CRADA INFORMATION

Each Party may designate and mark as Protected CRADA Information any qualifying Generated Information produced by its employees. For a period of up to five years from the date it is produced, the Party receiving such information from the producing Party agrees not to further disclose such Information except as necessary to perform this CRADA or to other DOE facilities with the same protection in place.

The Party will mark the cover of any document containing Protected CRADA Information with the following legend:

“PROTECTED CRADA INFORMATION”

THIS DOCUMENT CONTAINS PROTECTED CRADA INFORMATION WHICH WAS PRODUCED ON _____ [DATE] UNDER CRADA NO. 97-F001 AND IS NOT TO BE FURTHER DISCLOSED FOR A PERIOD OF _____ [NOT TO EXCEED 5 YEARS] FROM THE DATE IT WAS PRODUCED EXCEPT AS EXPRESSLY PROVIDED FOR IN THE CRADA.”

In addition, the Party will mark each page of the document with the following legend: “PROTECTED CRADA INFORMATION.”

ARTICLE IX: CESSATION OF OBLIGATIONS REGARDING PROTECTED AND PROPRIETARY INFORMATION

The obligations relating to the disclosure or dissemination, or both, of Protected CRADA Information and Proprietary Information shall end if any such information becomes inadvertently publicly known or is developed independently by a Party's employees who did not have access to the information or was known by the Party or is received by the Party from a third party without obligation as to secrecy.

ARTICLE X: RIGHTS IN GENERATED INFORMATION

Each Party shall have unlimited rights in all Generated Information or information provided to the Parties under this CRADA which is not marked as being Protected CRADA Information or Proprietary Information or which is not an invention disclosure which may later be the subject of a U.S. or foreign patent application.

ARTICLE XI: EXPORT CONTROL

EACH PARTY IS RESPONSIBLE FOR ITS OWN COMPLIANCE WITH SUCH LAWS AND REGULATIONS.

ARTICLE XII: REPORTS AND ABSTRACTS

At the time the CRADA is submitted to the Laboratory Director for approval, the Participant will provide an abstract suitable for public release. The Parties will jointly prepare a final report, to include a list of subject inventions.

Use of the name of the other Party or its employees in any promotional activity, with reference to this CRADA, requires written approval of the other Party.

ARTICLE XIII: RIGHTS TO INVENTIONS

Disposition and allocation of rights in any Subject Invention made under this CRADA by any employee of the Parties to this CRADA shall be subject to the patent policy of Section 9 of the Federal Non-nuclear Energy Research and Development Act of 1974, 42 U.S.C. 5908 and other appropriate laws, regulations or policy, and shall, to the extent permitted by law, be subject to negotiations between the Parties.

Each Party shall have the first option to retain title to any Subject Invention solely made by its employees during the work under this CRADA. Each Party agrees to disclose to the other Party every Subject Invention that may be patentable or otherwise protectable under the Patent Act. The Parties will disclose Subject Inventions to each other within two (2) months after the inventor first discloses the Subject Invention in writing to the person(s) responsible for patent matters of the disclosing Party. If the Party having the first option to retain title to the Subject Invention elects either not to retain title, not to file and prosecute a patent application to issuance, or not to maintain an issued patent, then the other Party shall have the option of electing to retain title to such Subject Invention under this Agreement.

If the Participant elects to retain title to a Subject Invention, or chooses an exclusive license to a FETC employee Subject Invention as provided below, the Government shall retain a nonexclusive, non-transferable, irrevocable, paid-up license to practice, or to have practiced, for or on its behalf all elected or exclusively licensed Subject Inventions throughout the world.

For Subject Inventions under this CRADA which are joint Subject Inventions made by the DOE and the Participant, the Participant shall have the option of electing to retain title to its undivided rights and, if this option is elected, title to such Subject Inventions shall be jointly owned by the DOE and the Participant.

The Participant shall have the option to choose an exclusive license for second generation pressurized fluidized bed combustion technology for any patents or patent applications made in whole or in part by employees of DOE/FETC under this CRADA. This option shall only be available to the Participant for a period not to exceed one year after the date on which a United States patent issues on the Subject Invention. Such license shall be evidenced by a mutually agreeable licensing agreement between the Parties, including reasonable compensation, commercialization milestones, a U.S. Competitiveness Clause, March-in Provisions and other reasonable terms and conditions.

ARTICLE XIV: REPORTS OF INVENTION USE

The Participant agrees to submit, upon request of DOE, reports no more frequently than annually on the efforts to obtain utilization of any waived Subject Invention to which the Participant holds title in accordance with 41 CFR 9-9.

ARTICLE XV: DOE MARCH-IN RIGHTS

The Participant recognizes that the DOE has certain march-in rights to any waived Subject Inventions in accordance with 48 CFR 27.304-1(g).

ARTICLE XVI: U.S. COMPETITIVENESS

The Parties agree that a purpose of this CRADA is to provide substantial benefit to the U.S. economy. In exchange for the benefits received under this CRADA, the Parties therefore agree to the following:

A. Products embodying Intellectual Property developed under this CRADA shall be substantially manufactured in the United States,

B. Processes, services, and improvements thereof which are covered by Intellectual Property developed under this CRADA shall be incorporated into the Participant's manufacturing facilities in the United States either prior to or simultaneously with implementation outside the United States. Such processes, services, and improvements, when implemented outside the U.S., shall not result in reduction of the use of the same processes, services, or improvements in the United States.

The requirement of this Article XVI may be waived by the DOE upon a showing by the Participant that reasonable but unsuccessful efforts have been made or that, under the circumstances, such requirements are not commercially reasonable.

ARTICLE XVII: FORCE MAJEURE

Neither Party will be liable for unforeseeable events beyond its reasonable control. However, in the event circumstances dictate, the Parties may mutually agree to a time extension covering delays caused by unforeseeable, or foreseeable but unavoidable, events.

ARTICLE XVIII: TERMINATION

Participation by FETC in this CRADA is subject to the availability of appropriated funds. This CRADA may be terminated by either Party upon thirty (30) days written notice to the other. Each Party shall be responsible for its costs incurred through the effective date of termination as well as its costs incurred after the effective date of termination and which are related to the termination. Any non-use or confidentiality obligations of the CRADA shall survive any termination of this CRADA except under the conditions provided for in Article IX.

ARTICLE XIX: NOTICES

A. Any communications required by this CRADA shall be deemed made if mailed by postage prepaid first class U.S. Mail addressed to the Party to receive the communication as of the day of receipt of such communication by the addressee or on the date given if by verified facsimile. Address changes shall be given in accordance with this Article and shall be effective thereafter. All such communications, to be considered effective, shall include this CRADA Number.

B. The points of contact for the Parties are as follows:

FETC

Technical Contact:	Administrative Contact:
Edward J. Boyle	R. Diane Manilla
U.S. Department of Energy	U.S. Department of Energy
P.O. Box 880	P.O. Box 880
Morgantown, WV 26505	Morgantown, WV 26505
Phone: (304) 285-4000	Phone: (304) 285-4086
Fax: (304) 285-4469	Fax: (304) 285-4469
E-mail: EBOYLE@METC.DOE.GOV	E-mail: RMANIL@METC.DOE.GOV

Participant

Technical Contact:	Administrative Contact:
Soung M. Cho	Mitchell D. Garber
Foster Wheeler Development	Foster Wheeler Development
Corporation	Corporation
12 Peach Tree Hill Road	12 Peach Tree Hill Road
Livingston, NJ 07039	Livingston, NJ 07039
Phone: (201) 535-2322	Phone: (201) 535-2533
Fax: (201) 535-2242	Fax: (201) 535-2242
E-mail: soung_cho@fwc.com	E-mail: mitch_garber@fwc.com

ARTICLE XX: ENTIRE CRADA AND MODIFICATIONS

A. This document represents the entire agreement reached between the Parties in performing the research described in Article II, Statement of Work, and becomes effective on the date the Laboratory Director signs the document. Any agreement to materially change any terms or conditions shall be valid only if the change is made in writing, and executed by the Parties.

B. The terms of the CRADA, unless otherwise specified, shall remain in effect for one (1) year, commencing on the date the Laboratory Director signs this agreement.

FOR DOE:

By
Rita A. Bajura
Director, FETC

Date

For Participant:
By
Folke Engstrom
Vice President, Foster Wheeler Development Corporation

Date

APPENDIX B: NETL COLD FLOW CIRCULATING FLUIDIZED BED SIMULATION

```
#  
# Simulation of FETC's  
#   Cold Flow Circulating Fluidized Bed System  
#  
# Simulation Uses Values Taken From Testing Performed On  
#   6/02/98 - Run L3 For PVC  
#  
# RISER  
#   60 feet tall  
#   12 inches ID  
#  
#   RISER FLOW  
#     Riser Flow is 39 KSCFH  
#     Riser Diameter is 12 in.  
#     Riser Area = pi*.5*.5 = .7854 ft^2  
#     Riser Velocity = 39,000/.7854 = 49,656 ft/hr  
#     Riser velocity = 49,656/3600 = 13.79 ft/sec  
#     Riser Velocity = 13.79 ft/sec * 12 * 2.54 = 420.4 cm/sec  
#  
# CROSSOVER  
#   4 feet long  
#   8 inches ID  
#   Top of Crossover is 7 in. from top of Riser  
#  
# CYCLONE  
#   2-D cyclone at the end of cross-over  
#   Discharge from cyclone is to the LEFT of the Cyclone  
#   Not out the top of the stanndpipe.  
#   This arrangement performs better than other configurations and  
#   Allows a more simple geometry.  
#  
# STAND PIPE  
#   10 inches ID  
#   Bottom of Move air enters across from "L" valve  
#   And bottom of slot is 4.75 inches above top of "L" valve  
#  
# "L" VALVE  
#   10 inches ID  
#  
# Rectangular geometry used assuming no wall effects from  
#   front and back walls  
#  
#  
# Move Air Velocity = 125 SCFH  
#   Since The Aeration Air Really Enters At Basicaly A Point  
#   Source (a 1 inch fitting in the side of the riser)  
#   Inlet Velocity Is Determined By Calculating  
#   Velocity Of Air Going Up Stand Pipe And Converting  
#   That Velocity To That Through The Inlet  
#  
#   125 SCFH / ((PI*5*5)/144) = 229 ft/hr = 0.0637 ft/sec  
#   0.0637 ft/sec = 1.94 cm/sec  
#  
#   1.94 cm/sec Up The Stand Pipe  
#  
# Note Assume that the aeration inlet is actually 12 cm in diameter  
#   (Simulation has a slot 12 cm tall)
```

```

#
# Therefore inlet velocity is
# 1.94 * (10*2.54)/12 = 4.11 cm/sec
#
#
# Aeration Air Velocity At Bottom Of Standpipe (Radius = 5 inch) is
# 80 SCFH / ((PI*5*5)/144) = 146.7 ft/hr = 0.041 ft/sec
# 0.041 ft/sec = 1.24 cm/sec
#
# L-Valve Has No Aeration!
#
# Solids flow from external to the system = 0.0
#
# Simulation time = 40 seconds
#
# Simulation starts out with riser filled with void fraction = 0.40
#
# Chris Ludlow
# September 10, 1999
#
# ****
# Run Control Section
# ****
#
#           RUN_NAME      =  'CFCFB'
#           DESCRIPTION   =  'COLD FLOW MODEL'
#           RUN_TYPE     =  'NEW'
#           UNITS        =  'CGS'
#           TIME         =  0.0
#           TSTOP        =  40.0
#           DT           =  1.00E-04
#
#           ENERGY_EQ    =  .FALSE.
#           SPECIES_EQ(0) =  .FALSE.
#           SPECIES_EQ(1) =  .FALSE.
#
#           UR_FAC(2)    =  0.2
#
#
# ****
# GEOMETRY SECTION
# ****
#
#           COORDINATES  =  'CARTESIAN'
#           XLENGTH     =  178.0 ! 70" = 177.8 cm
#           YLENGTH     =  1828.0 ! 60' = 720" = 1,829 cm
#           IMAX        =  89   ! X RATIO = 2:1
#           JMAX        =  457  ! Y RATIO = 4:1
#           NO_K        =  .TRUE.
#
#
# ****
# GAS-PHASE SECTION
# ****
#
#           MU_G0       =  1.80E-04
#           MW_AVG     =  29.0
#
#

```

```

# ****
# SOLIDS-PHASE SECTION
# ****
#
#          RO_S      =      1.42 !  PVC plastic
#          D_P      =      0.02 !  200 micron particles
#          E      =      0.8
#          PHI     =      45.0
#          EP_STAR =      0.387
#
#
# ****
# INITIAL CONDITIONS SECTION
# ****
#
# Establish overall initial condition
#
#          IC_X_W(1)  =      0.0
#          IC_X_E(1)  =     178.0
#          IC_Y_S(1)  =      0.0
#          IC_Y_N(1)  =    1828.0
#
#          IC_EP_G(1) =      1.0
#          IC_P_G(1)  =  1.013E+06
#
#          IC_U_G(1)  =      0.0
#          IC_V_G(1)  =      0.0
#
#          IC_T_G(1)  =     300.0
#
#
# ESTABLISH INITIAL BED WITHIN STANDPIPE
# STANDPIPE HAS 40 FEET OF INVENTORY
#
#          IC_X_W(2)  =      0.0
#          IC_X_E(2)  =     26.0
#          IC_Y_S(2)  =      0.0
#          IC_Y_N(2)  =    1216.0
#
#          IC_EP_G(2) =      0.388
#
#          IC_U_G(2)  =      0.0
#          IC_V_G(2)  =      0.0
#
#          IC_U_S(2,1) =      0.0
#          IC_V_S(2,1) =      0.0
#
#          IC_P_STAR(2) =      0.0
#          IC_T_G(2)   =     300.0
#
#
# ESTABLISH INITIAL BED INVENTORY IN "L" VALVE
#
#          IC_X_W(3)  =     26.0
#          IC_X_E(3)  =    148.0
#          IC_Y_S(3)  =     60.0
#          IC_Y_N(3)  =    84.0
#
#          IC_EP_G(3) =      0.388

```

```

    IC_U_G(3) = 0.0
    IC_V_G(3) = 0.0

    IC_U_S(3,1) = 0.0
    IC_V_S(3,1) = 0.0

    IC_P_STAR(3) = 0.0
    IC_T_G(3) = 300.0

#
#
#
# Establish "Cyclone" Gravity
#
#           C(1) = 200000 ! 200,000/980 = 204 g's
#                               ! Constant is Positive because
#                               ! Force is to the RIGHT
#
#
# BOUNDARY CONDITIONS
#
#
# *****
# GEOMETRY BOUNDARY CONDITIONS
# *****
#
# Block Of Cells Above Gas Cross Over
#
    BC_X_W(1) = 0
    BC_X_E(1) = 148
    BC_Y_S(1) = 1800
    BC_Y_N(1) = 1828
    BC_TYPE(1) = 'NSW'

#
# Block of Cells Between the Riser and Stand Pipe
#
    BC_X_W(2) = 26
    BC_X_E(2) = 148
    BC_Y_S(2) = 84
    BC_Y_N(2) = 1780
    BC_TYPE(2) = 'NSW'

#
# Block of Cells Under "L" valve
#
    BC_X_W(3) = 26
    BC_X_E(3) = 148
    BC_Y_S(3) = 0
    BC_Y_N(3) = 60
    BC_TYPE(3) = 'NSW'

#
# Block of Cells to Break up Solids Flow Down Standpipe Wall
#
    BC_X_W(4) = 0
    BC_X_E(4) = 4
    BC_Y_S(4) = 1592
    BC_Y_N(4) = 1596
    BC_TYPE(4) = 'NSW'

    BC_X_W(5) = 22
    BC_X_E(5) = 26
    BC_Y_S(5) = 1592

```

```

        BC_Y_N(5)      =      1596
        BC_TYPE(5)     =      'NSW'
#
# INTERNAL SEMI-PERMIABLE MEMBRANE SURFACE FOR THE OUTLET
# THIS IS TO ALLOW GAS OUT AND RETAIN SOLIDS
#
# THIS MAY BE ADJUSTED TO GIVE AN APPROPRIATE PRESSURE DROP
# FOR THE CYCLONE
#
        IS_X_W(1)      =      0.0
        IS_X_E(1)      =      0.0
        IS_Y_S(1)      =      1716.0
        IS_Y_N(1)      =      1748.0
        IS_TYPE(1)     =      'SP'
        IS_PC(1,1)     =      1.0E32
        IS_PC(1,2)     =      0.0
#
#
#
# *****
#      FLOW BOUNDARY CONDITIONS
# *****
#
#      Riser Inlet Gas Velocity = 13.8 ft/sec
#
        BC_X_W(6)      =      148.0
        BC_X_E(6)      =      178.0
        BC_Y_S(6)      =      0.0
        BC_Y_N(6)      =      0.0
        BC_TYPE(6)     =      'MI'

        BC_EP_G(6)     =      1.0

        BC_U_G(6)      =      0.0
        BC_V_G(6)      =      420.0 !13.8 ft/sec
        BC_U_S(6,1)    =      0.0
        BC_V_S(6,1)    =      0.0

        BC_P_G(6)      =      1.013E+06

        BC_T_G(6)      =      300.0
#
#
#      Exit Boundary Condition
#
        BC_X_W(7)      =      0.0
        BC_X_E(7)      =      0.0
        BC_Y_S(7)      =      1716.0
        BC_Y_N(7)      =      1748.0

        BC_TYPE(7)     =      'PO'

        BC_P_G(7)      =      1.013E+06

        BC_T_G(7)      =      300.0
#
#
#      Establish Aeration Air at the bottom of the stand pipe
#
        BC_X_W(8)      =      0.0

```

```

      BC_X_E(8)      =      26.0
      BC_Y_S(8)      =      0.0
      BC_Y_N(8)      =      0.0

      BC_TYPE(8)     =      'MI'

      BC_EP_G(8)     =      1.0

      BC_U_G(8)      =      0.0
      BC_V_G(8)      =      0.5 !Very Low Flow To Let Solids Settle
      BC_U_S(8,1)    =      0.0
      BC_V_S(8,1)    =      0.0

      BC_P_G(8)      =      1.013E+06

      BC_T_G(8)      =      300.0
#
# ADDITIONAL MOVE AIR ABOVE "L" VALVE
#
      BC_X_W(9)      =      0
      BC_X_E(9)      =      0
      BC_Y_S(9)      =      108
      BC_Y_N(9)      =      120
      BC_TYPE(9)     =      'MI'
      BC_EP_G(9)     =      1.0
      BC_U_G(9)      =      0.0 !No Move Air
      BC_V_G(9)      =      0.0
      BC_U_S(9,1)    =      0.0
      BC_V_S(9,1)    =      0.0
      BC_P_G(9)      =      1.013E+06
      BC_T_G(9)      =      300.0
#
#
#
# OUTPUT CONTROL
#
      RES_DT      =      0.0005
      SPX_DT(1)    =      0.010
      SPX_DT(2)    =      0.1
      SPX_DT(3)    =      0.1
      SPX_DT(4)    =      0.1
      SPX_DT(5)    =      100
      SPX_DT(6)    =      100
      SPX_DT(7)    =      100
      SPX_DT(8)    =      100
      NLOG        =      100
      FULL_LOG    =      .TRUE.

```

APPENDIX C: MFIX Code Modifications to “usr0.f” and “b-force2.inc”

```
DOUBLE PRECISION FUNCTION BFX_s(IJK, M)
USE param
USE param1
USE constant
USE geometry
USE indices

IMPLICIT NONE
INTEGER IJK, M
INTEGER i, j
INCLUDE 'function.inc'
i = I_OF(IJK)
j = J_OF(IJK)

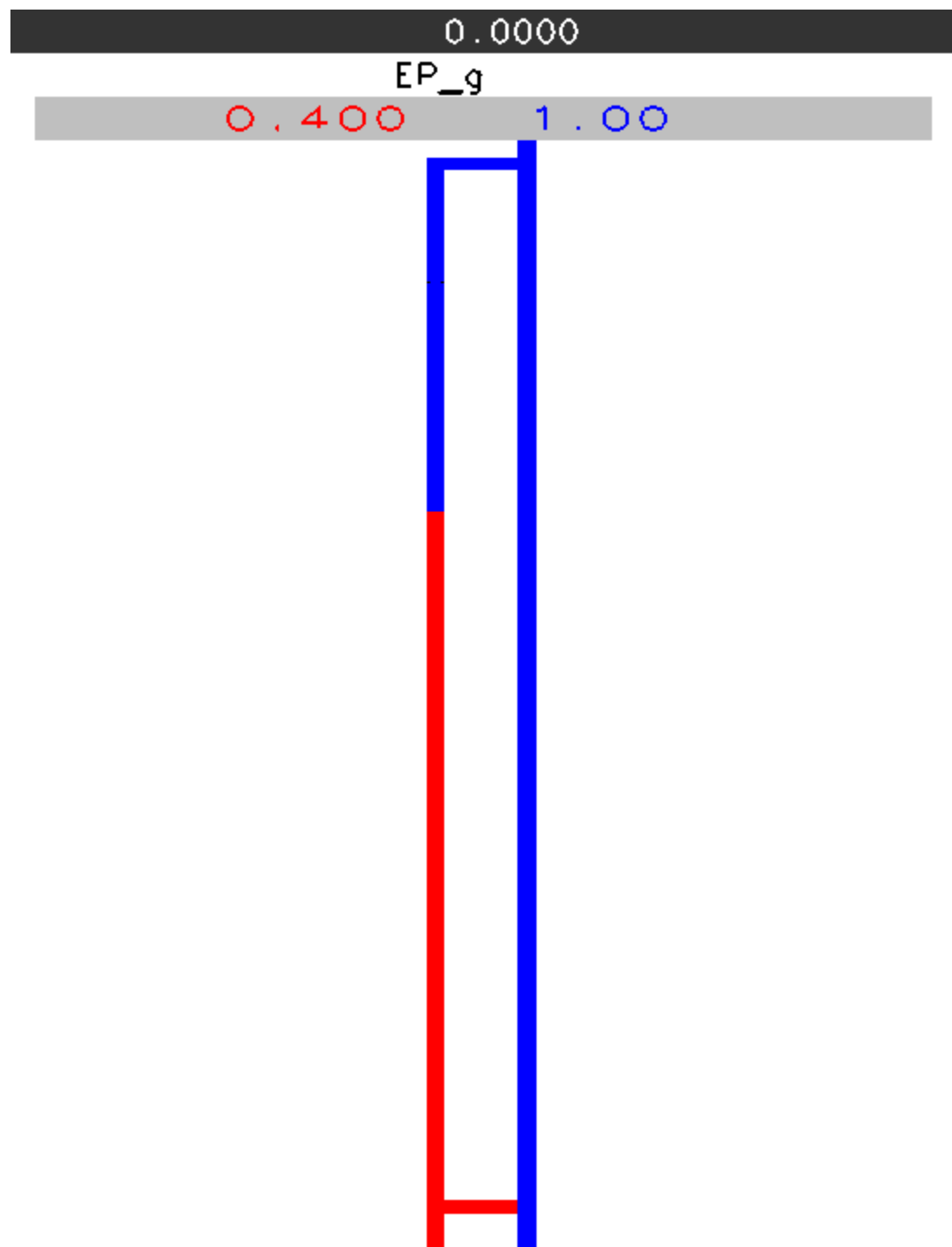
!      Specify a body force C(1) for the solids phase in the x direction
!      if 1>=i<=11 and 40>=j<=45.  When determining i and j, remember that
!      there is a one layer of fictitious cells at the boundary.
!      C(1) is specified in the input file
if(i .ge. 1 .and. i .le. 4 .and. &
   j .ge. 430 .and. j .le. 438) then
  BFX_s = C(1)
else
  BFX_s = ZERO
endif

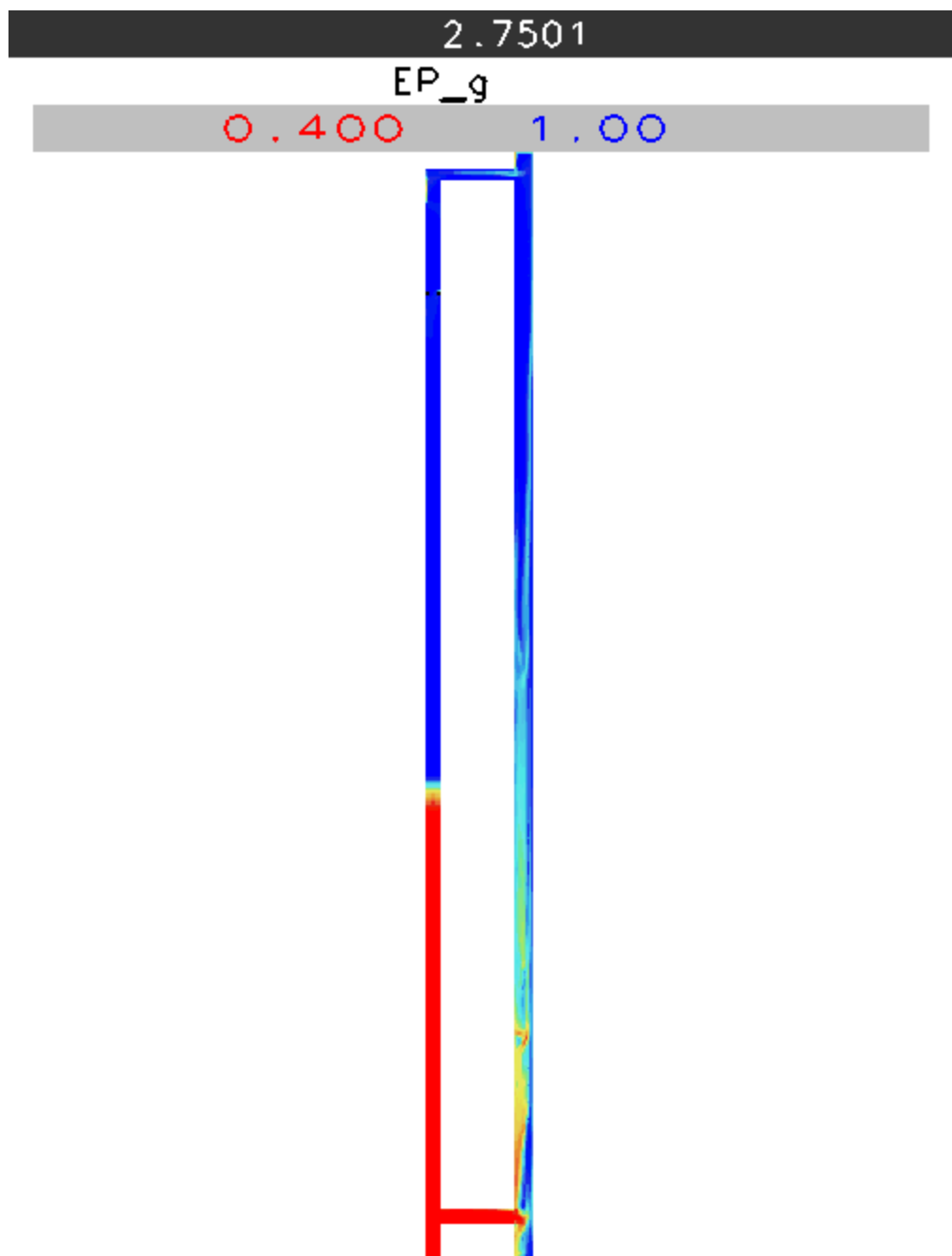
      return
      end

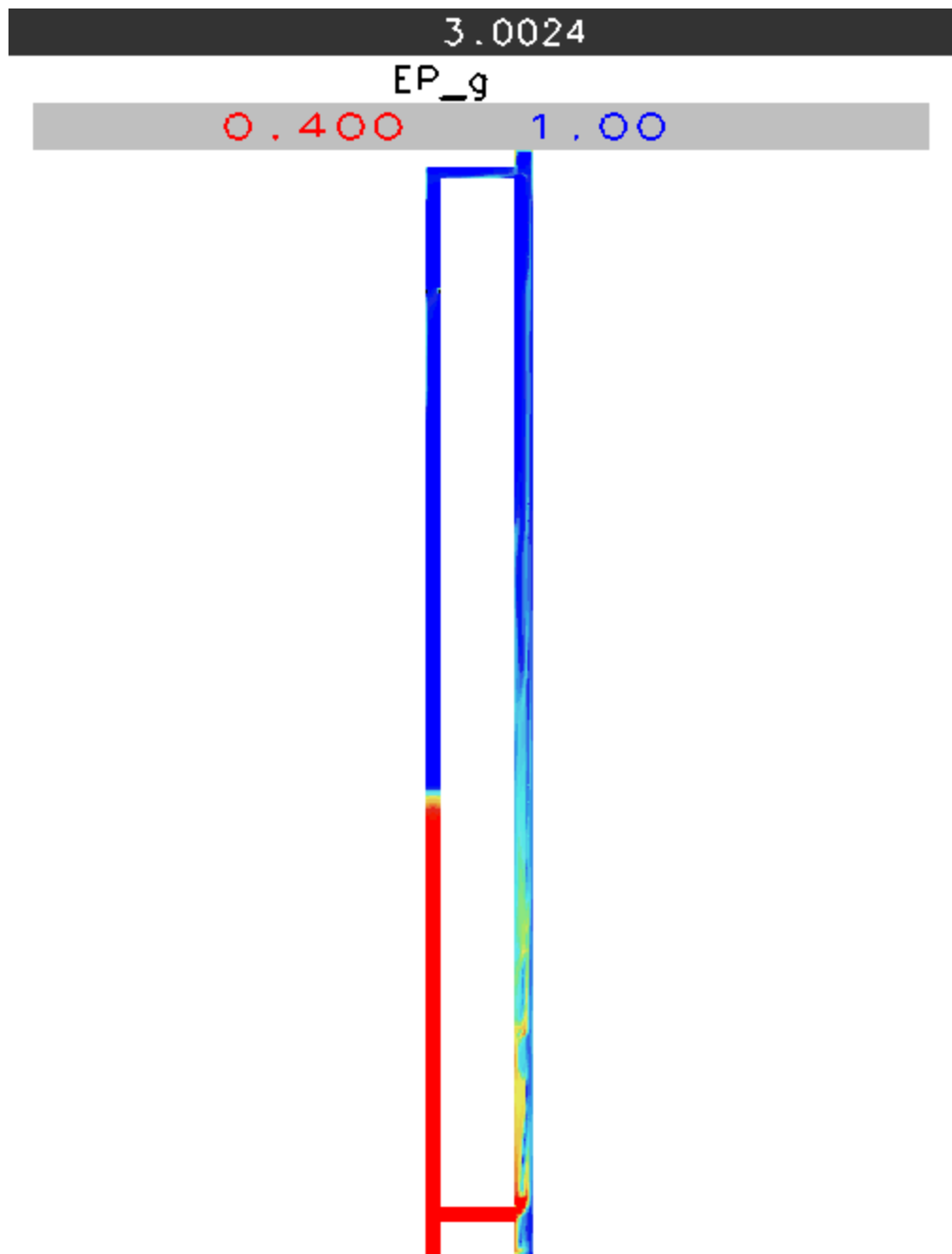
!vvvvvvvvvvvvvvvvvvvvvvvvvvvvvvvvvvvvvvvvvvvvvvvvvvvvvvvvvvvvvvvvvvvvvvvvvvvvvvvC
!                                         C
!  Module name: USR0                               C
!  Purpose: This routine is called before the time loop starts and is      C
!           user-definable.  The user may insert code in this routine      C
!           or call appropriate user defined subroutines.  This           C
!           can be used for setting constants and checking errors in      C
!           data.  This routine is not called from an IJK loop, hence      C
!           all indices are undefined.                           C
!
!           Author:                               Date: dd-mmm-yy   C
!           Reviewer:                            Date: dd-mmm-yy   C
!
!           Revision Number:                   C
!           Purpose:                           C
!           Author:                            Date: dd-mmm-yy   C
!           Reviewer:                           Date: dd-mmm-yy   C
!
!           Literature/Document References:   C
!
!           Variables referenced:           C
!           Variables modified:            C
!
!           Local variables:             C
!
!^^^^^^^^^^^^^^^^^^^^^^^^^^^^^^^^^^^^^^^^^^^^^^^^^^^^^^^^^^^^^^^^^^^^^^^^C
!
SUBROUTINE USR0
!...Translated by Pacific-Sierra Research VAST-90 2.06G5 12:17:31 12/09/98
!...Switches: -xf
```

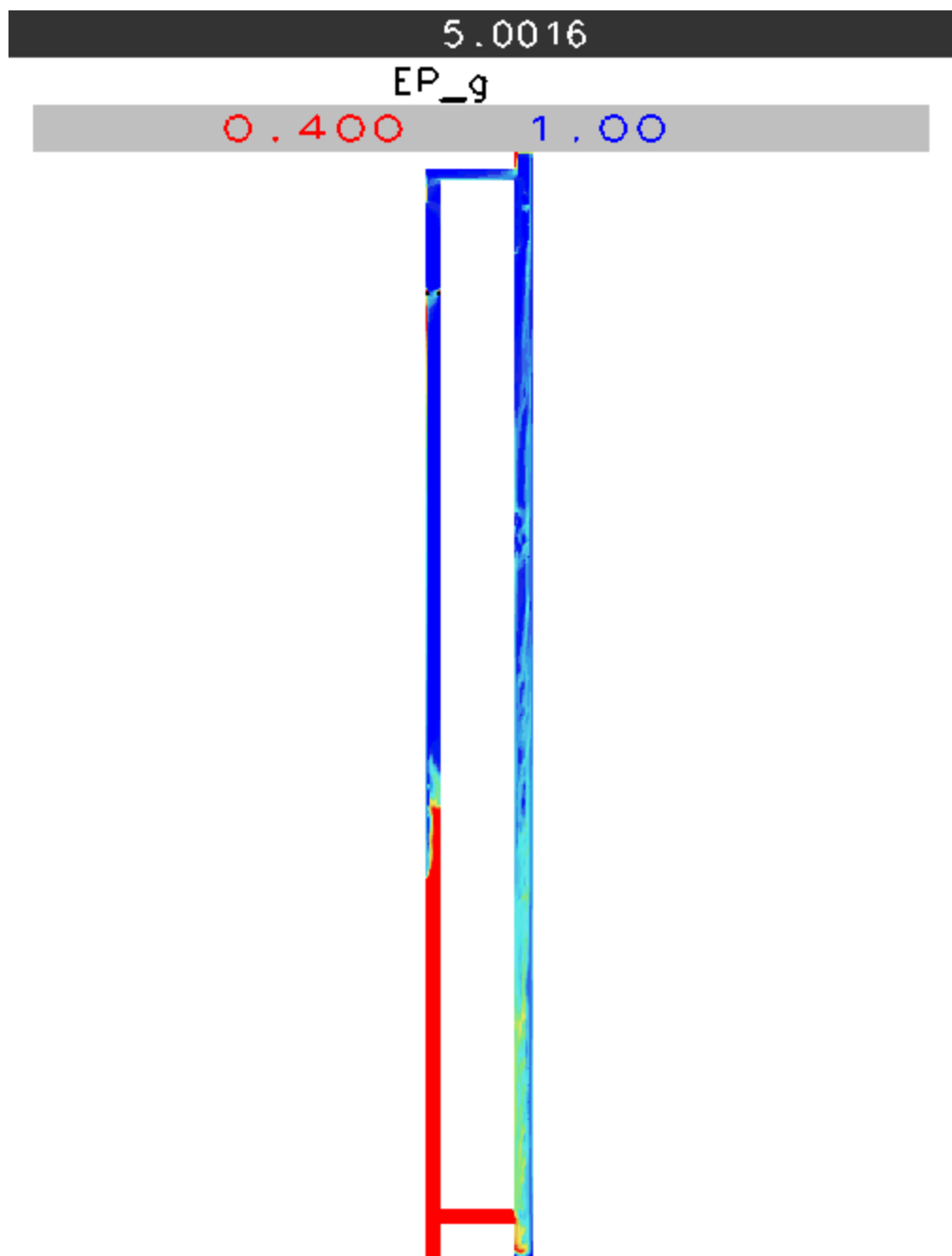
```
IMPLICIT NONE
!-----
!
! Include files defining common blocks here
!
!
! Define local variables here
!
!
! Include files defining statement functions here
!
!
! Insert user-defined code here
!
!
RETURN
END SUBROUTINE USR0
```

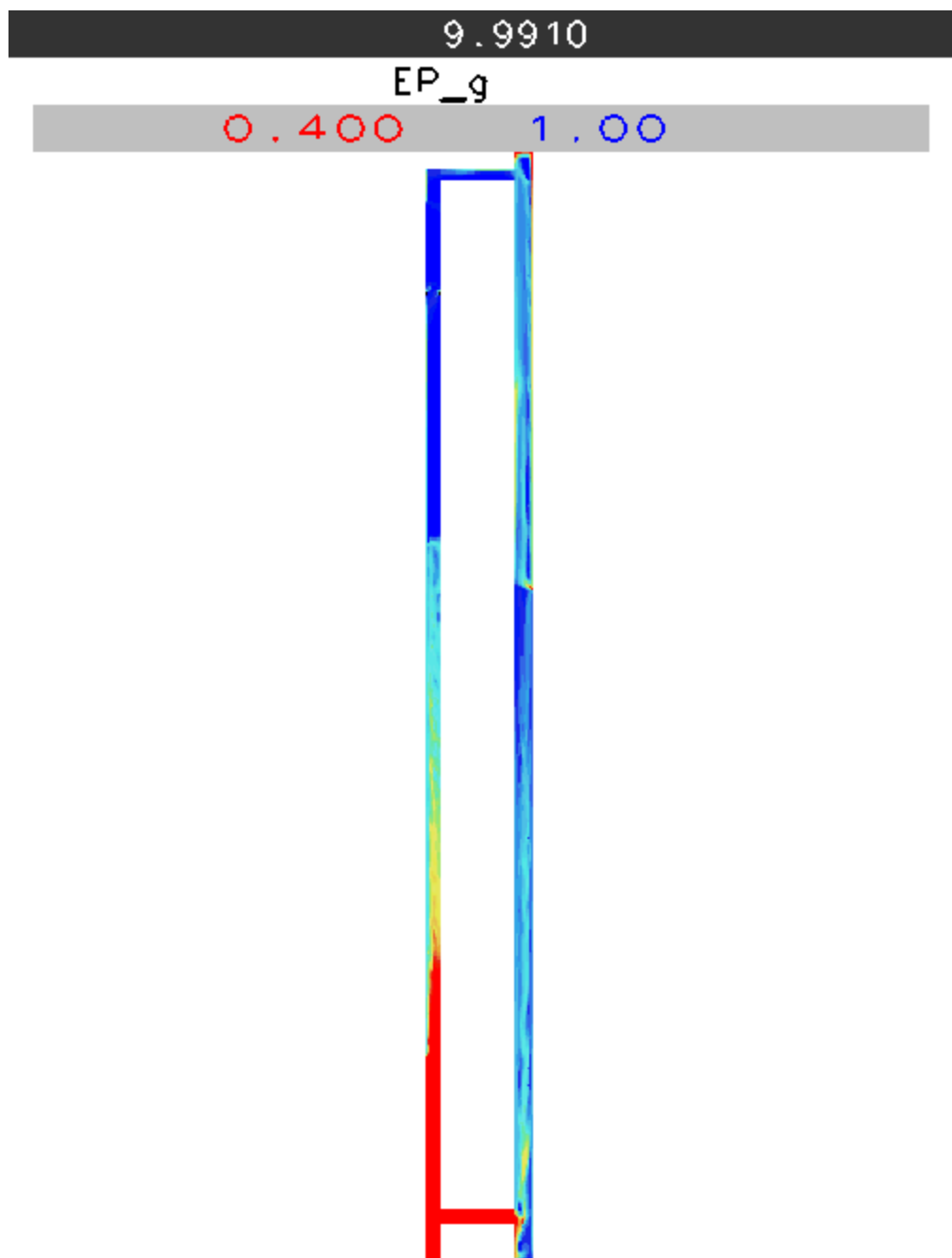
APPENDIX D: MFIX Predictions of Solids Distribution Within NRTL Circulating Fluidized Bed

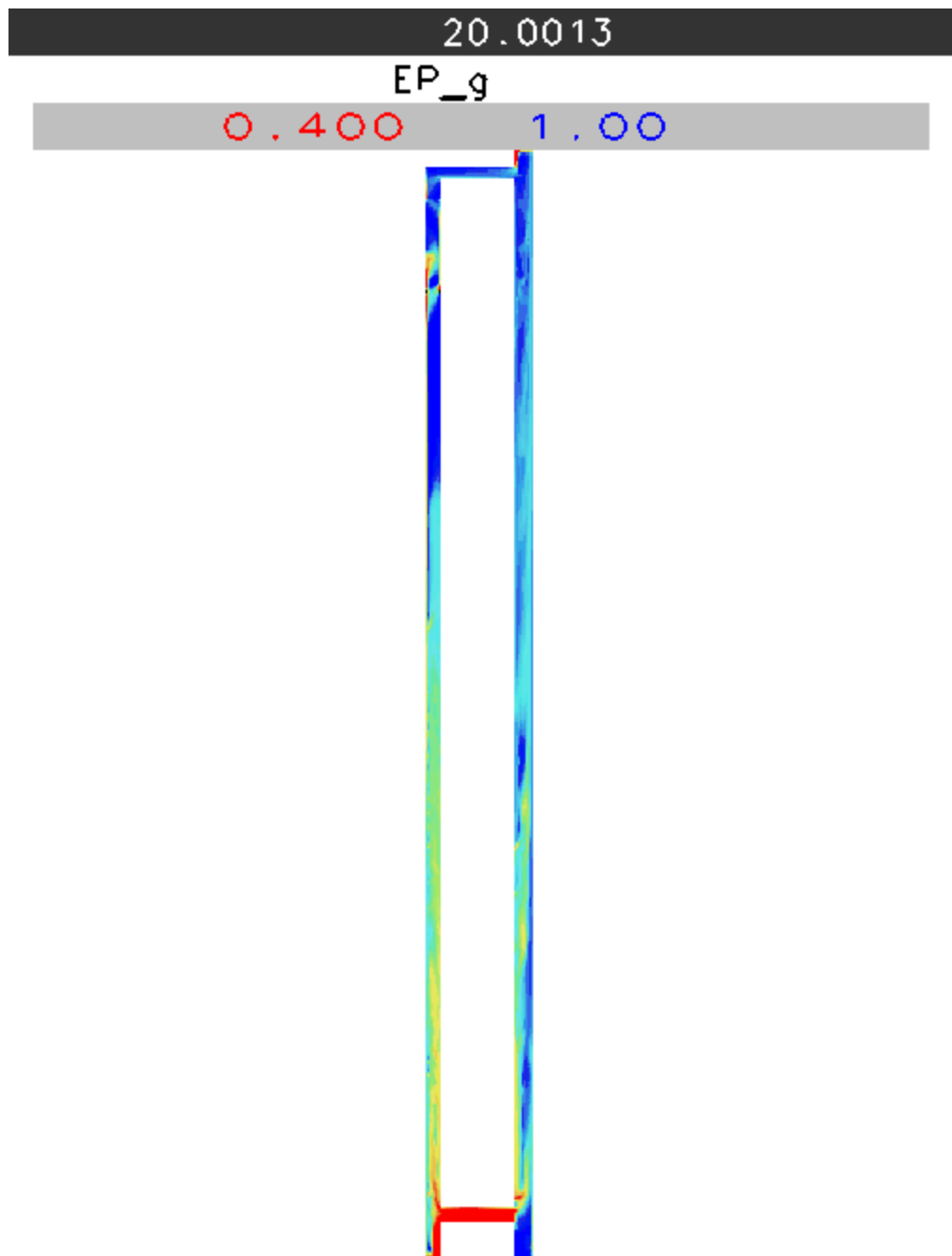


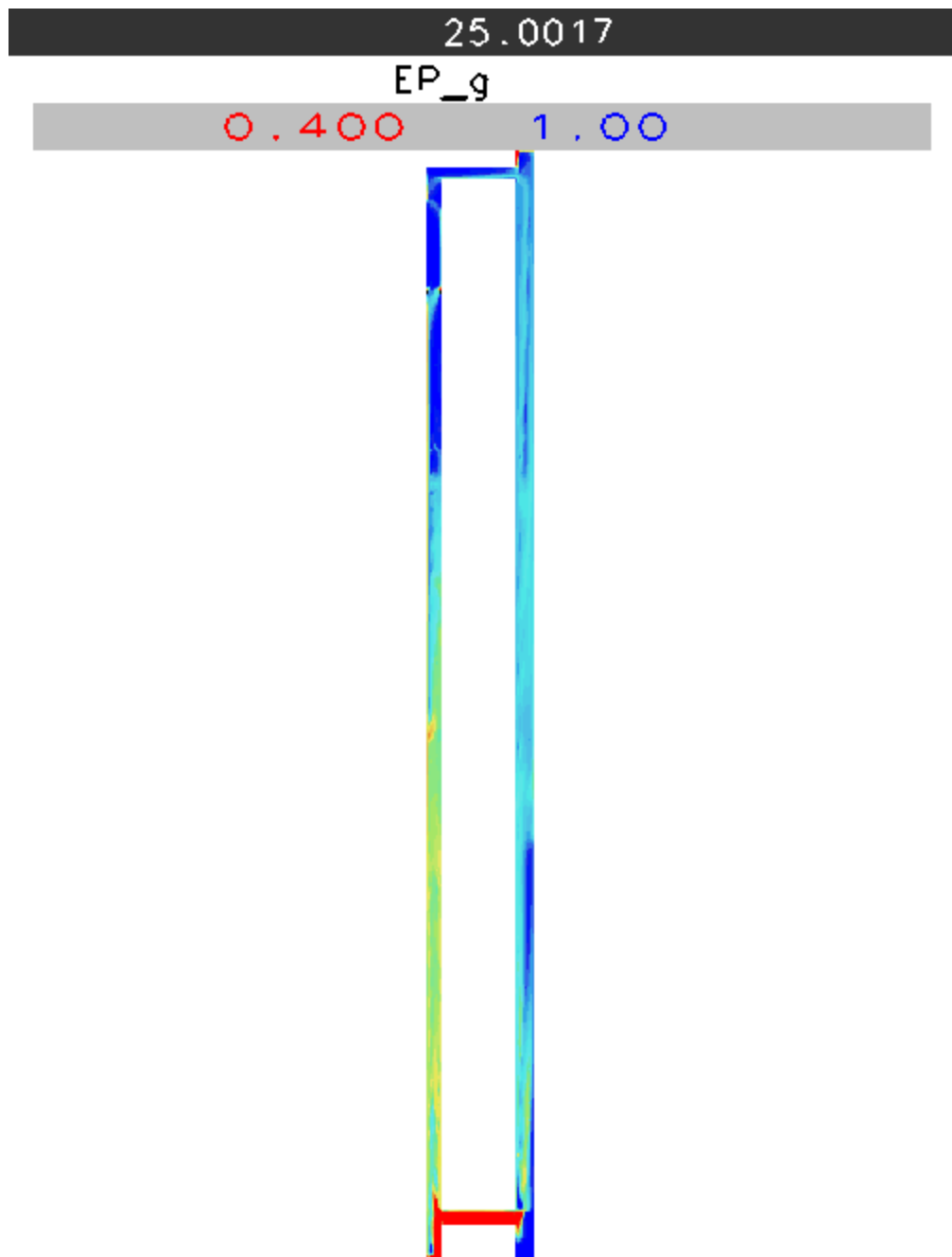


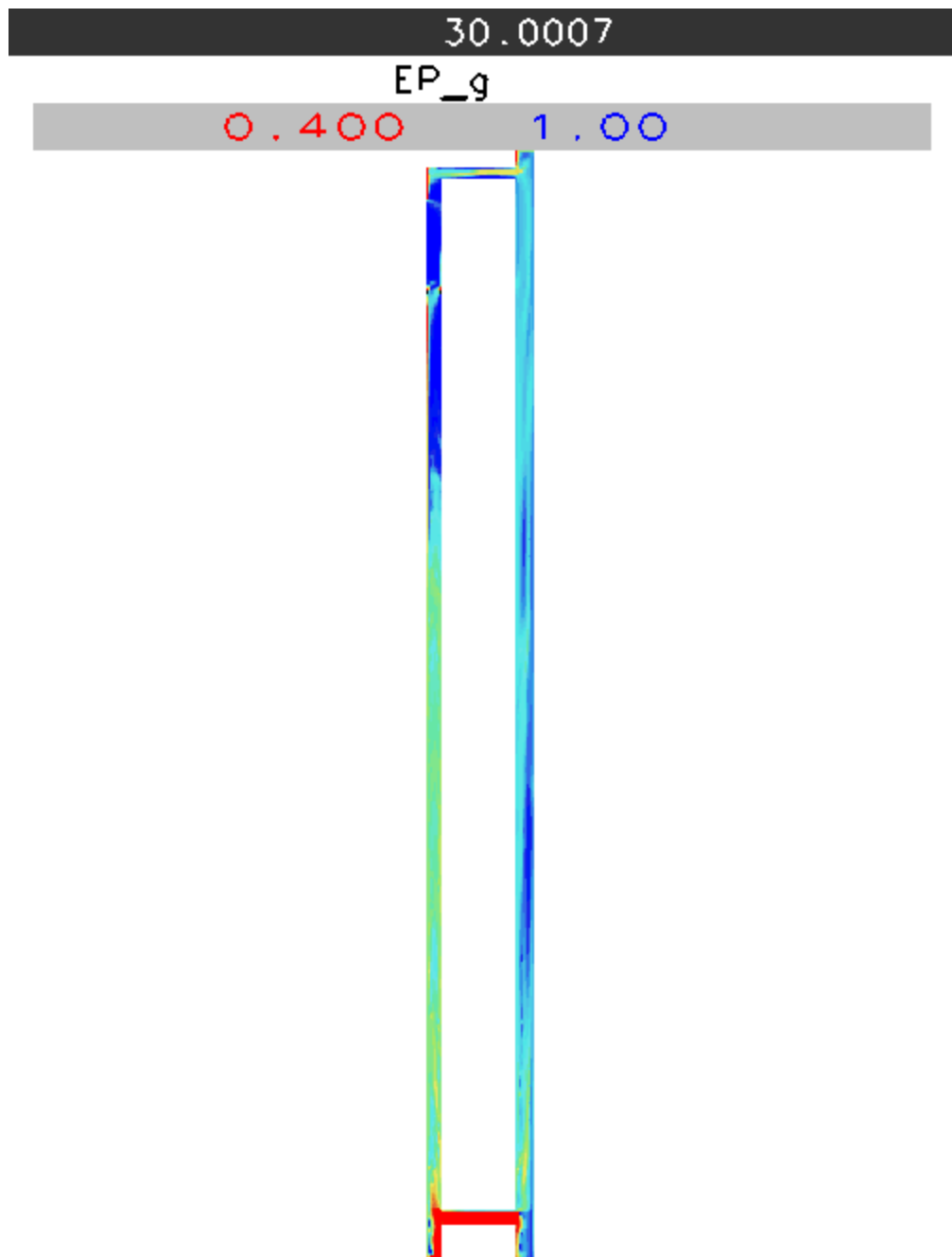


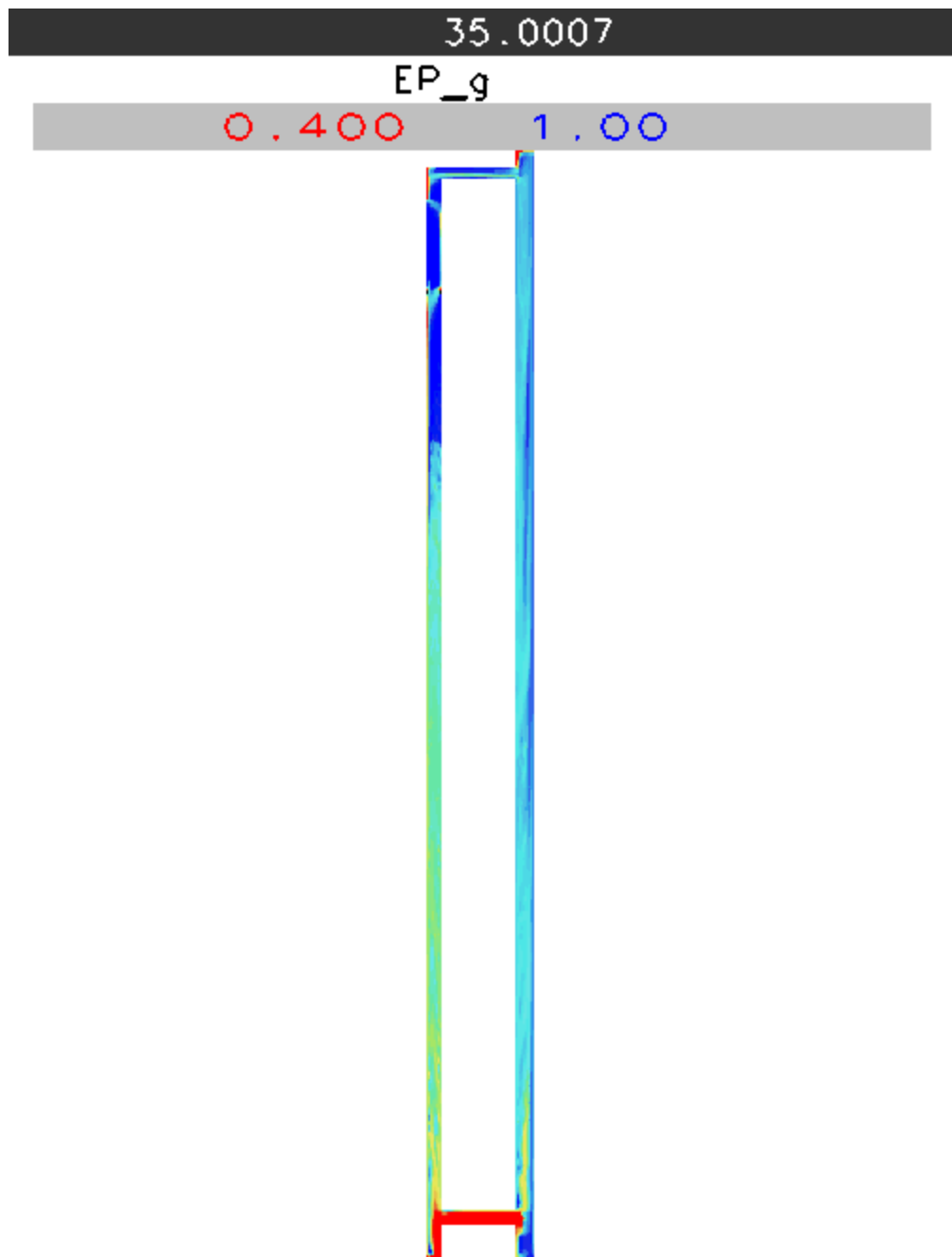


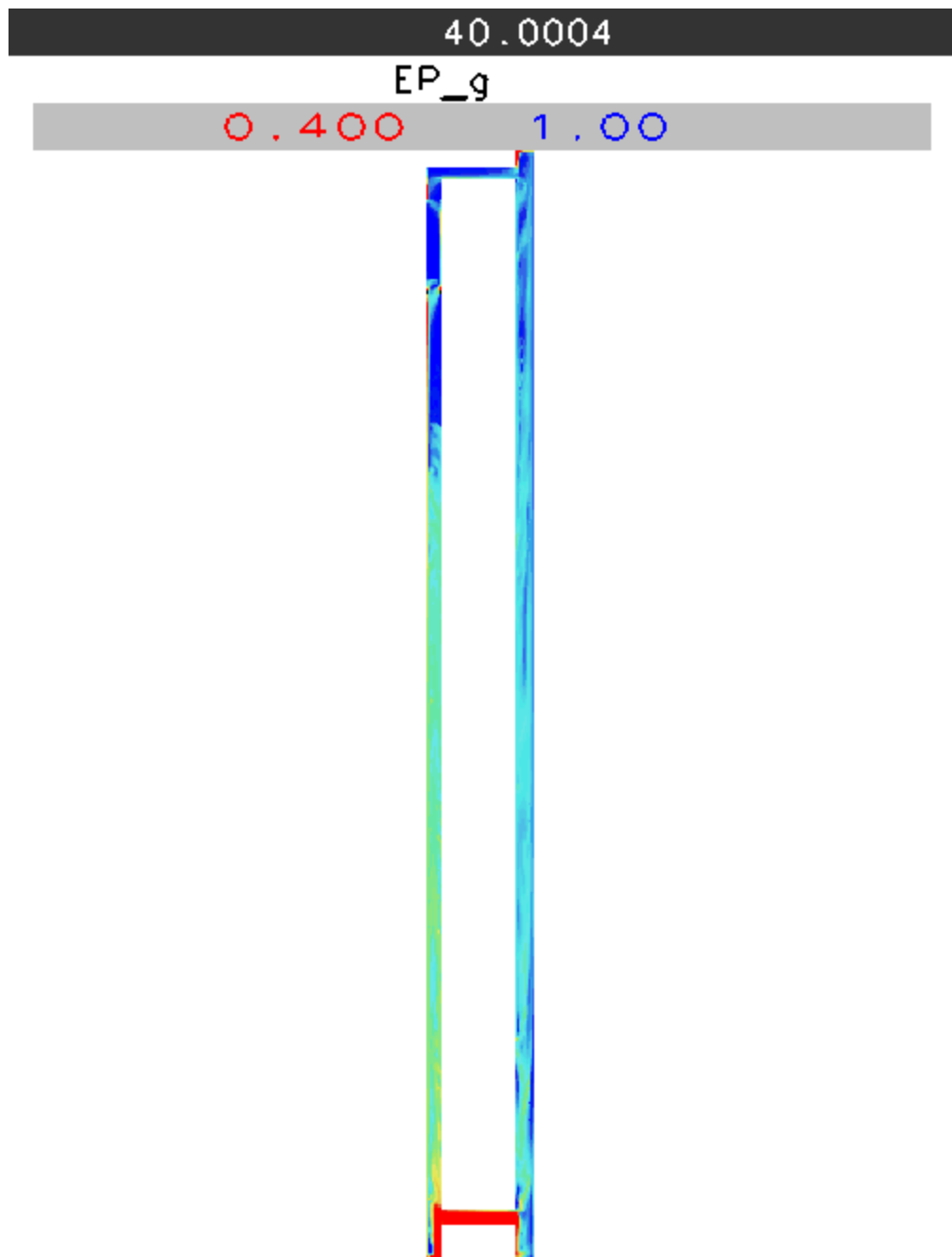












APPENDIX E: MFIX Input File for the Simulation of the FW Pilot Plant Cold Flow Unit

```
#FW CFB pilot plant cold model simulation for CRADA
#Modeler: Jinliang Ma of FWDC
#Date: 12/24/99

#RUN CONTROL SECTION
RUN_NAME='Case' !generic name for output files
DESCRIPTION='FW CFB Pilot Plant' !description
UNITS='CGS' !centimeter/gram/second unit system
RUN_TYPE='new' !new run, no restart
TIME=1.0 !start time
TSTOP=11.0 !stop time
DT=1.0e-4 !initial time step
ENERGY_EQ=.FALSE. !not solving energy equation
SPECIES_EQ(0)=.FALSE. !not solving gas species equations
SPECIES_EQ(1)=.FALSE. !not solving solid species equations
CALL_USR=.FALSE. !no user-defined routines

#PHYSICAL PARAMETERS
C_e=0.8 !coefficient of restitution, used to be e=0.8
Phi=0.0 !0.0=no plastic regime stress
ur_fac(2)=0.2 !solids phase urf, default 0.5

#GEOMETRY SECTION
COORDINATES='CARTESIAN' !Cartesian coordinate system
XLENGTH=213.4 !reactor depth
IMAX=21 !number of nodes in x direction
YLENGTH=1371.6 !reactor height, gravity in -y direction
JMAX=137 ! number of nodes in y direction
ZLENGTH=182.9 !reactor width
KMAX=3 !number of nodes in direction

#GAS SECTION
MW_avg=29.0 !constant molecular weight of gas
MU_g0=1.8e-4 !constant viscosity of gas

#PARTICLE SECTION
MMAX=1
D_p=0.0426 !average particle diameter
RO_s=1.51 !particle density
EP_star=0.4 !packed bed void fraction

# INITIAL CONDITIONS SECTION
IC_x_w(1)=0.0 !west wall
IC_x_e(1)=213.4 !east wall
IC_y_s(1)=0.0 !south wall
IC_y_n(1)=1371.6 !north wall
IC_z_b(1)=0.0 !bottom wall
IC_z_t(1)=182.9 !top wall
IC_ep_g(1)=1.0 !initial void fraction
IC_P_G(1)=1115830.0
IC_U_g(1)=0.0 !initial gas u-velocity
IC_V_g(1)=200.0 !initial gas v-velocity
IC_W_g(1)=0.0 !initial gas w-velocity
IC_T_g(1)=317.6 !initial gas temperature in [K]

# BOUNDARY CONDITIONS SECTION
!air inlet
BC_x_w(1)=0.0 !1st inlet face geometry
```

```

BC_x_e(1)=213.4
BC_y_s(1)=0.0
BC_y_n(1)=0.0
BC_z_b(1)=0.0
BC_z_t(1)=182.9
BC_TYPE(1)='MI' !mass_inflow boundary condition
BC_ep_g(1)=1.0 !void factor of inflow
BC_P_g(1)=1115830.0 !gas pressure at the inlet face
BC_T_g(1)=317.6 !gas temperature at the inlet face
BC_U_g(1)=0.0 !u-velocity of gas at the inlet face
BC_V_g(1)=243.8 !v-velocity of gas at the inlet face
BC_W_g(1)=0.0 !w-velocity of gas at the inlet face
BC_U_s(1,1)=0.0 !u-velocity of solid at the inlet face
BC_V_s(1,1)=0.0 !v-velocity of solid at the inlet
BC_W_s(1,1)=0.0 !w-velocity of solid at the inlet face
!solids inlet
BC_x_w(2)=94.0 !2nd inlet face geometry
BC_x_e(2)=119.4
BC_y_s(2)=61.0
BC_y_n(2)=139.7
BC_z_b(2)=0.0
BC_z_t(2)=0.0
BC_TYPE(2)='MI' !mass_inflow boundary condition
BC_ep_g(2)=0.4
BC_P_g(2)=1115830.0
BC_T_g(2)=317.6
BC_U_g(2)=0.0
BC_V_g(2)=0.0
BC_W_g(2)=10.0
BC_U_s(2,1)=0.0
BC_V_s(2,1)=0.0
BC_MASSFLOW_s(2,1)=0.1
!Gas-solids outlet
BC_x_w(5)=163.9
BC_x_e(5)=213.4
BC_y_s(5)=1163.3
BC_y_n(5)=1371.6
BC_z_b(5)=0.0
BC_z_t(5)=0.0
BC_TYPE(5)='PO' !pressure outlet boundary
BC_P_g(5)=1115830.0 !outlet pressure
BC_T_g(5)=317.6

#OUTPUT CONTROL SECTION
RES_DT=0.0005 !time inteval for restart file
SPX_DT(1)=0.01
SPX_DT(2)=0.1
SPX_DT(3)=0.1
SPX_DT(4)=0.1
SPX_DT(5)=100.
SPX_DT(6)=100.
SPX_DT(7)=100.
SPX_DT(8)=100.
NLOG=50 !interval in number of time steps for log file
FULL_LOG=.TRUE. !write residual on screen and to log file

```

APPENDIX F: MFIX Input File for Bubble Shape Simulation

```
#  
# Bubbling Fluidized Bed Simulation  
# 7-23-97  
#  
# 9.5 h on Octane, 11 Mb storage  
# Run-control section  
#  
RUN_NAME = 'KUIPERS'  
DESCRIPTION = 'KUIPERS EXPERIMENT'  
RUN_TYPE = 'new'  
UNITS = 'cgs'  
TIME = 0.0 TSTOP = 20.0 DT = 1.0E-4  
ENERGY_EQ = .FALSE.  
SPECIES_EQ = .FALSE. .FALSE.  
UR_FAC(2) = .2  
####  
#  
# SECOND ORDER CELL FACE INTERPOLATION FOR ALL THE  
# SEVEN EQUATIONS (7) i.e., PRESSURE, SOLIDS VOLUME FRACTION,  
# VELOCITY COMPONENTS FOR BOTH PHASES, TEMPERATURE, AND  
# MASS FRACTION USING THE SUPERBEE SCHEME (2) IS GIVEN BELOW.  
#  
DISCRETIZE = 7*2  
#  
#  
# TO IMPLEMENT THE HIGH ORDER DISCRETIZATION SCHEMES USING A  
# DEFERRED CORRECTION APPROACH SET DEF_COR = .TRUE.  
#  
DEF_COR = .TRUE.  
#  
#  
# Geometry Section  
#  
# COORDINATES = 'Cartesian'  
XLENGTH = 57.0 IMAX = 114  
YLENGTH = 100.0 JMAX = 200  
  
NO_K = .TRUE.  
#  
# Gas-phase Section  
#  
# MU_g0 = 1.8E-4  
# RO_g0 = .00128  
MW_avg = 29.  
#  
# Solids-phase Section  
#  
RO_s = 2.66  
D_p = 0.05  
  
e = 0.8  
Phi = 40.0  
EP_star = 0.4  
#  
# Initial Conditions Section  
#  
# ! Bed Freeboard  
IC_X_w = 0.0 0.0
```

```

IC_X_e          = 57.0          57.0
IC_Y_s          = 0.0           50.0
IC_Y_n          = 50.0          100.0

IC_EP_g          = 0.4           1.0
IC_X_g(1,1)      = 1.0           1.0
IC_X_s(1,1,1)    = 1.0           0.0
IC_U_g          = 0.0           0.0
IC_V_g          = (25.0/0.4)    25.0

IC_U_s(1,1)      = 0.0           0.0
IC_V_s(1,1)      = 0.0           0.
IC_P_star        = 0.0           0.0
IC_T_g          = 297.          297.

#
# Boundary Conditions Section
#
      !          Grid      Jet      Grid      Exit
BC_X_w          = 0.0          27.75    29.25    0.0
BC_X_e          = 27.75        29.25    57.0     57.0
BC_Y_s          = 0.0           0.0      0.0      100.0
BC_Y_n          = 0.0           0.0      0.0      100.0

BC_TYPE          = 'MI'         'MI'     'MI'     'PO'
BC_EP_g          = 1.0           1.0      1.0
BC_U_g          = 0.0           0.0      0.0
BC_V_g          = 25.0          1000.0   25.0

BC_P_g          = 4*1.01E6
BC_T_g          = 4*297.

#
# Output Control
#
RES_DT = 0.01
      !
      ! EP_g P_g          U_g   U_s   ROP_s      T_g   X_g
      !          P_star      V_g   V_s           T_s1  X_s
      !          W_g   W_s           T_s2
SPX_DT = 0.01 100.  1.0  0.01  100.  100. 100. 100. 100.
NLOG   = 100
full_log = .true.

```

Appendix G: MFIX Input File Used To Predict Spouted Bed Behavior

```
# Spouting bed experiment of U. of British Columbia          10-13-95
#
# He, Y.-L., J.R. Grace, S.-Z. Qin, and C.J. Lim, "Particle velocity
profiles
# and solid flow patterns in spouted beds," submitted to Can. J. Chem.
Eng.
# ubc100 -- fn B in drag formula adjusted to match exp Umf (assumed to be
equal
#          to Ums)
C(2) = 0.544
C(3) = 5.02382
#
# RUN CONTROL SECTION
#
RUN_NAME          = 'UBC100'
RUN_TYPE          = 'restart_1'
DESCRIPTION       = 'Spouting Bed -- 1.1 * Ums'
UNITS             = 'CGS'
ENERGY_EQ         = .FALSE.
SPECIES_EQ        = .F.          .F.
GRANULAR_ENERGY  = .T.

DISCRETIZE        = 8*2
DEF_COR           = .T.

TIME              = 0.0
TSTOP             = 10.
DT                = 1.0e-4

#
# GEOMETRY SECTION
#
COORDINATES      = 'CYLINDRICAL'
NO_K              = .TRUE.

XLENGTH           = 7.6
DX                = 20*0.0475 !0.95
DX(21)            = 0.05          !1
DX(22)            = 0.06          !1.06
DX(23)            = 0.07          !1.13
DX(24)            = 0.08          !1.21
DX(25)            = 0.09          !1.3
DX(26)            = 0.1           !1.4
DX(27)            = 0.11          !1.51
DX(28)            = 0.12          !1.63
DX(29)            = 0.13          !1.76
DX(30)            = 0.14          !1.9
DX(31)            = 0.15          !2.05
DX(32)            = 0.17          !2.22
DX(33)            = 0.19          !2.41
DX(34)            = 0.21          !2.62
DX(35)            = 0.23          !2.85
DX(36)            = 0.25          !3.1
DX(37)            = 0.28          !3.38
```

```

DX( 38) = 0.31 !3.69
DX( 39) = 0.34 !4.03
DX( 40) = 0.37 !4.4
DX( 41) = 0.41 !4.81
DX( 42) = 0.45 !5.26
DX( 43) = 0.468 !5.728
DX( 44) = 0.468 !6.196
DX( 45) = 0.468 !6.664
DX( 46) = 0.468 !7.132
DX( 47) = 0.468 !7.6
IMAX = 47

YLENGTH = 90
JMAX = 360

ZLENGTH = @ ( 2*pi )
KMAX = 1

#
# Numerical parameters
#
UR_FAC( 2) = 0.2
#
# GAS SECTION
#
MU_g0 = 1.19e-4
MW_avg = 29.

l_scale0 = 0.36
Mu_gmax = 0.2

#
# PARTICLE SECTION
#
e = 0.8
Phi = 30.0
EP_star = 0.412

MMAX = 1

D_p = 0.141
RO_s = 2.503

#
# INITIAL CONDITIONS SECTION
#
! bed freeboard
IC_x_w = 0.0 0.0
IC_x_e = 7.6 7.6
IC_y_s = 0.0 32.5
IC_y_n = 32.5 90.0

IC_U_g = 0.0 0.0
IC_V_g = 2.0 2.0

IC_ep_g = 0.412 1.0

```

```

IC_U_s(1,1)      =  0.0          0.0
IC_V_s(1,1)      =  0.0          0.0

IC_T_g           =  294.0      294.0
IC_T_s           =  294.0      294.0
IC_Theta_m       =  0.0          0.0

IC_P_star        =  0.0          0.0

#
# BOUNDARY CONDITIONS SECTION
#
!

      !           Central Jet      top exit
BC_x_w           =  0.0          0.0
BC_x_e           =  0.95         7.6
BC_y_s           =  0.0          90.0
BC_y_n           =  0.0          90.0

BC_TYPE          =  'MI'        'PO'

BC_ep_g          =  1.0

BC_U_g           =  0.0
BC_V_g           =  @(1.1*3448.)

BC_P_g           =  1.05E6     1.0129E6
BC_T_g           =  293.0      293.0
BC_T_s           =  293.0      293.0

!
! conical section at the bottom
!
BC_i_w(10)       =  24
BC_i_e(10)       =  25
BC_j_s(10)       =  1
BC_j_n(10)       =  2
BC_Uw_s(10,1)    =  0.0
BC_Vw_s(10,1)    =  0.0
BC_Thetaw_m(10,1) =  0.0

BC_TYPE(10)      =  'NSW'

BC_i_w(11)       =  25
BC_i_e(11)       =  27
BC_j_s(11)       =  1
BC_j_n(11)       =  3

BC_Uw_s(11,1)    =  0.0
BC_Vw_s(11,1)    =  0.0
BC_Thetaw_m(11,1) =  0.0

BC_TYPE(11)      =  'NSW'

BC_i_w(12)       =  28
BC_i_e(12)       =  28
BC_j_s(12)       =  1
BC_j_n(12)       =  4

BC_Uw_s(12,1)    =  0.0

```

```

BC_Vw_s(12,1)      = 0.0
BC_Thetaw_m(12,1)  = 0.0

BC_TYPE(12)         = 'NSW'

BC_i_w(13)          = 29
BC_i_e(13)          = 29
BC_j_s(13)          = 1
BC_j_n(13)          = 5

BC_Uw_s(13,1)       = 0.0
BC_Vw_s(13,1)       = 0.0
BC_Thetaw_m(13,1)  = 0.0

BC_TYPE(13)         = 'NSW'

BC_i_w(14)          = 30
BC_i_e(14)          = 30
BC_j_s(14)          = 1
BC_j_n(14)          = 6

BC_Uw_s(14,1)       = 0.0
BC_Vw_s(14,1)       = 0.0
BC_Thetaw_m(14,1)  = 0.0

BC_TYPE(14)         = 'NSW'

BC_i_w(15)          = 31
BC_i_e(15)          = 31
BC_j_s(15)          = 1
BC_j_n(15)          = 7

BC_Uw_s(15,1)       = 0.0
BC_Vw_s(15,1)       = 0.0
BC_Thetaw_m(15,1)  = 0.0

BC_TYPE(15)         = 'NSW'

BC_i_w(16)          = 32
BC_i_e(16)          = 32
BC_j_s(16)          = 1
BC_j_n(16)          = 8

BC_Uw_s(16,1)       = 0.0
BC_Vw_s(16,1)       = 0.0
BC_Thetaw_m(16,1)  = 0.0

BC_TYPE(16)         = 'NSW'

BC_i_w(20)          = 33
BC_i_e(20)          = 33
BC_j_s(20)          = 1
BC_j_n(20)          = 9

BC_Uw_s(20,1)       = 0.0
BC_Vw_s(20,1)       = 0.0
BC_Thetaw_m(20,1)  = 0.0

BC_TYPE(20)         = 'NSW'

```

BC_i_w(21)	= 34
BC_i_e(21)	= 34
BC_j_s(21)	= 1
BC_j_n(21)	= 10
BC_Uw_s(21,1)	= 0.0
BC_Vw_s(21,1)	= 0.0
BC_Thetaw_m(21,1)	= 0.0
BC_TYPE(21)	= 'NSW'
BC_i_w(22)	= 35
BC_i_e(22)	= 35
BC_j_s(22)	= 1
BC_j_n(22)	= 11
BC_Uw_s(22,1)	= 0.0
BC_Vw_s(22,1)	= 0.0
BC_Thetaw_m(22,1)	= 0.0
BC_TYPE(22)	= 'NSW'
BC_i_w(23)	= 36
BC_i_e(23)	= 36
BC_j_s(23)	= 1
BC_j_n(23)	= 13
BC_Uw_s(23,1)	= 0.0
BC_Vw_s(23,1)	= 0.0
BC_Thetaw_m(23,1)	= 0.0
BC_TYPE(23)	= 'NSW'
BC_i_w(24)	= 37
BC_i_e(24)	= 37
BC_j_s(24)	= 1
BC_j_n(24)	= 15
BC_Uw_s(24,1)	= 0.0
BC_Vw_s(24,1)	= 0.0
BC_Thetaw_m(24,1)	= 0.0
BC_TYPE(24)	= 'NSW'
BC_i_w(25)	= 38
BC_i_e(25)	= 38
BC_j_s(25)	= 1
BC_j_n(25)	= 16
BC_Uw_s(25,1)	= 0.0
BC_Vw_s(25,1)	= 0.0
BC_Thetaw_m(25,1)	= 0.0
BC_TYPE(25)	= 'NSW'
BC_i_w(26)	= 39
BC_i_e(26)	= 39
BC_j_s(26)	= 1
BC_j_n(26)	= 18

BC_Uw_s(26,1)	= 0.0
BC_Vw_s(26,1)	= 0.0
BC_Thetaw_m(26,1)	= 0.0
BC_TYPE(26)	= 'NSW'
BC_i_w(30)	= 40
BC_i_e(30)	= 40
BC_j_s(30)	= 1
BC_j_n(30)	= 20
BC_Uw_s(30,1)	= 0.0
BC_Vw_s(30,1)	= 0.0
BC_Thetaw_m(30,1)	= 0.0
BC_TYPE(30)	= 'NSW'
BC_i_w(31)	= 41
BC_i_e(31)	= 41
BC_j_s(31)	= 1
BC_j_n(31)	= 23
BC_Uw_s(31,1)	= 0.0
BC_Vw_s(31,1)	= 0.0
BC_Thetaw_m(31,1)	= 0.0
BC_TYPE(31)	= 'NSW'
BC_i_w(32)	= 42
BC_i_e(32)	= 42
BC_j_s(32)	= 1
BC_j_n(32)	= 26
BC_Uw_s(32,1)	= 0.0
BC_Vw_s(32,1)	= 0.0
BC_Thetaw_m(32,1)	= 0.0
BC_TYPE(32)	= 'NSW'
BC_i_w(33)	= 43
BC_i_e(33)	= 43
BC_j_s(33)	= 1
BC_j_n(33)	= 29
BC_Uw_s(33,1)	= 0.0
BC_Vw_s(33,1)	= 0.0
BC_Thetaw_m(33,1)	= 0.0
BC_TYPE(33)	= 'NSW'
BC_i_w(34)	= 44
BC_i_e(34)	= 44
BC_j_s(34)	= 1
BC_j_n(34)	= 32
BC_Uw_s(34,1)	= 0.0
BC_Vw_s(34,1)	= 0.0
BC_Thetaw_m(34,1)	= 0.0

```

BC_TYPE( 34 )           =  'NSW'

BC_i_w( 35 )           =  45
BC_i_e( 35 )           =  45
BC_j_s( 35 )           =   1
BC_j_n( 35 )           =  35

BC_Uw_s( 35,1 )         =  0.0
BC_Vw_s( 35,1 )         =  0.0
BC_Thetaw_m( 35,1 )    =  0.0

BC_TYPE( 35 )           =  'NSW'

BC_i_w( 36 )           =  46
BC_i_e( 36 )           =  46
BC_j_s( 36 )           =   1
BC_j_n( 36 )           =  38

BC_Uw_s( 36,1 )         =  0.0
BC_Vw_s( 36,1 )         =  0.0
BC_Thetaw_m( 36,1 )    =  0.0

BC_TYPE( 36 )           =  'NSW'

BC_i_w( 40 )           =  47
BC_i_e( 40 )           =  47
BC_j_s( 40 )           =   1
BC_j_n( 40 )           =  42

BC_Uw_s( 40,1 )         =  0.0
BC_Vw_s( 40,1 )         =  0.0
BC_Thetaw_m( 40,1 )    =  0.0

BC_TYPE( 40 )           =  'NSW'

BC_i_w( 41 )           =  48
BC_i_e( 41 )           =  48
BC_j_s( 41 )           =   1
BC_j_n( 41 )           =  46

BC_Uw_s( 41,1 )         =  0.0
BC_Vw_s( 41,1 )         =  0.0
BC_Thetaw_m( 41,1 )    =  0.0

BC_TYPE( 41 )           =  'NSW'

#
# OUTPUT CONTROL SECTION
#
!   OUT_DT = 1.0
RES_DT = 0.01
!
!   EP_g      P_g      U_g      U_s      ROP_s    T_g      X_g      Theta   Scalar
!           P_star   V_g      V_s      T_s1      T_s2
!
SPX_DT = 0.01           0.1      0.1      0.1     100.     100.     100.    0.1    100.

NLOG = 25
FULL_LOG = .TRUE.

```